Characterisation of Enzymes involved in Tetrapyrrole Biosynthesis

Von der Fakultät für Lebenswissenschaften
der Technischen Universität Carolo-Wilhelmina
zu Braunschweig
zur Erlangung der Grades einer
Doktorin der Naturwissenschaften
(Dr. rer. nat.)
genehmigte
D i s s e r t a t i o n

von Claudia Schulz
aus Celle

1. Referent: Professor Dr. Dieter Jahn
2. Referentin: Dr. Gunhild Layer
eingereicht am: 07.07.2010
mündliche Prüfung (Disputation) am: 19.08.2010

Druckjahr 2010

Vorveröffentlichungen der Dissertation

Teilergebnisse aus dieser Arbeit wurden mit Genehmigung der Fakultät für Lebenswissenschaften, vertreten durch den Mentor der Arbeit, in folgenden Beiträgen vorab veröffentlicht:

PUBLIKATIONEN

Silva, P.J.*, Schulz, C.*, Jahn, D., Jahn, M. & Ramos, M. J. (2010)
A tale of two acids: when arginine is a more appropriate acid than H_3O^+.
J Phys Chem B **114**: 8994-9001 *these authors contributed equally to this paper

„Zwei Dinge sind zu unserer Arbeit nötig: Unermüdliche Ausdauer und die Bereitschaft, etwas, in das man viel Zeit und Arbeit gesteckt hat, wieder wegzuwerfen.“

Albert Einstein

Meiner Familie und Freunden

TABLE OF CONTENTS

ABBREVIATIONS

A	ampere
ALA	5-aminolaevulinic acid
ALAS	5-aminolaevulinic acid synthase
amp	ampicillin
APS	ammonium peroxidisulfate
ATP	adenosine triphosphate
BCA	bicinchoninic acid
BCIP	5-brom-4-chloro-3-indolylphosphate
BLAST	basic local alignment search tool
bp	base pair
BSA	bovine serum albumin
C	Celsius (°C)
CHAPS	3-[(3-cholamidopropyl)dimethylammonio]-1-propansulfonate
cm	chloramphenicol
CPO	coproporphyrinogen III oxidase
Da	Dalton
ddNTP	didesoxy nucleotide triphosphate
DMBA	4-(dimethylamino)-benzaldehyde
DMF	dimethylenformamide
DNA	desoxyribonucleic acid
dsDNA	double stranded DNA
dNTP	desoxy nucleotide triphosphate
Dnase	desoxyribonuclease
DTT	1,4-dithio-D,L-threitol
EDTA	ethylenediamine tetraacetic acid
et al.	*et alteri* (and others)
e.g.	*exempli gratia* (for example)
FAD	flavin adenine dinucleotide
FC	ferrochelatase
Fig.	figure
FPLC	fast protein liquid chromatography
for	forward

g	centrifugation: earth gravity (x *g*)
	weight: gram
GST	glutathione-S-transferase
GluTR	glutamyl-tRNA-reductase
GSA	glutamate-1-semialdehyde
GSAM	glutamate-1-semialdehyde-2,1-aminomutase
h	hour
HemE	uroporphyrinogen III decarboyxlase
HemF	oxygen-dependent coproporphyrinogen III oxidase
HemN/Z	oxygen-independent coproporphyrinogen III oxidase
HPLC	high performance liquid chromatography
IPTG	isopropyl-β-D-thiogalactopyranoside
k	kilo
kb	kilobase
kan	kanamycin
L	litre
λ	wavelength
LB	Luria Bertani
m	scale unit: milli
	unit of length: meter
M	molar (mol/L)
µ	micro
MC	magnesiumchelatase
min	minute
MOPS	3-(N-morpholino)-propan sulfonacid
M_r	relative molecular mass
n	nano
NAD(P)	nicotine adenine dinucleotide (phosphate), reduced form
NBT	nitroblue-tetrazolium
Ni^{2+}-NTA	nickel agarose with chelating agent nitrilo-tir-acetic acid
rpm	rotation per minute
OD_λ	optical density at a wavelength λ in nm
PBG	porphobilinogen
PBGS	porphobilinogen synthase

PBGD	porphobilinogen deaminase
PBS	phosphate buffered saline
PCR	polymerase chain rection
PEG	polyethyleneglycol
rev	reverse
RNase	ribunuclease
PCT	porphyria cutanea tarda
PLP	pyridoxal-5'-phosphate
PPO	protoporphyrinogen IX oxidase
psi	pound-force per square inch
PVDF	polyvinylidene fluoride
RT	room temperature
sec	second
SAM	*S*-adenosyl-*L*-methionine
SDS	sodium dodecyl sulphate
SDS-PAGE	sodium dodecyl sulphate polyacrylamide gel electrophoresis
sp.	species
str	streptomycin
T	temperature
Tab.	table
TEMED	tetramethylen diamine
tet	tetracycline
Tris	Tris-(hydroxymethyl)-aminomethane
tRNA	transfer ribonucleic acid
uro'gen III	uroporphyrinogen III
uro'gen I	uroporphyrinogen I
uro III	uroporphyrin III
UROD	uroporphyrinogen III decarboxylase
UROS	uroporphyrinogen III synthase
UV	ultraviolet
V	volt
v/v	volume per volume
WT	wildtype
w/v	weight per volume

1 INTRODUCTION

1.1 Structure and Functions of Tetrapyrroles

Tetrapyrroles are nearly present ubiquitous in all organisms. They are involved in the eukaryotic as well as in prokaryotic cell physiology. The basic structure consists of four pyrrole rings which are either linked to a ring system or a linear molecule. The universal basic structure of the cyclic tetrapyrroles is the porphyrin ring whose pyrrole derivates are connected by four methine bridges. The four pyrrole rings are denoted A, B, C and D in a clockwise direction. The carbon and nitrogen atoms are serially numbered with C1-C20 and N21-N24 (Figure 1.1). The α-position denotes the carbons which are close to the nitrogen atoms. The carbons which form the methine bridges are in meso-position and the remaining carbons are in β-position (Chadwick and Ackrill, 1994; Jordan, 1991; Warren and Smith, 2008).

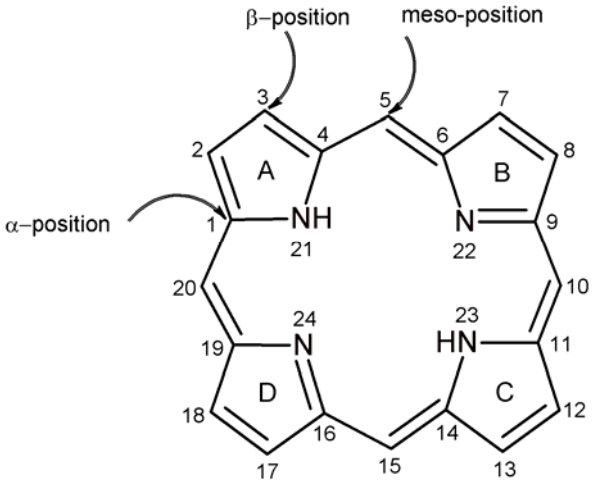

Figure 1.1: Basic structure of all cyclic tetrapyrroles, the porphyrin ring.

The four pyrrole rings are denoted A, B, C and D in a clockwise direction. The carbon and nitrogen atoms are serially numbered with C1-C20 and N21-N24. The α-position denotes the carbons which are close to the nitrogen atoms. The carbons which form the methine bridges are in meso-position and the remaining carbons are in β-position.

Cyclic tetrapyrroles discriminate in their variable oxidation state of their ring system, the nature of the chelated metal ion and the ring substituents at the β-position of the pyrrole rings. The centred nitrogen atoms are able to chelate different metal ions like iron, magnesium, cobalt or nickel (Frankenberg *et al.*,

2003; Heinemann *et al.*, 2008; Layer *et al.*, 2010). Because of their conjugated π-electron system tetrapyrroles are able to absorb different parts of the visual light. For example, haem is responsible for the red colour in blood or chlorophyll colours plants green. Linear tetrapyrroles derive from cleavage of cyclic tetrapyrroles. They are divided into bile pigments, phycobilins and degradation products of the macrocycles (Dammeyer and Frankenberg-Dinkel, 2008). Based on their characteristics the tetrapyrroles are divided into eight classes: haem (Munro *et al.*, 2008; Rodgers, 1999), chlorophyll, bacteriochlorophyll (Beale, 1999; Vavilin and Vermaas, 2002), corrinoids, sirohaem (Raux *et al.*, 2003), haem d_1 (Chang and Wu, 1986; Chang, 1994), cofactor F_{430} (Thauer and Bonacker, 1994) and open-chain tetrapyrroles. Because of the leak of the fourth carbon bridge (C20, see Figure 1.1) the corrinoides form an exception (Battersby, 2000; O'Brian and Thony-Meyer, 2002). All cyclic tetrapyrroles are derived from the common precursor uroporphyrinogen III (Figure 1.2).

Tetrapyrroles play vital roles in various biological processes. Magnesium containing chlorophylls and bacteriochlorophylls serve as essential macromolecules in photosynthesis by absorbing light and transferring light energy or electrons to other molecules (Beale, 1999). Haemoglobin and myoglobin utilise iron-chelating haem for oxygen and carbon dioxide transport. Moreover, haem is found in cytochromes and enzymes as prosthetic group where they are involved in electron transport and enzymatic reactions (Panek and O'Brian, 2002). The iron-chelating sirohaem is a cofactor involved in assimilatory nitrite or sulfite reduction (Chang, 1994; Raux *et al.*, 2003). Corrinoids, such as the cobalt chelating vitamin B_{12}, are involved in radical-depended nucleotide reduction and in methyl transfer (Warren and Smith, 2008). The nickel chelating coenzyme F_{430} takes part in the methanogenesis in archaea (Friedmann *et al.*, 1990; Thauer and Bonacker, 1994). Linear tetrapyrroles do not contain a tightly bound metal ion. They can be found as bile pigments in humans and chromophores, as parts of the plant photoreceptors and in cyanobacteria (Frankenberg and Lagarias, 2003). The diversity and wide dispersal of this class of cofactors implies the importance in nature. In eukaryotes the tetrapyrrole biosynthesis is restricted to haem, sirohaem, chlorophyll and biline formation. Prokaryotes are additionally able to synthesise corrinoids, coenzyme F_{430} and haem d_1 (Jahn *et al.*, 1996; Vavilin and Vermaas, 2002).

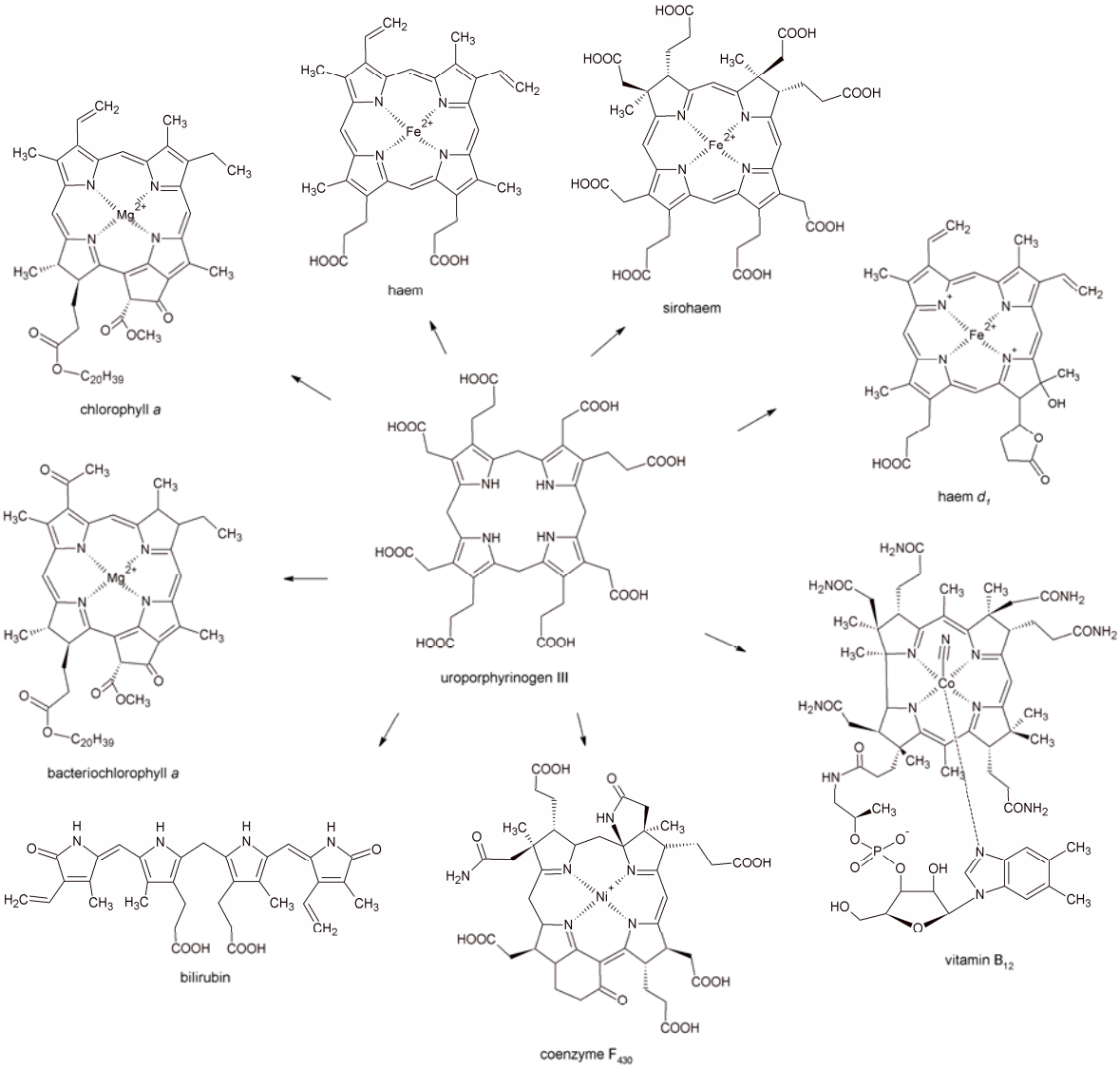

Figure 1.2: Representative structures of the eight tetrapyrrole classes and their common precursor uroporphyrinogen III.

Tetrapyrroles are divided into eight classes: haem, chlorophyll, bacteriochlorophyll, corrinoids, sirohaem, haem d_1, cofactor F_{430} and open-chain tetrapyrroles. All cyclic tetrapyrroles are derived from the common precursor uroporphyrinogen III. Linear tetrapyrroles result from the cleavage of cyclic tetrapyrroles.

1.2 Tetrapyrrole Biosynthesis

The tetrapyrrole biosynthesis is a highly conserved mechanism which is controlled by different regulation mechanisms in the cell. 5-aminolaevulinic acid (ALA) is the common precursor for all tetrapyrroles, which contains all carbon and nitrogen atoms required to build the porphyrin macrocycle. The major branching point occurs after the formation of the first cyclic tetrapyrrole, uroporphyrinogen III. This is either converted into protoporphyrin IX or precorrin-2. Protoporphyrin IX is the

precursor for so called porphyrins like haem, chlorophyll and bacteriochlorophyll, which are characterised by their completely conjugated planar ring system, while precorrin-2 serves as basic frame for porphinoids like sirohaem, haem d_1, coenzyme F_{430} and corrinoids (Warren and Smith, 2008).

1.2.1 Two Pathways for the Biosynthesis of 5-Aminolaevulinic Acid

The first step in the tetrapyrrole biosynthesis in all organisms is the formation of 5-aminolaevulinic acid (ALA), which is synthesised in nature in two unrelated pathways.

Vertebrates, yeasts and α-proteobacteria form ALA by condensation of glycine and succinyl-CoA with subsequently release of carbon dioxide and coenzyme A (CoA; Figure 1.3). This reaction is catalysed by the pyridoxal-5'-phosphate-dependent 5-aminolaevulinic acid synthase (ALAS; encoded by *hemA*; EC 2.3.1.37). The pyridoxal-5'-phosphate is covalently linked to an essential active site lysine, forming an internal aldimine. The reaction starts when glycine binds to the active site and forms an external aldimine with the pyridoxal-5'-phosphate cofactor. This is followed by the stereo-specific abstraction of the pro-*R* proton of glycine, leading to the formation of a quinonoid intermediate. This condenses with succinyl-CoA to form a 2-amino-3-ketoadipate intermediate by coenzyme A and CO_2 release. Then a proton replaces the glycine-derived carboxyl group and ALA is released as the internal aldimine is restored (Hunter *et al.*, 2007; Hunter and Ferreira, 2009).

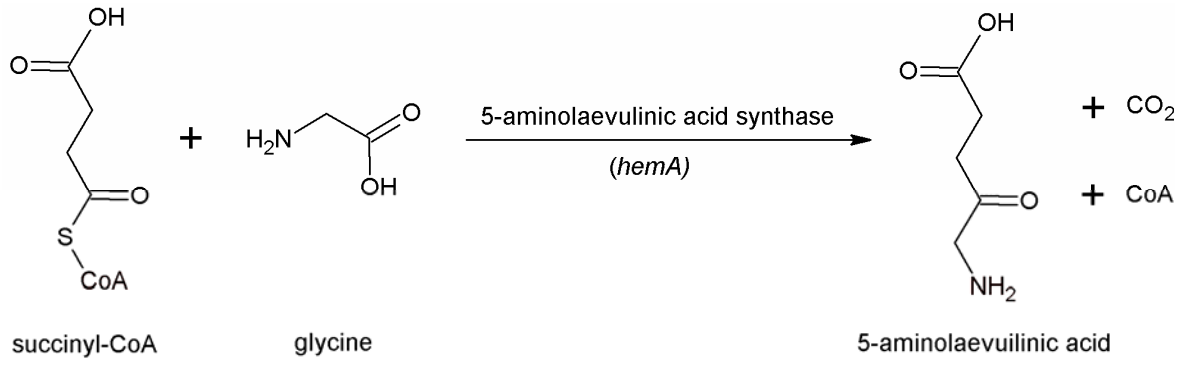

Figure 1.3: Shemin way: formation of 5-aminolaevulinic acid.

Biosynthesis of 5-aminolaevulinic acid in vertebrates, yeasts and α-proteobacteria takes place *via* condensation of glycine and succinyl-CoA by 5-aminolaevulinic acid synthase (*hemA*).

The catalytic reaction was named after its discoverer Shemin. In 1945 Shemin and Rittenberg reported for the first time that the nitrogen atom originates from glycine in haem (Shemin and Rittenberg, 1945, 1946). Therefore, Shemin himself ingested ^{15}N-labled glycine over a period of three days and took regularly blood samples. Based on his results, Shemin concluded that porphyrin is synthesised *in vivo* from glycine and other compounds. Years later the Shemin group identified succinyl-CoA as the second source of carbon atoms in haem (Shemin and Kumin, 1952). Finally, ALA was suggested to be the source of all atoms of protoporphyrin (Kikuchi *et al.*, 1958; Shemin and Russel, 1953).

Plants, archaea and the vast majority of bacteria use the so called C5-way. Here, glutamyl-tRNA serves as initial substrate. Then, two enzymatic steps are required to form ALA (Figure 1.4).

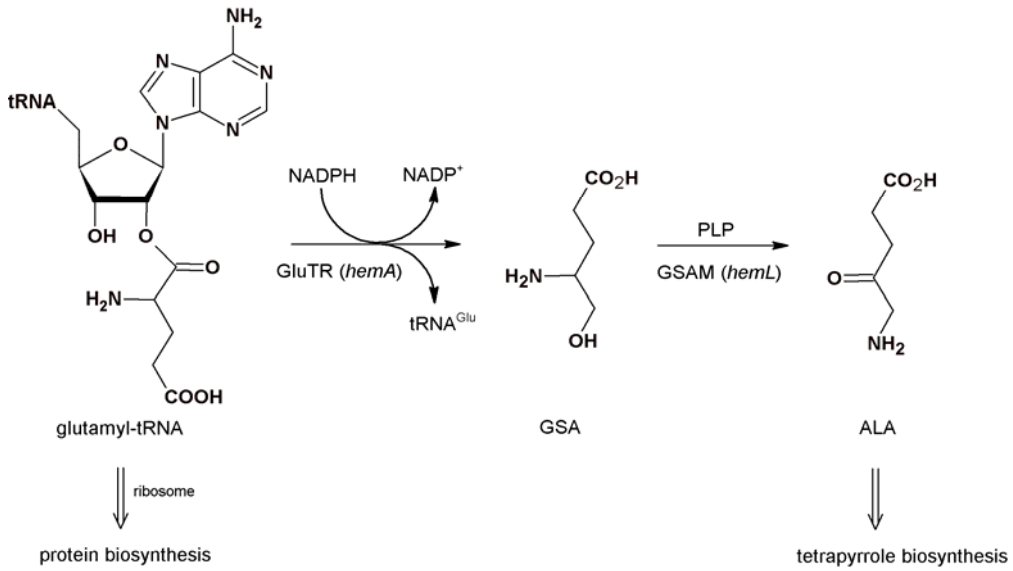

Figure 1.4: C-5 way: formation of 5-aminolaevulinic acid.

Glutamyl-tRNA reductase (GluTR) reduces glutamyl-tRNA by use of NADPH under $tRNA^{Glu}$ release to glutamate-1-semialdehyde (GSA). GSA is converted to 5-aminolaevulinic acid (ALA) in a pyridoxal-5'-phosphate dependent reaction by glutamate-1-semialdehyde-2,1-aminomutase (GSAM).

The glutamyl-tRNA reductase (**GluTR**, encoded by *hemA*; EC 6.1.1.17) uses the glutamylated tRNA as substrate in an NADPH-depended reaction. The chemical high reactive glutamate-1-semialdehyde (GSA) is emerged from this reduction, while $tRNA^{Glu}$ is released. Subsequently, GSA is converted to ALA in a pyridoxal-5'-phosphate (PLP) dependent transamination reaction by the glutamate-1-

semialdehyde-2,1-aminomutase (**GSAM**, encoded by *hemL*; EC 5.4.3.8; Beale and Castelfranco, 1973; Jahn *et al.*, 1992). GSA is a highly reactive aldehyde. For that reason an earlier proposal suggested that GluTR and GSAM form a complex, which is in line with the structural complementary of the two enzymes (Moser *et al.*, 2002) and was finally proven to exist *in vivo* (Luer *et al.*, 2005).

1.2.2 Conversion of 5-Aminolaevulinic Acid to Haem

In the first common step in the biosynthesis two ALA molecules are asymmetric condensed to porphobilinogen by porphobilinogen synthase (**PBGS**; encoded by *hemB*; EC 4.2.1.24), which uses metal ion as cofactors. In different organisms variable cations are chelated for example zinc, magnesium or potassium (Frankenberg *et al.*, 1999a; Frankenberg *et al.*, 1999b; Jaffe, 2003; Shoolingin-Jordan *et al.*, 2002). By elimination of NH_3 the porphobilinogen deaminase (**PBGD**; encoded by *hemC*; EC 4.3.1.8) links four porphobilinogen molecules to the instable linear pre-uroporphyrinogen (Figure 1.5; Louie *et al.*, 1992; Warren and Jordan, 1988). Porphobilinogen deaminase contains dipyrromethane, an unusual cofactor consisting of two molecules of porphobilinogen. Dipyrromethane is covalently attached to the enzyme and serves as the starting point of tetramerisation of porphobilinogen without being integrated into the final product (Jordan and Warren, 1987; Jordan, 1994a). Subsequently the uroporphyrinogen III synthase (**UROS**; encoded by *hemD*; EC

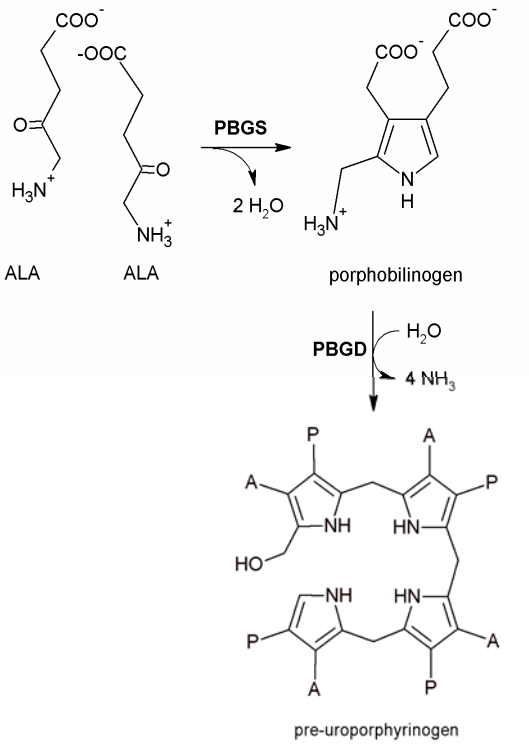

Figure 1.5: Conversion of 5-aminolaevulinic acid (ALA) into pre-uroporphyrinogen
Porphobilinogen synthase (PBGS) catalyses the formation of porphobilinogen (PBG) by asymmetric condensation of two 5-aminolaevulinic acid (ALA) molecules. Four PBG molecules are linked to the unstable linear pre-uroporphyrinogen by porphobilinogen deaminase (PBGD) *via* NH_3 elimination. A = acetate side chain; P = propionate side chain.

4.2.1.75) forms the common cyclic precursor uroporphyrinogen III by condensation. At this point the important step is the inverting of the tetrapyrrole D ring *via* a spiro-mechanism with spiro-pyrrolenine as an intermediate to form an asymmetric tetrapyrrole (Chadwick and Ackrill, 1994). Then the biosynthesis of the various tetrapyrroles divides. On the one hand uroporphyrinogen III is methylated at C2 and C7 by uroporphyrin III C-methyltransferase (EC 2.1.1.107) to form dihydrosirohydrochlorin (precorrin-2) which is the precursor of corrinoids, sirohaem, haem d_1 and coenzyme F_{430} (Jahn *et al.*, 1996). On the other hand haem, chlorophyll and bacteriochlorophyll are formed. The next step in the haem and chlorophyll pathway is the decarboxylation of four acetate side chains to methyl groups by uroporphyrinogen III decarboxylase (**UROD**; encoded by *hemE*; EC 4.1.1.37; Akhtar, 1994). The decarboxylation proceeds in an ordered manner beginning with the acetate chain of ring D, followed by A, B and finally C (Figure 1.6). Subsequently, the originated coproporphyrinogen III is modified by converting the propionate groups on ring A and B into vinyl side chains by coproporphyrinogen III oxidase (**CPO**; encoded by *hemN* or *hemF*; EC 1.3.3.3). This reaction can be catalysed by two structurally non-related enzymes: the oxygen-dependent enzyme HemF, which uses molecular oxygen as an electron acceptor and the oxygen-independent “radical SAM”-enzyme HemN, which utilises

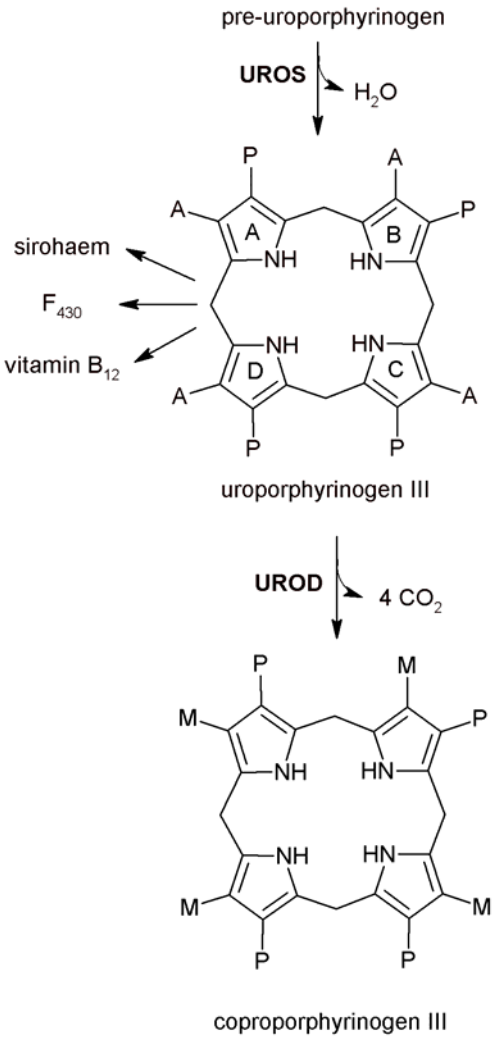

Figure 1.6: First steps of haem formation
Uroporphyrinogen III synthase (UROS) forms the first asymmetric cyclic tetrapyrrole uroporphyrinogen III by inverting the D ring. At this branching point in the biosynthesis uro-porphyrinogen III is either converted into precorrin-2 the precursor for sirohaem, vitamin B_{12}, haem d_1 and coenzyme F_{430} or into coproporphyrinogen III *via* converting the acetate chains into methyl chains by uro-porphyrinogen III decarboxylase (UROD). A = acetate side chain; P = propionate side chain; M = methyl side chain.

alternative electron acceptors (Breckau *et al.*, 2003; Layer *et al.*, 2002). The side chain modification is completed with the formed protoporphyrinogen IX. The next enzyme, protoporphyrinogen IX oxidase (**PPO**; encoded by *hemG* and *hemY*; EC 1.3.3.4), catalyses the oxidation to protoporphyrin IX, which requires the elimination of six electrons and results in the formation of a system of completely conjugated double bonds. Like CPO two structurally non related enzymes exist. Oxygen-dependent PPO (HemY) uses a flavin cofactor and molecular oxygen as an terminal electron acceptor (Hansson and Hederstedt, 1994; Koch *et al.*, 2004), whereas oxygen-independent PPO (HemG) was shown to transport the electrons to anaerobic respiratory chains with alternative terminal electron acceptors such as nitrate or fumarate (Jacobs and Jacobs, 1975, 1976). Recently, studies revealed that under aerobic conditions this HemG transfers the abstracted electrons *via* ubiquinone, cytochrome *bo*$_3$ and cytochrome *bd* to oxygen. While under anaerobic conditions the electrons are transferred *via* menaquinone, fumarate and nitrate reductase (Möbius *et al.*, 2010). Here is the next branching point in the biosynthesis. By inserting iron, which is catalysed by the ferrochelatase (**FC**; encoded by *hemH*; EC 4.99.1.1), protohaem IX (haem *b*) is formed, whereof all haems derive from. By chelating a magnesium ion into the protoporphyrin IX by magnesiumchelatase (**MC**), the synthesis of chlorophyll and bacteriochlorophyll is initiated (Figure 1.7; Jordan, 1994b; Jordan, 1991).

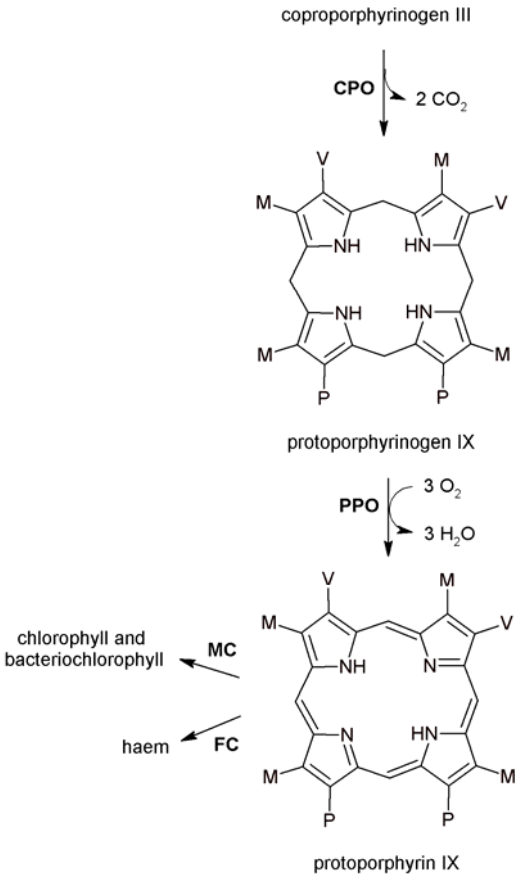

Figure 1.7: Last steps of haem formation
Converting the propionate groups into vinyl groups by coproporphyrinogen III oxidase (CPO) is the last side chain modification step. The completely modified tetrapyrrole protoporphyrinogen IX is finally oxidised into protoporphyrin IX by protoporphyrinogen IX oxidase (PPO). On the one hand haem *b* is formed *via* inverting a Fe^{2+} by ferrochelatase (FC) on the other hand the precursor for chlorophyll and bacteriochlorophyll is formed via inverting Mg^{2+} by magnesium-chelatase (MC). P = propionate side chain; V = vinyl side chain; M = methyl side chain

The variety of functions fulfilled by tetrapyrroles underscores their importance in nature, and explains the extensive effect of disorders in tetrapyrrole anabolism. These disorders cause toxic stress symptoms and cellular damage *via* peroxidation of membrane lipids (Meissner *et al.*, 1996). In humans, the rare heterogeneous metabolic disorders are commonly known as porphyrias (see chapter 1.7). However, there are still open questions, for example how do the enzymes cooperate *in vivo* to prevent solvent exposure and accumulation of biosynthesis intermediates, although they are located in different compartments in the cell (inner mitochondrial membrane, cytosol or chloroplast). For the two last enzymes in haem biosynthesis, PPO and FC, a complex formation was shown *in vitro* by co-immunoprecipitation and *in vivo via* immunogold labelling and electron microscopy in *Thermosynechococcus elongatus* (Masoumi *et al.*, 2008). The next chapter summarises the state-of-the-art knowledge about the enzymes used in this study.

1.3 Porphobilinogen Synthase

Porphobilinogen synthase (PBGS; or 5-aminolaevulinic acid dehydratase) is the first common enzyme in the tetrapyrrole biosynthesis. PBGS is encoded by the gene *hemB* and catalyses the asymmetric condensation of two molecules 5-aminolaevulinic acid (ALA) *via* the release of two molecules water to form porphobilinogen (PBG). PBGS from various organisms has been investigated *e.g. Escherichia coli* (Erskine *et al.*, 1999b), *Pseudomonas aeruginosa* (Frankenberg *et al.*, 1999b), *Homo sapiens* (Breinig *et al.*, 2003; Jaffe *et al.*, 2001) and *Saccharomyces cerevisiae* (Erskine *et al.*, 1999a). PBGSs share a high degree of sequence similarity. The most common active form is a homo-octamer with a molecular mass of 280’000-320’000. For all PBGSs a use of metal ion cofactors *e.g.* Zn^{2+} and/or Mg^{2+} have been described. During substrate recognition and substrate attachment the PBGS has to treat two identical molecules discretely to ensure defined asymmetric condensation at the catalysis (Shoolingin-Jordan and Cheung, 1999).

Crystal structures of PBGS from various sources confirm the presence of two distinct binding sites for each ALA molecule, the so called A- and P-site. Thus, the

product molecules sites are discriminated into an A- and P-site. This depends on the two substrate molecules ALA according to which the acetate and propionate side chain, respectively, originate from. The synthesis of PBG requires a successive formation of a C-C bond and a C-N bond between the substrate molecules. For the PBGS from *P. aeruginosa* it was shown that the reaction is initiated by formation of Schiff base bonds between the two ALA substrate molecules and two conserved lysine residues in the active site (Figure 1.8). Inhibitor studies revealed that the Aldol condensation (C-C bond formation) of the two ALA substrate molecules is the first reaction step, followed by the Schiff base C-N bond (Frere *et al.*, 2002; Frere *et al.*, 2006).

The recently discovered antibacterial compound alaremycin was isolated from the actinomycete *Streptomyces* sp. A012304 (Awa *et al.*, 2005). Alaremycin structurally closely resembles ALA. PBGSs of Gram-positive and Gram-negative bacteria revealed alaremycin inhibition. Cocrystallisation of alaremycin and recombinant produced *P. aeruginosa* PBGS demonstrated that the active site is efficiently blocked. The results revealed that PBGS is a molecular target of alaremycin (Heinemann *et al.*, 2010).

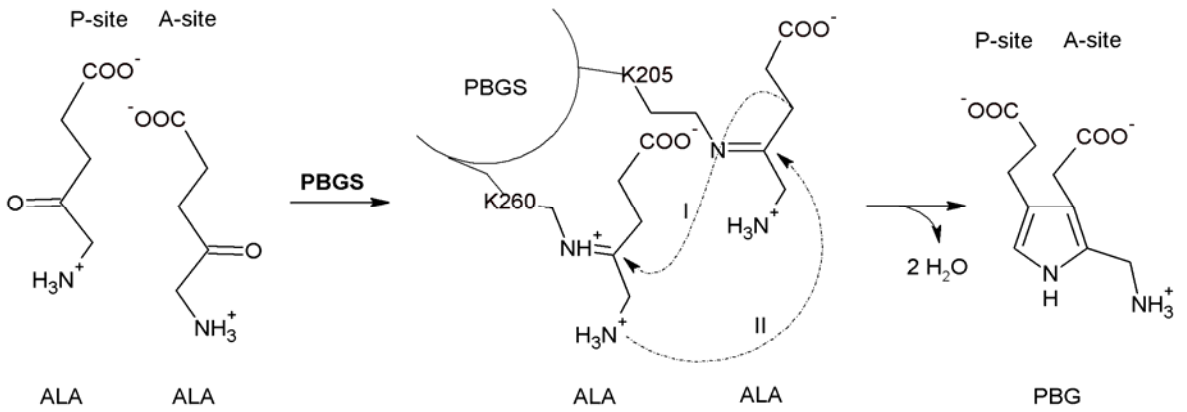

Figure 1.8: Reaction mechanism of porphobilinogen synthase.

Enzymatic reaction catalysed by *P. aeruginosa* porphobilinogen synthase (PBGS) during tetrapyrrole biosynthesis; two molecules of 5-aminolaevulinic acid (ALA) are condensed asymmetrically to form the first pyrrole porphobilinogen (PBG). Crystal structures of PBGS from various sources confirm the presence of two district binding sites for each ALA molecule, the so called A and P-site. Denotations of the substrate binding sites are ensued towards the occurred product side chains. This depends on the two substrate molecules ALA according to which the acetate and propionate side chain, respectively, originate from (modified after Frere *et al.*, 2005).

1.4 Uroporphyrinogen III Synthase

Uroporphyrinogen III synthase (UROS; formally uroporphyrinogen III cosynthase) was described by Bogorad and Granick in 1953 for the first time (Bogorad and Granick, 1953). UROS is encoded by the gene *hemD* and catalyses the fourth step in the tetrapyrrole biosynthesis. It was shown for the conversion of the monopyrrole porphobilinogen into the first cyclic tetrapyrrole uroporphyrinogen III (Uro'gen III) two enzymes porphobilinogen deaminase (PBGD), as well as UROS are required (Bogorad, 1958a, 1958b). PBGD catalyses the formation of the instable intermediate pre-uroporphyrinogen (Burton *et al.*, 1979), which serves as substrate for the UROS (Jordan *et al.*, 1979; Jordan and Berry, 1980). Uroporphyrinogen III synthases were isolated and characterised from several organisms: *Euglena gracilis* (Hart and Battersby, 1985), *Bacillus subtilis* (Stamford *et al.*, 1995), *Anacystis nidulans* (Roessner *et al.*, 2002), *E. coli* (Jordan *et al.*, 1988), *H. sapiens* (Mathews *et al.*, 2001; Omata *et al.*, 2004), *Rattus sp*. (Kohashi *et al.*, 1984), *Synechocystis sp.* PCC 6803 (Kaneko *et al.*, 1995), *S. cerevisiae* (Amillet and Labbe-Bois, 1995) and *Arabidopsis thaliana* (Tan *et al.*, 2008), respectively. To date, the enzyme is shown to be a monomer in all examined organisms with an average size of 28'000 to 35'000, which contains no reversible bound cofactors or metal ions.

In contrast to other enzymes of the tetrapyrrole biosynthesis UROS does not show a high amino acid sequence homology (Jahn *et al.*, 1996). Since then, many controversial catalytic mechanisms have been postulated. Today it is assumed that it is an interlude between PBGD and UROS to prevent the release of pre-uroporphyrinogen, which would spontaneously and irreversible cyclised to the symmetric toxic uroporphyrinogen I (uro'gen I; Battersby *et al.*, 1979). This hypothesis is supported by the fact that the two encoding genes (*hemC* and *hemD*) are organised in the same operon in many so far examined bacteria. Thus, a coproduction of the enzymes are preventing the formation of uro'gen I (Figure 1.9; Jordan and Warren, 1987; Jordan and Woodcock, 1991). On the one hand uroporphyrinogen III methyltransferase would not be able to form the precursor dihydrosirohydrochlorin for corronoids, sirohaem, haem d_1 and coenzyme F_{430}. On the other hand coproporphyrinogen III, the precursor for haem, chlorophyll and bacteriochlorophyll, can not be formed by the

uroporphyrinogen III decarboxylase. Uro'gen I can be metabolised by uroporphyrinogen III decarboxylase but this leads to an accumulation of the toxic coproporphyrinogen I. To date, there is no evidence of substrate channelling or complex formation between PBGD and UROS *in vivo* as it was verified for the last two biosynthesis enzymes, protoporphyrinogen IX oxidase and ferrochelatase in *T. elongatus* (Masoumi *et al.*, 2008).

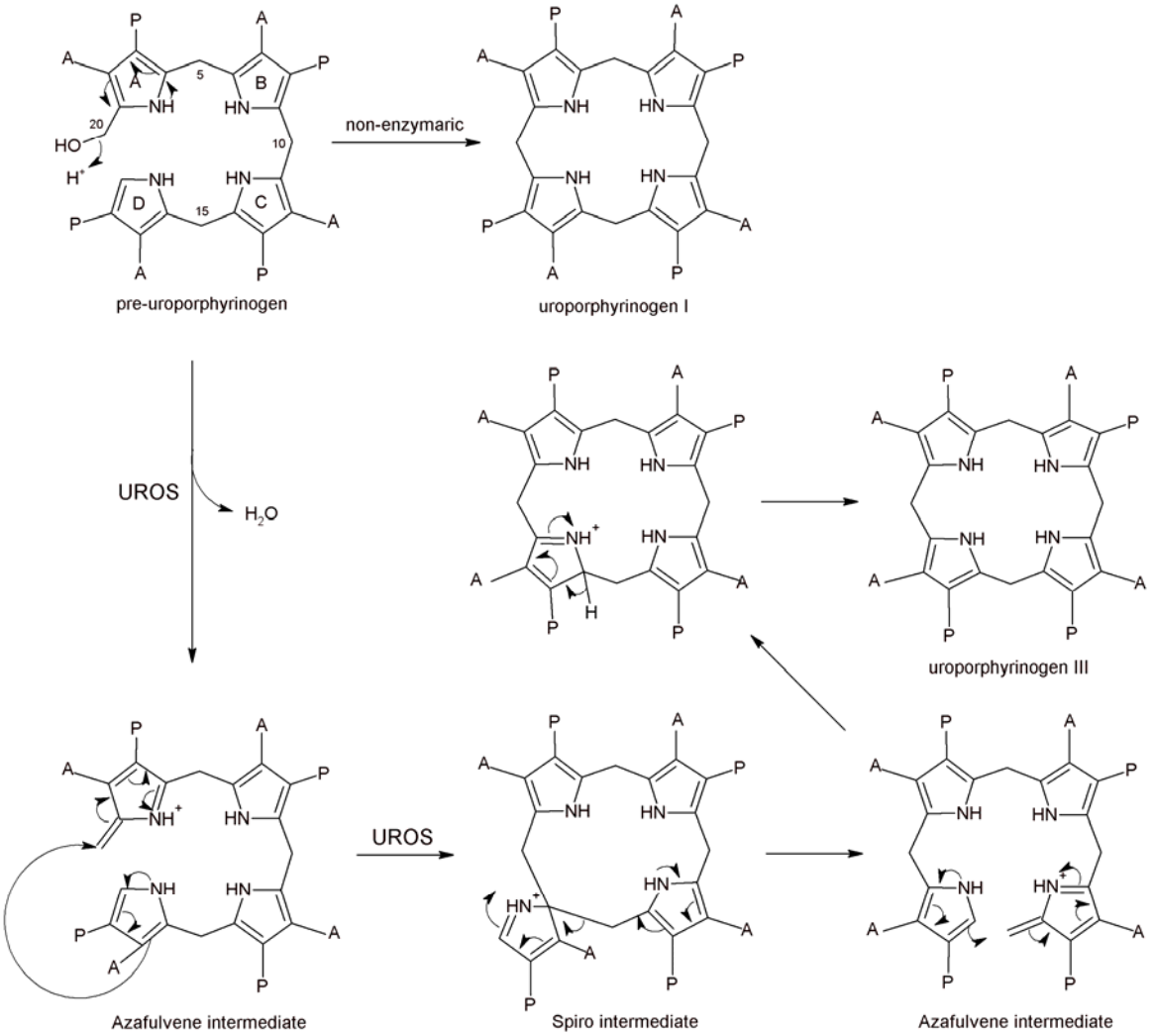

Figure 1.9: The spiro mechanism of the uroporphyrinogen III synthase.

Pre-uroporphyrinogen is cyclised via an azafluvene and spiro intermediate to uroporphyrinogen III by uroporphyrinogen III synthase (UROS); at this the inversion of the D-pyrrole ring is important. Without UROS uroporphyrinogen III is non-enzymatically formed into the symmetric and toxic uroporphyrinogen I. A: acetyl side chain; P: propionate side chain (modified after Roessner *et al.*, 2002).

In nature the enzymatic cyclisation reaction of pre-uroporphyrinogen to uroporphyrinogen III (Figure 1.9) requires an isomerisation of the D-pyrrole ring

(Battersby and Leeper, 1990). At first a carbo-cation (Azafulvene intermediate) is formed by water elimination from the pre-uroporphyrinogen. A so called spiro intermediate occurs by the conjunction of the A-pyrrole ring carbon C1 and the carbon C16 of the D-pyrrole ring. Finally, uroporphyrinogen III is formed by inversion of the electrophilic addition with a cleavage between the C- and D-pyrrole ring and a following electrophilic substitution. The intermediate stability is guaranteed *via* free electron pairs of the nitrogen atoms in the C- and D-pyrrole ring which can be shifted into the ring system (Battersby *et al.*, 1978; Cassidy *et al.*, 1996; Chadwick and Ackrill, 1994; Crockett *et al.*, 1991).

1.5 Uroporphyrinogen III Decarboxylase

Uroporphyrinogen III decarboxylase (UROD) is a cytosolic enzyme which catalyses the conversion of uroporphyrinogen III to coproporphyrinogen III by decarboxylation of the four acetic side chains into methyl chains. In plants, bacteria and yeast, UROD must compete for uroporphyrinogen III with uroporphyrinogen III methylase, the first enzyme of the pathway to sirohaem and corrin biosynthesis. Both naturally occurring isomers of uroporphyrinogen (I & III) are substrates for UROD, but only coproporphyrinogen III can be ultimately converted to haem (Phillips and Kushner, 1999). There is a general interest in the enzyme since mutations in the corresponding gene cause the rare human disease porphyria cutanea tarda (Elder and Roberts, 1995).

UROD from several organisms has been investigated *e.g.* *Synechococcus elongatus* PCC 7942 (Saito *et al.*, 2008); *E. gracilis Z* (Juknat *et al.*, 1989); *Rhodobacter sphaeroides* (Jones and Jordan, 1993); rat liver (Smith and Francis, 1979); *S. cerevisiae* (Felix and Brouillet, 1990); *E. coli* (Nishimura *et al.*, 1993); *B. subtilis* (Fan *et al.*, 2007; Hansson and Hederstedt, 1992); *Plasmodium falciparum* (Nagaraj *et al.*, 2009); *Nicotiana tabacum* (Martins *et al.*, 2001a; Martins *et al.*, 2001b); *H. sapiens* (de Verneuil *et al.*, 1983; Phillips *et al.*, 1997; Romeo *et al.*, 1986) and *Gallus gallus* (Seki *et al.*, 1986). URODs subunits have a relative molecular weight of around 40'000. Except for human, tobacco and chicken URODs, whose structures reveal a homodimer, until now all others seem to be monomeric. To date all studies indicate that there is no requirement for

cofactors or prosthetic groups for enzymatic activity which mark UROD as a very unusual decarboxylase (de Verneuil *et al.*, 1980; de Verneuil *et al.*, 1983; Straka and Kushner, 1983). There are hypothetically 24 possible pathways between uroporphyrinogen III and coproporphyrinogen III involving up to 14 intermediates. Nevertheless, early studies revealed that at high substrate concentrations the decarboxylation sequence is random. However, at physiological substrate concentrations the reaction runs in a specific order starting at ring D followed in a clockwise direction with ring A, B and C. It has been demonstrated that the reaction is a biphasic process in which the first acetate group is removed at a faster rate than the remaining three (Jackson *et al.*, 1976; Jones and Jordan, 1993; Luo and Lim, 1993; Tomio *et al.*, 1970). The reaction mechanism is hardly understood. Because of lack of a cofactor, the enzyme itself has to be the proton donor. Comparisons of the amino acid sequences reveal a 10 % identity and 33 % similarity with a highly conserved stretch of residues like proline, glycine, histidine and arginine in all to date examined species.

The human structure shows many conserved residue clusters at the active site cleft including invariant amino acids like Arg37, Arg41, His339, Asp86, Tyr164 and Ser219 which probably function in substrate binding and catalysis (Whitby *et al.*, 1998). Inhibition, mutation and density-functional calculation studies exclude several amino acids and confirm that Asp86 or Arg37 play a direct role in catalysis (Silva and Ramos, 2005). The human dimer structure serves to make a deep cleft where the negative charged substrate is nestled in a lot of positively charged residues in the active centre. The crystal structure also indicates that the substrate and the intermediates are hydrogen bound to the enzyme by aspartate carboxyl oxygen linked to the pyrrole nitrogen. So it was proposed that Asp86 stabilises the pyrrole and the reactive Arg37, which is located in a very short distance to the pyrrole, successively protonates the pyrrole rings. To date no further biochemical attempts have been made to identify Arg37 or further amino acids as proton donor (Figure 1.10; Lewis and Wolfenden, 2008; Martins *et al.*, 2001a; Martins *et al.*, 2001b; Phillips *et al.*, 2003; Silva and Ramos, 2005; Whitby *et al.*, 1998; Wyckoff *et al.*, 1996). Recently, studies indicate that each UROD subunit is able to function independent as an active catalytically site and is able to perform all four decarboxylation steps on one substrate molecule. Reaction intermediates are rather released from the enzyme then shuttled to the partner active site for the

next step in coproporphyrinogen III formation. The dimer formation seems to be important for UROD folding and conformation stability (Phillips *et al.*, 2009).

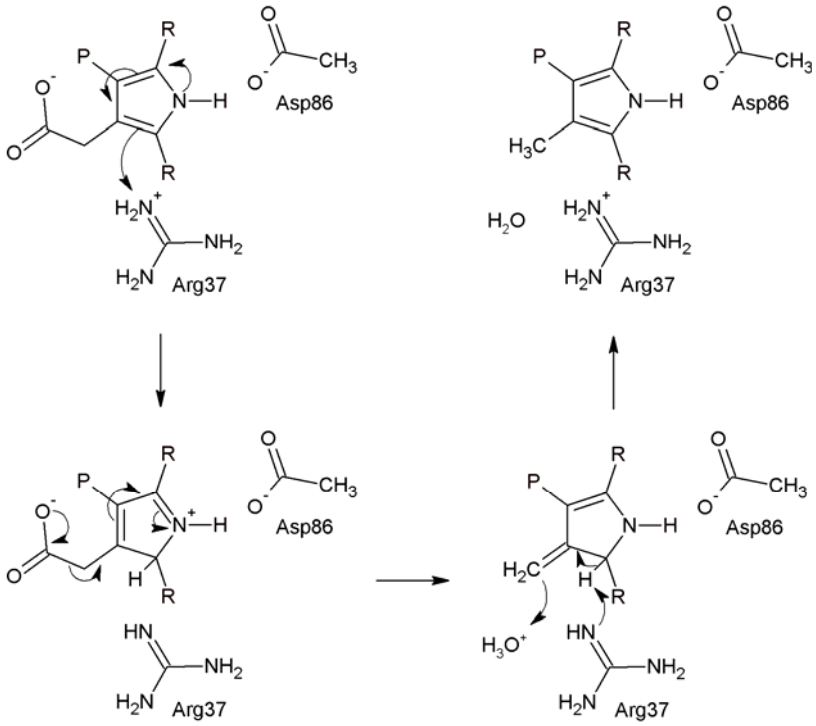

Figure 1.10: Proposed reaction mechanism for uroporphyrinogen III decarboxylase.

The acetate side chains of uroporphyrinogen III are converted into methyl groups by uroporphyrinogen III decarboxylase. To date it is proposed that in the active centre Arg37 serves as H^+ donor to the Asp86-stabilised substrate. R = tetrapyrrole; P = propionate side chain (modified after Lewis and Wolfenden, 2008; Silva and Ramos, 2005)

1.6 Coproporphyrinogen III Oxidase

Coproporphyrinogen III oxidase is the sixth enzyme in the tetrapyrrole biosynthesis. It catalyses an oxidative decarboxylation which results in a conversion of the propionate side chains of ring A and B of coproporphyrinogen III to the corresponding vinyl groups to yield protoporphyrinogen IX. Two molecules CO_2 are released during the reaction and a final electron acceptor is required to take up two electrons from each side chain (Figure 1.11).

In nature two different types of enzymes are found: the oxygen-dependent form encoded by *hemF* and the oxygen-independent enzyme encoded by *hemN*. Both share no obvious amino acid sequence identity which indicates an independent evolution.

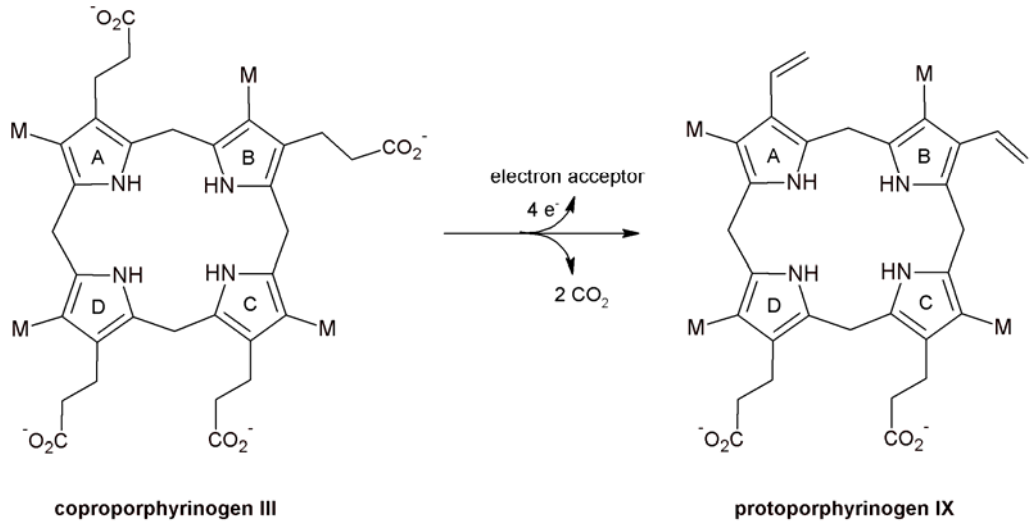

Figure 1.11: The oxidative decarboxylation of coproporphyrinogen III to protoporphyrinogen IX.

Coproporphyrinogen III is oxidatively decarboxylated to protoporphyrinogen IX whereby the propionate side chains of ring A and B are converted into the corresponding vinyl groups. Two molecules CO_2 are released during the reaction and a final electron acceptor is required to take up four electrons from the modified side chains. M = methyl group (modified after Layer *et al.*, 2006)

Oxygen-dependent coproporphyrinogen III oxidase (HemF) is principally found in eukaryotes, only some bacteria possess the *hemF* gene (Panek and O'Brian, 2002). The enzyme has been investigated from several organisms like yeast (Zagorec *et al.*, 1988), mammals (Kohno *et al.*, 1993; Martasek *et al.*, 1994), plants (Madsen *et al.*, 1993), *S. typhimurium* (Xu and Elliott, 1993) as well as *E. coli* (Troup *et al.*, 1994). The amino acid sequences from different organisms are highly conserved. HemF is a homodimer of two identical subunits carrying different metal ions *e.g.* manganese in *E. coli*, copper in mouse and iron in yeast. In contrast, the human structure was shown to be metal free. Molecular oxygen is required as terminal electron acceptor which results in a release of carbon dioxide (Breckau *et al.*, 2003; Kohno *et al.*, 1996; Labbe *et al.*, 1985; Medlock and Dailey, 1996; Phillips *et al.*, 2004). Early studies revealed that the propionate on ring A is decarboxylated prior to that on ring B (Jackson *et al.*, 1980a; Jackson *et al.*, 1980b). However, the mechanism is poorly understood and several proposals had been made (Lash, 2005; Lee *et al.*, 2005; Silva and Ramos, 2008).

Most bacteria utilise the oxygen-independent coproporphyrinogen III oxidase (HemN). Activity under anaerobic conditions was first described in cell free extract from *R. sphaeroides* with a complex mixture of cofactors like $NADP^+$, NADH, $MgSO_4$, L-methionine, ATP and *S*-adenosyl-*L*-methionine (SAM; Tait, 1969,

1972). Since then, *hemN* genes from several bacteria have been cloned and sequenced *e.g. S. typhimurium*, *E. coli*, *R. sphaeroides*, *Alcaligenes eutrophus* and *B. subtilis*. Furthermore, a HemN like enzyme was described in *B. subtilis*. The so called HemZ has an amino acid homology to HemN and has been proposed to be involved into an oxygen-independent reaction (Coomber *et al.*, 1992; Homuth *et al.*, 1999; Lieb *et al.*, 1998; Troup *et al.*, 1995; Xu and Elliott, 1994). HemN belongs to the family of radical SAM enzymes (Layer *et al.*, 2002; Sofia *et al.*, 2001). The crystal structure of *E. coli* HemN revealed a monomer which contains a catalytical essential [4Fe-4S] cluster coordinated by a conserved amino acid motif which consists of three cysteine residues (Layer *et al.*, 2003). The enzyme requires additionally SAM for catalysis (Figure 1.12).

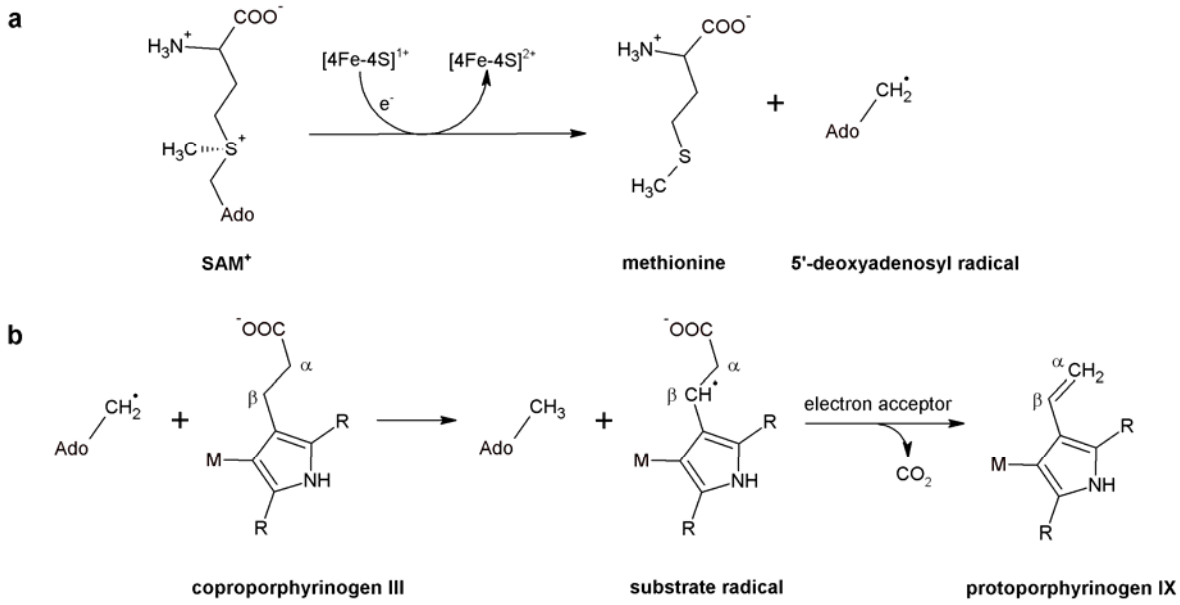

Figure 1.12: The proposed oxidative decarboxylation of coproporphyrinogen III to protoporphyrinogen IX by HemN.

(a) The *S*-adenosyl-*L*-methionine (SAM) cleavage reaction catalysed by radical SAM enzymes. The reduced [4Fe-4S] cluster is used for the homolytic cleavage of SAM to yield methionine and a catalytically active 5'-deoxyadenosyl radical (Ado). (b) The proposed reaction mechanism for the HemN reaction. The adenosyl radical (Ado) is proposed to abstract a hydrogen atom from the β-carbon of the coproporphyrinogen III propionate side chains resulting in the formation of a substrate radical. Release of CO_2 and uptake of the remaining electron by an external electron acceptor leads to protoporphyrinogen IX formation. M = methyl groups; R = tetrapyrrole (modified after Layer *et al.*, 2006).

HemN uses the iron-sulphur cluster to transfer an electron from an electron donor such as ferredoxin to SAM. Thereby, methionine and a 5-desoxyadenosyl radical is produced (Layer *et al.*, 2002; Layer *et al.*, 2005). The 5-desoxyadenosyl radical

then abstracts a hydrogen atom from the β-carbon of substrate propionate side chain resulting in the formation of a coproporphyrinogenyl radical and 5'-deoxyadenosine (Layer *et al.*, 2006). Finally, decarboxylation and transfer of a remaining single electron to a yet unidentified final electron acceptor leads to formation of the corresponding vinyl group of reaction product (Figure 1.12). This reaction has to pass through twice. Recently, it could be shown that HemN decarboxylates the propionate of ring A prior to ring B (Rand *et al.*, 2010).

1.7 Disorders in Tetrapyrrole Biosynthesis Lead to Diseases

Tetrapyrroles are essential cofactors in most archaea, bacteria and eukaryotes. Perturbation in the biosynthesis pathway causes diverse dysfunctions and damages to the cells. The tetrapyrrole biosynthesis is subjected to strict regulation mechanism. In plants, perturbation of tetrapyrrole anabolism induces cell damage based on accumulation of photoreactive chlorophyll intermediates, which can result in a reduced photosynthesis capacity (Lermontova *et al.*, 1997; Mock and Grimm, 1997; Mock *et al.*, 1999). In humans, haem is synthesised in every cell for respiratory and oxidation-reduction reactions. A variety of gene mutations concerning the synthesis enzymes cause rare heterogeneous metabolic disorders commonly known as porphyrias (Roehl *et al.*, 1998). Porphyrias manifest with broad range of cutaneous symptoms and/or acute neurological attacks because of the synthesis intermediates toxicity. Depending on their solubility, the overproduced porphyrins and porphyrin precursors accumulate and are excreted in urine and stool. Cutaneous photosensitivity is a result of the production of free radicals when porphyrins, like uro-, copro- and protoporphyrinogen, deposited in the skin are exposed to ultraviolet light at a wavelength of approximately 400 nm (Sandberg and Romslo, 1981; Wood *et al.*, 1995). Neurovisceral symptoms are believed to result from neurotoxicity of 5-aminolaevulinic acid and porphobilinogen. Usually, haem production in the cells is controlled *via* negative feedback regulation of the 5-aminolaevulinic acid synthase activity by haem (Fraser *et al.*, 2002; Thunell, 2006) and by iron availability in the erythropoietic cells (Smith and Cox, 1997). Except for porphyria cutanea tarda (PCT), all types of porphyria show an autosomal inheritance pattern. PCT is the most common type which is caused by

uroporphyrinogen III decarboxylase (HemE) deficiency. Twenty five percent of the PCT cases are classified as familial type which results from an autosomal-dominant inheritance with a 50 % enzyme activity deficit in all tissues. The remaining 75 % are described as acquired sporadic type whereby enzymatic deficiency is exclusively expressed in liver. Trigger factors like alcohol abuse, haemodialysis, iron overload, oestrogen and viral infections have been described to initiate this PCT type (Kauppinen, 2005; van Serooskerken *et al.*, 2010).

1.8 Aim of This Study

Several open questions related to various steps of haem biosynthesis in humans and bacteria should be investigated in the cause of this thesis.

Recently newly density-functional studies of the mechanism for the cofactor-free decarboxylation performed by human uroporphyrinogen III decarboxylase revealed new potential arginine residues of the enzyme active site which may serve as proton donor for catalysis. In order to investigate the influence of these highly conserved arginine residues (R37 and R41) for decarboxylation, mutant variants of UROD were generated and biochemically characterised. The determination of kinetic parameters was aimed to resolve their contribution for catalysis.

The second objective of this work was to study interactions and the existence of protein complexes of different enzymes involved in early steps of tetrapyrrole biosynthesis in *T. elongatus*. For this purpose, the *T. elongatus* genes coding for HemB, HemD, HemE and HemN should be cloned into expression vectors and their encoded proteins recombinantly produced. Subsequently, antibodies were aimed to be generated directed against the purified recombinant proteins. Finally, these antibodies should provide the basis for coimmunoprecipitation and electron microscopic experiments in order to prove the existence of interaction and complex formation *in vitro* as well as *in vivo.*

2 MATERIALS AND METHODS

2.1 Instruments and Chemicals

2.1.1 Instruments

Agarose gel electrophoresis	Agagel	Biometra
Agarose gel documentation	GelDoc	Bio-Rad
Anaerobic chamber	MACS-MG-1000 anaerobic workstation	DW Scientific
Autoclave	LVSA 50/70	Zirbus
Blotting equipment	Semidry-Blot Trans-Blot®SD	BioRad
Centrifuges	5804	Eppendorf
	Minispin	Eppendorf
	Biofuge primoR	Heraeus
	Avantis®J-26XP	Beckmann Coulter
	RC 5B Plus	Sorvall
	Qik Spin QS 7000	Edwards Instruments
	Speed Vac SPD 110B	Savant
DNA sequencing	Genetic Analyzer ABI Prism™ 310	Applied Biosystems
Electrophoresis power supply	PowerPac 300	BioRad
FPLC	Äkta Purifier™ 900 series	Amersham Biosciences
French press	French® Pressure Cell Press	Amersham Biosciences
Homogenizer	FastPrep 24 Instruments	MP Biomedicals
HPLC	Jasco 1500 series	Jasco
pH-determination	pH Meter C 6840 B	Schott
Pipettes	Reference	Eppendorf
Scales	BL 1500	Sartorius
	BL 61S	Sartorius
	SBA 52	Scaltec
SDS-PAGE-system	Mini Protean II	Bio-Rad
Thermocycler	Tpersonal	Biometra
	Tgradient	Biometra
Thermomixer	Thermomixer compact	Eppendorf
Ultrasonic bath		Merck eurolab
Ultrasound device	Sonoplus HD 2070	Bandelin
UV/visible spectrophotometer	Ultrospec 2000	Amersham Biosciences
Vortex	Vortex-Genie 2	Scientific Industries
Water bath shaker	Aquatron	Infors AG
Water purification	Milli-Q System	Millipore

2.1.2 Chemicals and Kits

Antibodies	anti-His_6 (murine)	GE Healthcare
	anti-mouse (Fc-specific; goat) alkaline phosphatase conjugated	Sigma-Aldrich
	anti-GST (rabbit)	Sigma-Aldrich
	anti-rabbit (Fc-specific) ImmunoPure®Goat alkaline phosphatase conjugated	Pierce
Blotting material	Gel blotting Paper	Roth
	Roti-PVDF-membrane	Roth
Chemicals	5-aminolaevulinic acid	Merck
	Coproporphyrin III	Porphyrin Products
	Uroporphyrin III	Porphyrin Products
	Bicinchoninic Acid Kit for Protein Determination	Sigma – Aldrich
	Complete Mini, protease inhibitor cocktail tablets	Roche
Enzymes	Phusion™ DNA Polymerase	Finnzymes
	Benzonase® Nuclease	Novagen
	T4 DNA Ligase	New England Biolabs
	Restriction enymes	New England Biolabs
Kits	BigDye Terminater v1.1 Cycle Sequencing Kit	Applied Biosystems
	QIAquick Gel Extraction Kit	Qiagen
	QIAquick PCR Purification Kit	Qiagen
	QuikChange®II Site-Directed Mutagenesis Kit	Stratagene
Molecular weight standards	GeneRuler™ DNA Ladder Mix	MBI Fermentas
	MassRuler™ DNA Ladder Mix	MBI Fermentas
	PageRuler™ Prestained Protein Ladder	MBI Fermentas
	Unstained Protein Molecular Weight Marker	MBI Fermentas
PCR materials	Oligonucleotides	Metabion, Biomers
	Nucleotides (dNTPs)	Fermentas
Other materials	Dialysis VISKING, type 27/32 exclusion 14,000	Roth
	Glutathione sepharose 4 FF	GE Healthcare
	InstantBlue™	Expedeon
	Ni^{2+}-NTA column, HiTrap™Chelating HP	Amersham Biosciences
	Steril filter (0.2 µm)	Millipore
	Vivaspin concentrator	Vivascience

Chemicals and reagents not specifically listed were purchased from the following manufacturers: Amersham Biosciences, Fluka, Gebru, Merck, Roth, Fisher Scentific and Sigma-Aldrich.

2.2 Strains and Plasmids

All strains and plasmids used for this work are listed in Table 1 and Table 2.

Table 1: Employed bacterial strains.

Strains	Description	Reference
Escherichia coli DH10β	F⁻*mcr*A Δ(*mrr-hsd*RMS-*mcr*BC) Φ80*lac*ZΔM15 Δ*lac*X74 *rec*A1 *end*A1 *ara*Δ139 Δ(*ara*,*leu*)7697 *gal*U *gal*K λ⁻ *rps*L (*str*^{R}) *nup*G	Invitrogen
Escherichia coli BL21(DE3)RIL	F⁻ *omp*T *hsd*S($r_B^-m_B^-$) *dcm*$^+$ *tet*^{R} *gal*λ(DE3) *end*A Hte[*arg*U *ile*Y *leu*W *cm*^{R}]	Stratagene
Escherichia coli BL21(DE3)pLysS	F⁻ *omp*T *hsd*S($r_B^-m_B^-$) *dcm*$^+$ *gal*λ(DE3) [pLysS *cm*^{R}]	Stratagene
Escherichia coli Rossetta (DE3)pLysS	F⁻ *omp*T *hsd*S_B($r_B^-m_B^-$) *dcm*$^+$ *gal* (DE3) [pLysSRARE *cm*^{R}]	Novagen
Escherichia coli Rosetta gami 2 (DE3)	Δ(*ara-leu*)7697 Δ*lac*X74 Δ*pho*A P*vul*l *pho*R *ara*D139 *ahp*C *gal*E *gal*K *rps*L (DE3) F[*lac*$^+$ *lacI*^{q} *pro*] *gor*5*22*::Tn*10* *trx*B pRARE2 (*cm*^{R}, *str*^{R}, *tet*^{R})	Novagen
Thermosynechococcus elongatus BP-1	wild type	Yamaoka *et al.*, 1978
Bacillus megaterium MS941	Δ*npr*M mutant of wild type strain *B. megaterium* DSM319	Wittchen and Meinhardt, 1995

Table 2: Plasmids used in this study.

Plasmid	Description	Reference
pET32a	Expression vector carrying C-terminal His-Tag® and S-tag sequence, T7 promotor, *amp*^{R}	Novagen
pGEX-6P-1	Expression vector carrying N-terminal sequence for GST from *Schistosoma japonicum* and recognition sequence from PreScission™ Protease, *lac* promoter, *amp*^{R}	Amersham Biosciences

Table 2 (continued): Plasmids used in this study.

Plasmid	Description	Reference
pHT#77	pAED4 derivate encoding human UROD, *amp*^{R}	Phillips *et al.*, 1997
pHT#77-R37A	pHT#77 with exchange of triplet CGC (nucleotides 109-111) to GCC, protein carries alanine instead of arginine	this work
pHT#77-R37K	pHT#77 with exchange of triplet CGC (nucleotides 109-111) to AAA, protein carries lysine instead of arginine	this work
pHT#77-R41A	pHT#77 with exchange of triplet CGA (nucleotides 121-123) to GCC, protein carries alanine instead of arginine	this work
pHT#77-R41K	pHT#77 with exchange of triplet CGA (nucleotides 121-123) to AAA, protein carries lysine instead of arginine	this work
pGA15hemD_T._elongatus	pGA15 derivate encoding *T. elongatus* UROS with optimised codon usage for intracellular production of protein in *B. megaterium*, *kan*^{R}	GeneArt AG
pN-HIS-TEV1622	pSTOP1622 derivate; vector for intracellular production of N-terminal His_6-tagged proteins in *B. megaterium*; P_{xylA}-His_6-Tag-TEV-MCS-Stop, *tet*^{R}*, B. megaterium; amp*^{R}*, E. coli*	Biedendieck *et al.*, 2007
pKMBm4	pSSBm44 derivate; vector for intracellular production of proteins in *B. megaterium*; *tet*^{R}*, B. megaterium; amp*^{R}*, E. coli*	Stammen *et al.*, 2010
pN-HIS-TEV1622-hemD	pN-HIS-TEV1622 derivate encoding UROS from *T. elongatus* with optimised codon usage for intracellular production of protein in *B. megaterium*	this work
pKMBm4-hemD	pKMBm4 derivate encoding UROS from *T. elongatus* with optimised codon usage and additional N-terminal His_6-tagged for intracellular production of protein in *B. megaterium*	this work
pET32a-TEhemB	pET32a derivate encoding PBGS from *T. elongatus*	this work
pGEX6P-1hemD	pGEX-6p-1 derivate encoding UROS from *T. elongatus*	Frese, 2008

Table 2 (continued): Plasmids used in this study.

Plasmid	Description	Reference
pET32a-TEhemE	pET32a derivate encoding UROD from *T. elongatus*	this work
pGEX-TEhemN	pGEX-6p-1 derivate encoding CPO from *T. elongatus*	this work

2.3 Growth Media and Media Additives

2.3.1 Growth Media

As a standard medium for growth of all *Escherichia coli* and *Bacillus megaterium* strains Luria Bertani (LB) medium was used (Sambrook and Russell, 2001), unless indicated otherwise. All strains were grown at 37 °C and 200 rpm.
All media were autoclaved for 20 min at 121 °C. For solid media 15 g/L agar-agar was added before sterilisation.

LB-Medium	tryptone	10 g/L
	NaCl	5 g/L
	yeast extract	5 g/L
	in $H_2O_{dest.}$	

2.3.2 Media Additives

Antibiotics and other additives were prepared as concentrated stock solutions, sterilised by filtration and added to the sterile medium. Stock solutions were stored at -20 °C. Solutes and concentrations are summarised in Table 3.

Table 3: Media Additives

Substance	Solute	Concentration of stock solution	Final concentration
Ampicillin	H_2O_{dest}	100 mg/mL	100 µg/mL
Chloramphenicol	70 % ethanol (v/v)	34 mg/mL	34 µg/mL
Tetracycline	70 % ethanol (v/v)	5 mg/mL	5-10 µg/mL
Isopropyl-1-thio-ß-D-galactopyranoside (IPTG)	H_2O_{dest}	1 M	100-400 µM
Xylose	H_2O_{dest}	50 % (w/v)	0.5 % (w/v)

2.4 Microbiological Techniques

2.4.1 Sterilisation

All media, solutions and glass equipments were vapour sterilised at 121 °C and 1 bar positive pressure for 20 min. Temperature sensitive solutions were sterilised by filtration (pore width 0.2 µm).

2.4.2 Cultivation of Bacteria

Precultures (volume 5 up to 200 mL) of *E. coli* strains containing appropriate plasmids were grown in LB (with required additives) overnight at 37 °C and 200 rpm in baffled flasks. After inoculation with preculture (1:100), 500 mL cultures were grown at 37 °C to an OD_{578} of 0.6. Protein production was induced with indicated amounts of Isopropyl-1-thio-ß-D-galactopyranoside (IPTG). After induction, cultures were incubated at 25 °C for 6 h or overnight.
100 mL precultures of *B. megaterium* MS941 were grown in LB with tetracycline (10 µg/mL) at 100 rpm and 37 °C overnight. 250 mL cultures for protein production, inoculated with preculture (1:100), were grown at 37 °C until induction of protein production with 0.5 % (w/v) xylose.
Agar plates were either utilized for plating 50-100 µL of bacterial cell suspension with a Drigalski spatula, or for streaking cells with an inoculating loop with liquid culture or with a single colony. Plates were incubated at 37 °C overnight.

2.4.3 Determination of Cell Density

The cell density of liquid cultures was determined by measuring the optical density (OD_λ) at a wavelength of 578 nm. An OD_{578} of 1 corresponds to approximately 1×10^9 *E. coli* cells per millilitre.

2.4.4 Storage of Bacterial Strains

E. coli strains were stored on agar plates at 4 °C for up to four weeks and *B. megaterium* for up to 10 days, respectively. To prevent dehydration the plates were sealed with Parafilm®. For long-term storage glycerol stocks were prepared. Therefore, 0.4 mL overnight cultures were mixed with 1.2 mL sterile glycerol (80 % (v/v)), cooled on ice for 30 min, immediately frozen and stored at -80 °C.

2.5 Molecular Biology Techniques

2.5.1 Preparation of DNA

2.5.1.1 Genomic DNA

Thermosynechococcus elongatus BP-1 cells were provided by Frederike Frese (Frese, 2008). After harvesting by centrifugation (5 min at 7,000 x *g*), cells were washed once in TE buffer and suspended in 4 mL lysis buffer A supplemented with 0.2 mg/mL RNase A and 50 µg lysozyme. The samples were incubated at 37 °C for 45 min. After addition of 500 µL N-laurosylsarcosinine (20 % (w/v)) and further incubation for 5 min at 37 °C the suspension was mixed with one volume of phenol and incubated under constant motion for 30 min at room temperature (RT). After subsequent centrifugation (20 min at 7,000 x *g*), the upper aqueous phase was transferred into a fresh tube and submitted to 4 mL phenol/chloroform/isoamylalcohol (24:24:1). Following 15 min of incubation, samples were centrifuged again and the phenol-chloroform extraction was repeated. The upper aqueous phase of this step was transferred into a fresh tube and DNA precipitation was initiated by addition of 10 mL pure ice cold ethanol and 500 µL of a 3 M sodium acetate solution (pH 4.8). The sample was centrifuged for 30 min (7,000 x *g* and 4 °C) and the DNA was washed twice with 500 µL 70 % (v/v) ethanol. After evaporation of residual ethanol, the DNA was solubilised in 200 µL TE buffer and stored at 4 °C.

Lysis buffer A	NaCl	100 mM
	EDTA	50 mM
	in H_2O_{dest}; pH 8.0	

TE buffer	Tris-HCl	10 mM
	EDTA	1 mM
	in H_2O_{dest}; pH 8.0	

2.5.1.2 Plasmid DNA (Mini Prep)

Four mL of an *E. coli* DH10β overnight culture were harvested by centrifugation (5 min at 14,000 x *g*). The sedimented cells were suspended in 300 µL of buffer P1. For cell lyses 300 µL of buffer P2 were added, carefully mixed by inverting the tube and incubated for 5 min at room temperature (RT). After addition of 300 µL of buffer P3 the sample was mixed carefully again and incubated on ice for 5 min. Cell debris and degraded proteins were sedimented by centrifugation (15 min at 14,000 x *g*). 600 µL of supernatant were transferred to 600 µL isopropanol into a fresh tube, incubated for 10 min at RT and centrifuged (30 min at 14,000 x *g*). The sedimented plasmid DNA was washed twice with 70 % (v/v) ethanol. After all traces of ethanol had evaporated, the DNA was solubilised in 50-100 µL H_2O_{dest}.

Buffer P1	Tris-HCl	50 mM
	EDTA	10 mM
	RNase A	100 mg/L
	in H_2O_{dest}; pH 8.0	
Buffer P2	NaOH	200 mM
	sodium dodecyl sulfate (SDS)	1 % (w/v)
	in H_2O_{dest}	
Buffer P3	potassium acetate	3 M
	in H_2O_{dest}; pH 5.5 adjusted with acetic acid	

2.5.2 Determination of DNA Concentration

The concentration of a DNA solution was determined by measuring the absorbance at 260 nm and additionally at 280 nm to account for protein impurities. For a pure DNA solution an OD_{260} of one corresponds to a dsDNA concentration of 50 µg/mL (Sambrook and Russell, 2001). The purity of the DNA solution can be deduced from the ratio of OD_{260} to OD_{280}. With an OD_{260}/OD_{280} ratio of 1.8-2.0 the DNA was considered as pure.

2.5.3 Agarose Gel Electrophoresis

For the analytical separation of DNA fragments, agarose gels consisting of 1 % (w/v) agarose in TAE buffer were prepared. Depending on the gel size, a voltage of 90-110 V was applied. DNA fragments migrate towards the anode with a velocity that is proportional to the negative logarithm of their size. Prior to loading, DNA samples were mixed with loading dye to facilitate loading and to indicate the progress of the samples in the gel. GeneRuler™ DNA Ladder Mix and MassRuler™ DNA Ladder Mix were used as size standard according to the manufacturer's manual (Fermentas). After electrophoresis, gels were incubated in an ethidium bromide solution for 15-30 min and DNA was detected *via* its fluorescence under UV light (λ = 312 nm).

TAE buffer	Tris-acetate	40 mM
	EDTA	1 mM
	in H_2O_{dest}; pH 8.0	
DNA loading dye (5x)	bromphenol blue	0.35 mM
	xylene cyanol FF	0.45 mM
	orange G	0.25 mM
	glycerol	20 % (v/v)
	in H_2O_{dest}	
Ethidium bromide	ethidium bromide	0.1 % (v/v)
	in H_2O_{dest}	

2.5.4 Cloning of DNA

2.5.4.1 Amplification of DNA by Polymerase Chain Reaction (PCR)

For amplification of haem genes involved in the haem biosynthesis of *T. elongatus* by PCR, oligonucleotide primers were designed with additional recognition sequences for restriction endonucleases. Oligonucleotides primers are listed in Table 4. Recognition sequences of restriction endonucleases are underlined.

Table 4: Oligonucleotide primers used for amplification of DNA fragments.
"for" refers to forward and "rev" to reverse primer. Restriction sites are underlined

Primer designation	Sequence of oligonucleotide primer (5'→ 3')	Additional information
hemBEcoR1for	CGCCCGGAATTCATGGAGCTAACC	*Eco*RI restriction site
hemBNot1rev	TTGCGGCCGCATAGTTCAATCCC	*Not*I restriction site
TE_hemE_EcoR1for	CCCCGGAATTCATGACCACCC	*Eco*RI restriction site
TE_hemE_Not1rev	TTGCGGCCGCATTAGGCGAGG	*Not*I restriction site
TE_hemN_EcoR1for	CCCCGGAATTCATGAGTGTGGTTC	*Eco*RI restriction site
TE_hemN_Not1rev	CTATTGCGGCCGCACTAAATGGCCTTAG	*Not*I restriction site

Phusion™ DNA polymerase (Finnzymes) was used for all reactions. PCR was performed in a total volume of 50 µL. After an initial DNA denaturation step, a cycle consisting of the three steps denaturation, primer annealing and primer elongation was completed 30 times. The reaction terminated by a final elongation step. The denaturation temperature of 98 °C and the elongation temperature of 72 °C remained unchanged. The annealing temperature depended on oligonucleotide length and G+C content and was furthermore influenced by the insertion of mismatches. The melting temperature (T_m) was calculated as followed:

$$T_m\ [°C] = 69.3 + 0.41(\%\ G+C) - 650/n$$

% G+C represented the G+C content of the primer in % and n represented the number of nucleotides.

The duration of the elongation step was chosen according to the length of the DNA fragment to be amplified according to the manufacturer's manual.

Standard thermocycler program for Phusion™ DNA polymerase:

denaturation	98 °C	5 min	
denaturation	98 °C	30 sec	30x
annealing	60-70 °C	30 sec	
elongation	72 °C	30 sec/kb	
elongation	72 °C	10 min	

2.5.4.2 Restriction of DNA

Restriction of DNA (vector and PCR products) was carried out using restriction endonucleases purchased from New England Biolabs (Frankfurt am Main, Germany). Reaction buffers, concentrations of enzymes and DNA as well as incubation temperatures were chosen according to the manufacturer's manual. The digestion was allowed to proceed for 5-6 h and was, if possible, followed by heat inactivation of the restriction endonucleases (20 min at 65 °C or 80 °C, depending on the enzyme).

2.5.4.3 Purification of DNA

For removal of polymerase, buffer and unbound nucleotides after amplification of DNA by PCR, the resulting PCR products were purified using the QIAquick® PCR Purification Kit (Qiagen; Hilden, Germany). Restriction endonucleases and buffer were removed from digested DNA (vector and PCR products) by agarose gel electrophoresis. The DNA fragment was excised from the gel and purified using the QIAquick® Gel Extraction Kit (Qiagen; Hilden, Germany). All kits were used according to the manufacturer's manual.

2.5.4.4 Ligation of DNA

Ligation of DNA was carried out using T4 DNA ligase (New England Biolabs; Frankfurt am Main, Germany) according to the manufacturer's manual. An amount of 25-50 ng vector DNA was mixed with insert DNA (insert to vector ratio with regard to molar concentration ~ 5:1) in a final volume of 10 µL. Moreover, control reactions in the absence of ligase or insert were carried out. The reaction was incubated for 2 h at RT or at 17 °C overnight.

2.5.5 Site-Directed Mutagenesis of DNA

Single amino acids in a protein of interest can be exchanged by site-directed mutagenesis into the DNA sequence of the corresponding gene. The QuikChange® II Site-Directed Mutagenesis Kit (Stratagene; Böblingen, Germany) was employed in this work for mutational analysis of human uroporphyrinogen III decarboxylase (UROD). The method utilises a dsDNA plasmid carrying the gene of interest and two synthetic oligonucleotide primers which contain the desired mutation (see Table 5) and are complementary to opposite strands of the vector. During PCR with *PfuUltra HF* DNA polymerase a mutated plasmid is generated (figure 2.1). The PCR product was treated with *Dpn*I, an endonuclease specifically digesting partially methylated DNA, here, the parental template DNA. This allows isolation of the newly *in vitro* synthesized unmethylated DNA of the mutated plasmid with which a suitable *E. coli* strain was subsequently transformed. PCR reactions with the QuikChange® II Site-Directed Mutagenesis Kit were carried out according to the manufacturer's manual. However, the volume of the PCR reaction was reduced to 25 µL. Compentent *E. coli* XL 1 Blue cells were transformed with the mutated plasmids.

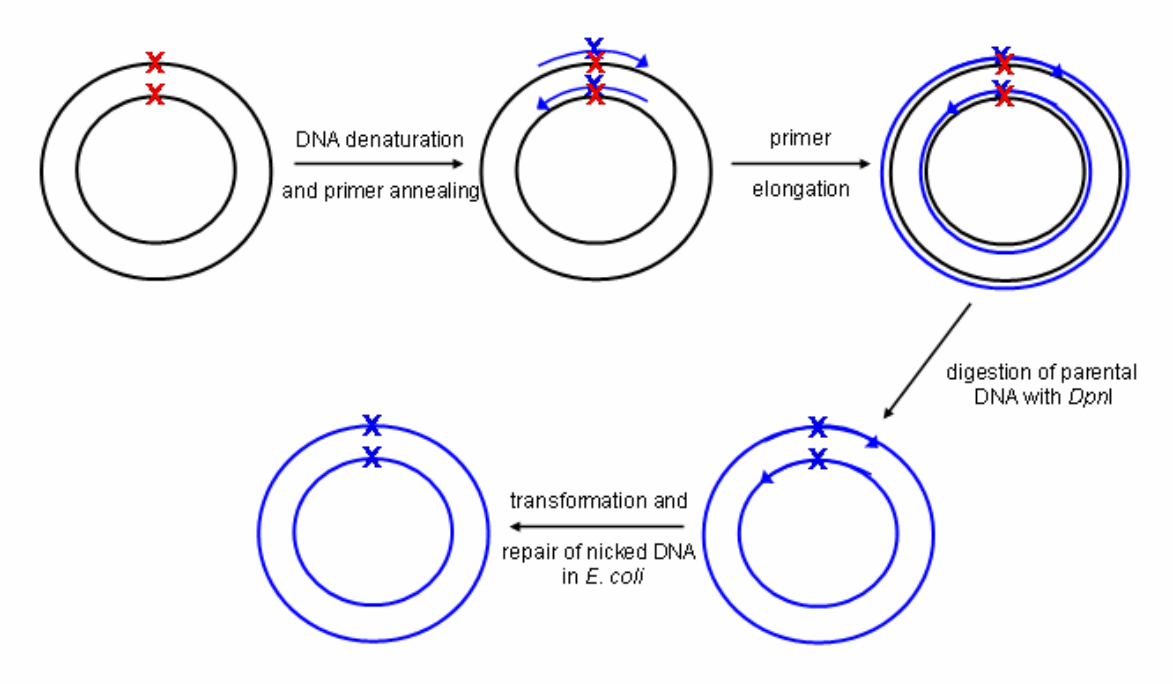

Figure 2.1: Outline of the QuikChange® Procedure.

Overview of the QuikChange® Site-Directed mutagenesis method (modified from Stratagene Instruction Manual, 2007) **—** parental DNA, — mutated DNA, X position of the desired mutation, → mutagenic primer, X introduced mutation. A detailed description is given in the text.

Table 5: Oligonucleotide primers used for site-directed mutagenesis of human uroporphyrinogen III decarboxylase.
"for" refers to forward and "rev" the reverse primer. Changed nucleotides are underlined

Primer designation	Sequence of oligonucleotide primer (5'→ 3')
R37Afor	GTTTGGTGCATGGCCCAGGCAGGCCG
R37Arev	CGGCCTGCCTGGGCCATGCACCAAAC
R37Kfor	GTTTGGTGCATGAAACAGGCAGGCCG
R37Krev	CGGCCTGCCTGTTTCATGCACCAAAC
R41Afor	CGCCAGGCAGGCGCCTACTTACCAGAG
R41Afrev	CTCTGGTAAGTAGGCGCCTGCCTGGCG
R41Kfor	CGCCAGGCAGGCAAATACTTACCAGAG
R41Krev	CTCTGGTAAGTATTTGCCTGCCTGGCG

2.5.6 Transformation of Bacteria

2.5.6.1 Transformation of *Escherichia coli* Cells by the $RbCl_2$ Method

E. coli cells were grown in 500 mL LB with required additives under aeration. When the culture obtained an OD_{578} of 0.6 cells were harvested by centrifugation (10 min at 6,000 x *g* and 4 °C), subsequently gently suspended in 200 mL ice cold TFB1 and incubated on ice for 5 min. Once more the cells were harvested (5 min at 3,000 x *g* and 4 °C) and suspended in 2 volumes of ice cold TFB2 (referring to the volume of cell sediment), incubated on ice for 45 min and divided into 50 µL aliquots. These were either immediately used for transformation or stored at -80 °C.

For transformation, 40 µL $RbCl_2$-competent cells were combined with 1-2 µL DNA solution (50 µg/mL) and incubated for 30 min on ice. Afterwards the transformation mix was subjected to a heat shock for 45 sec at 42 °C and cooled on ice for 3 min. One mL of preheated LB medium was added and cells were incubated at 37 °C for 45 min. Depending on the expected colony density, different volumes were streaked on agar plates containing the appropriate antibiotics. Plates were incubated overnight at 37 °C.

TFB1	potassium acetate	30 mM
	$CaCl_2$	10 mM
	$MnCl_2$	50 mM
	$RbCl_2$	100 mM
	glycerol	15 % (v/v)
	in H_2O_{dest}; pH 5.8 adjusted with acetic acid	
TFB2	MOPS	10 mM
	$CaCl_2$	75 mM
	$RbCl_2$	10 mM
	glycerol	15 % (v/v)
	in H_2O_{dest}; pH 6.5 adjusted with potassium hydroxide	

2.5.6.2 Protoplast Transformation of *Bacillus megaterium* Cells

The *B. megaterium* MS941 protoplasts were provided by Simon Stammen (Institut für Mikrobiologie, TU Braunschweig, Germany). For transformation of the protoplasts, 5 µg plasmid DNA were dried and dissolved in 10 µL SMMP for 20 min at 37 °C. A 500 µL aliquot of protoplasts was gently mixed with the plasmid DNA and added to 1.5 mL PEG-P solution. After incubation for 2 min at RT, 5 mL SMMP were added and the reaction was gently mixed. The protoplasts were harvested by centrifugation (10 min at 1,300 x *g* and RT), subsequently the protoplast were carefully suspended in 500 µL SMMP and incubated at 30 °C for 45 min without shaking, followed by 45 min of smooth shaking at 300 rpm (Thermomixer compact). The regenerated protoplasts were mixed with 2.5 mL of 42 °C CR5-top agar and added on a preheated agar plate containing tetracycline (10 µg/mL). The plates were incubated at 30 °C for up to 24 h. Formed colonies were streaked out on new LB medium agar plates containing tetracycline (10 µg/mL).

SMMP	2 x AB3 and 2 x SMM; mixed 1 : 1		
2 x AB3	antibiotic medium No.3 (Difco)	35	g/L
2 x SMM	malic acid	40	mM
	$MgCl_2$	40	mM
	NaOH	80	mM
	sucrose	1	M
	in H_2O_{dest}; pH 6.5		
PEG-P solution	PEG 6000	40	% (w/v)
	in 1 x SMM		
C5R-top agar	solution A	1.25	mL
	solution B	713	µL
	8 x CR5-salts	288	µL
	L-proline (12 % (w/v))	125	µL
	D-glucose (20 % (w/v))	125	µL
Solution A	sucrose	602	mM
	MOPS	58	mM
	NaOH	30	mM
	in H_2O_{dest}; pH 7.3		

Solution B	agar agar	4	% (w/v)
	casamino acids	0.2	% (w/v)
	yeast extract	10	% (w/v)
	in H_2O_{dest}		
8 x CR5-salts	K_2SO_4	11	mM
	$MgCl_2$	394	mM
	KH_2PO_4	3	mM
	$CaCl_2$	159	mM
	in H_2O_{dest}		

2.5.7 DNA Sequencing

The modification of DNA (cloning as well as site-directed mutagenesis) was confirmed by sequence determination of the respective DNA region based on the Sanger method (Sanger *et al.*, 1977). DNA sequences were obtained with an Abi Prism™ 310 Genetic Analyzer (Applied Biosystems). The required preparatory PCR with fluorescence-labeled ddNTPs and purification of the PCR product were carried out as described by the manufacturer.

2.6 Protein Biochemical Methods

2.6.1 Recombinant Production and Purification of *Thermosynechococcus elongatus* Haem Proteins

2.6.1.1 Cell Growth for Protein Production

For recombinant production of haem proteins in *E. coli*, 2 x 500 mL LB medium containing ampicilin (100 µg/mL) and chloramphemicol (34 µg/mL) were inoculated (ratio 1:100) with an overnight culture of *E. coli* Rosetta gami2 (DE3) carrying pET32a-TEhemB for porphobilinogen synthase (PBGS) or pET32a-TEhemE for uroporphyrinogen III decarboxylase (UROD), respectively. *E. coli* Rosetta (DE3)pLysS carrying pGEX6P-1hemD was used for uroporphyrinogen III synthase (UROS) and pGEX-TEhemN for coproporphyrinogen III oxidase (CPO), respectively. Cultures were grown aerobically in 1 L Erlenmeyer flasks at 37 °C and 200 rpm to an OD_{578} of 0.6. The production of proteins was induced by

addition of IPTG to a final concentration of 400 µM. Incubation was continued overnight at 25 °C and 180 rpm. Cells were harvested by centrifugation for 15 min at 4,000 x *g* and 4 °C. The cell sediments were stored at -20 °C.
For recombinant production of proteins in *B. megaterium* MS941, carrying pN-HIS-TEV1622-hemD and pKMBm4-hemD, respectively, 100 mL precultures were inoculated by a single colony from a LB agar plate and grown in LB with tetracycline (10 µg/mL) at 100 rpm and 37 °C overnight. 250 mL cultures were inoculated at a ratio of 1:100 with the preculture. The cultures were incubated at 37 °C and 250 rpm in a water bath shaker. After reaching an OD_{578} of 0.4, recombinant protein production was induced by adding 0.5 % (w/v) xylose. Incubation was continued for 8 h. For analysis of the intracellular protein fractions (see chap. 2.6.3.2), samples were taken at different time points after induction. Cells were harvested by centrifugation for 15 min at 4,000 x *g* and 4 °C. The cell sediments were stored at -20 °C.

2.6.1.2 Cell Disruption

The *E. coli* cell sediments were suspended in lysis buffer B and disrupted by a single passage through a French Press® homogenizer at 19,200 psi. Cell debris and insoluble protein fraction were removed by centrifugation for 90 min at 4 °C and 25,000 x *g*. The resulting supernatant was loaded onto a glutathione sepharose column for GST-tagged proteins or onto a Ni^{2+}-NTA column for His-tagged proteins. Proteins solutions were stored an ice.

Lysis buffer B	Tris-HCl	50 mM
	NaCl	150 mM
	$MgCl_2$	10 mM
	glycerol	10 % (v/v)
	lysozyme	5 mg/mL
	Benzonase® Nuclease	0.1 % (v/v)
	protease inhibitor	1 Tablet
	in H_2O_{dest}; pH 7.5	

To increase the protein solubility optional detergents such as CHAPS, Tesit octyl glycoside or TritonX-100 (concentration 0.2-2 % (v/v) or (w/v)) were added.

2.6.1.3 Purification of *Thermosynechococcus elongatus* Porphobilinogen Synthase (PBGS) by Affinity Chromatography

Recombinant produced PBGS was purified by a Ni^{2+}-NTA affinity chromatography using an ÄKTA Purifier^{TM} with a 5 mL column, which was equilibrated with 10 volumes of buffer A. All steps were carried out at RT, proteins were stored on ice. After loading the cell free extract on the column at a flow rate of 0.5 mL/min, the column was washed with 10 volumes of buffer A to remove unbound proteins. Bound proteins were eluted using a linear gradient of 0-200 mM imidazole in buffer A at a flow rate of 0.5 mL/min. Fractions containing PBGS were identified by SDS-PAGE and stored at 4 °C.

Buffer A	Tris-HCl	50 mM
	NaCl	150 mM
	$MgCl_2$	10 mM
	glycerol	10 % (v/v)
	in H_2O_{dest}; pH 7.5	

2.6.2 Recombinant Production and Purification Human Uroporphyrinogen III Decarboxylase (UROD)

2.6.2.1 Cell Growth for Protein Production

For recombinant production of human UROD in *E. coli*, 20 x 500 mL LB medium containing ampicilin (100 µg/mL) and chloramphemicol (34 µg/mL) were inoculated (ratio 1:100) with an overnight culture of *E. coli* BL21(DE3)pLysS carrying pHT#77 for the wild type and pHT#77-R37K for the mutant variant R37K, respectively, or *E. coli* BL21(DE3)RIL transformed with pHT#77-R37A, pHT#77-R41A or pHT#77-R41K for the mutant variants R37A, R41A and R41K, respectively. Cultures were grown aerobically in 1 L Erlenmeyer flasks at 37 °C and 200 rpm to an OD_{578} of 0.6 and production of proteins was induced by addition of IPTG to a final concentration of 400 µM. Incubation was continued for

6 h at 25 °C and 180 rpm. Cells were harvested by centrifugation for 15 min at 4,000 x *g* and 4 °C. The cell sediments were stored at -20 °C.

2.6.2.2 Cell Disruption

The cell sediments were suspended in lysis buffer C and disrupted by a single passage through a French Press® homogeniser at 19,200 psi. Cell debris and insoluble protein fraction were removed by centrifugation for 90 min at 4 °C and 25,000 x *g*. The resulting supernatants were loaded onto a Ni^{2+}-NTA column. Proteins solutions were stored on ice.

Lysis buffer C	NaCl	300	mM
	Sørensen's buffer; pH 6.8	50	mM
	glycerol	10	% (v/v)
	Benzonase® Nuclease	0.1	% (v/v)
	protease inhibitor	1	Tablet

2.6.2.3 Purification by Affinity Chromatography

Recombinant human UROD was purified by a Ni^{2+}-NTA affinity chromatography using an ÄKTA Puifier™ with a 5 mL column, which was equilibrated with 10 volumes of buffer B. All steps were carried out at RT, proteins were stored on ice. After loading the cell free extract at a flow rate of 0.5 mL/min, the column was washed with 10 volumes of buffer B to remove unbound proteins. Bound proteins were eluted using a linear gradient of 0-250 mM imidazole in buffer B at a flow rate of 0.5 mL/min. Fractions containing UROD were identified by SDS-PAGE and stored at 4 °C.

Buffer B	NaCl	300	mM
	Sørensen's buffer; pH 6.8	50	mM
	glycerol	10	% (v/v)

2.6.3 Protein Characterisation

2.6.3.1 Bicinchoninic Acid (BCA) Test

Concentrations of protein solutions were determined using the Bicinchoninic Acid Kit for Protein Determination according to manufacturer's instructions. Proteins reduce alkaline Cu(II) to Cu(I) in a concentration-dependent manner. Bicinchoninic acid is a highly specific chromogenic reagent for Cu(I) forming a purple complex with an absorbance maximum at 562 nm. The absorbance is directly proportional to protein concentration. Bovine serum albumin was used as a standard.

2.6.3.2 Analysis of the Intracellular Protein Fractions from *B. megaterium*

For analysis of the intracellular proteins fractions, samples containing 3 x 10^9 *B. megaterium* cells were harvested (14,000 x *g*; 4 °C; 15 min) and the supernatant was completely removed afterwards. Subsequently, the cells were suspended in 30 µL lysis buffer D supplemented with 2 µL/mL benzonase and incubated at 37 °C at 1,000 rpm (Thermomixer compact) for 30 min. After centrifugation (14,000 x *g*; 4 °C; 30 min), 26 µL of the supernatant containing the soluble proteins were mixed with SDS loading dye and stored on ice. The sediment, containing the cell debris and the insoluble proteins, was suspended in 30 µL of urea buffer and centrifuged for cell debris elimination (14,000 x *g*; 30 min and 4 °C). For analysis of the insoluble proteins, 26 µL supernatant were mixed with SDS loading dye. The samples were analysed by SDS-PAGE (see chapt. 2.6.3.3)

Lysis buffer D	Na_3PO_4	100 mM
	$MgSO_4$	2 mM
	lysozyme	5 mg/mL
	in H_2O_{dest}; pH 6.5	
Urea buffer	Tris-HCl	50 mM
	urea	8 M
	in H_2O_{dest}; pH 7.5	

5 x SDS loading dye	Tris-HCl	100 mM
	glycerol	40 % (v/v)
	β-mercaptoethanol	10 % (v/v)
	SDS	3.2 % (w/v)
	bromphenol blue	0.2 % (w/v)
	in H_2O_{dest}; pH 6.8	

2.6.3.3 Discontinuous Sulphate Polyacrylamide Gel Electrophoresis

Proteins were analyzed by sodium dodecyl sulphate polyacrylamide gel electrophoresis (SDS-PAGE) as described by Laemmli (Laemmli, 1970) with modifications by Righetti (Righetti *et al.*, 1990) for discontinuous SDS-PAGE. Protein samples were denatured by heating at 95 °C for 5 min in SDS loading dye. Samples were loaded onto the gel which was run at 45 mA. During electrophoresis, proteins were first focused in the stacking gel and subsequently separated according to their relative molecular mass in the running gel. The size standard employed was Protein Molecular Weight Marker. Gels were stained with staining solution and destained with destaining solution A or InstantBlue™ until protein bands were clearly visible.

SDS gel

	running gel [12 % (v/v)]	stacking gel [6 % (v/v)]
Acrylamide stock solution	2 mL	500 µL
Buffer for running gel	1.25 mL	-
Buffer for stacking gel	-	625 µL
H_2O_{dest}	1.75 mL	1.375 mL
APS solution	50 µL	25 µL
Tetramethylethylen diamine (TEMED)	5 µL	2.5 µL

Acrylamide stock solution	Rotiphorese® Gel 30 (37.5:1)	(Roth)
Buffer for running gel	Tris-HCl	1.5 M
	SDS	0.4 % (w/v)
	in H_2O_{dest}; pH 8.8	
Buffer for stacking gel	Tris-HCl	0.5 M
	SDS	0.4 % (w/v)
	in H_2O_{dest}; pH 6.8	

APS solution	ammonium peroxodisulfate in H_2O_{dest}	10	% (w/v)
Tetramethylethylen diamine	TEMED p.a. for electrophoresis (Roth)	99	%(v/v)
Electrophoresis buffer	Tris-HCl	25	mM
	glycine	190	mM
	SDS	0.1	% (w/v)
	in H_2O_{dest}; pH 8.4		
5 x SDS loading dye	Tris-HCl	100	mM
	glycerol	40	% (v/v)
	β-mercaptoethanol	10	% (v/v)
	SDS	3.2	% (w/v)
	bromphenol blue	0.2	% (w/v)
	in H_2O_{dest}; pH 6.8		
Staining solution A	ethanol	30	% (v/v)
	acetic acid	10	% (v/v)
	Coomassie Brillant Blue G-250	0.25	% (w/v)
	in H_2O_{dest}		
Destaining solution	ethanol	30	% (v/v)
	acetic acid	10	% (v/v)
	in H_2O_{dest}		

2.6.3.4 Western Blot

Proteins immobilised on a polyvinylidene fluoride (PVDF)-membrane (Roth) can be detected by antibodies. The primary antibody is directed against an epitope of the protein of interest and the secondary antibody is directed against the primary antibody. Furthermore the secondary antibody is coupled with an enzyme which catalyses a detectable colour developing reaction. For immunochemical detection, electrophoretically separated proteins were transferred in a semi-dry process onto a PVDF-membrane which binds the proteins by polar interactions. Therefore, the PVDF-membrane was activated in methanol for 15 min and, similarly to the SDS gel and the Whatman blotting paper, incubated for 15 min in Towbin buffer. Proteins were blotted onto the membrane for 15 min at 15 V per gel according to the manufacturer's instructions. Non-specific binding sites of the membrane were

saturated overnight in blocking solution at 4 °C and slight shaking. Proteins immobilised on the PVDF-membrane were specifically detected by antibodies. For the detection of the His-tagged proteins, the membrane was incubated for 1 h (RT) and slightly shaking with the primary anti-His antibody, which was diluted 1:3,000 in blocking solution. After washing with washing solution thrice for 10 min and subsequent incubation for 45 min with the secondary antibody (1:5,000 diluted in washing solution), which is directed against the primary antibody and coupled with alkaline phosphatase, the membrane was washed four times for 10 min with PBS/Tween. After 5 min of incubation with alkaline phosphate buffer the chemiluminescence reaction was performed with staining solution B until bands became visible. During exposure alkaline phosphatase, the enzyme bound to the antibody catalyses the reaction of 5-brom-4chloro-3indolylphosphate (BCIP) with nitroblue-tetrazolium (NBT).

Towbin buffer	Tris-HCl	25	mM
	glycine	150	mM
	methanol	10	% (v/v)
	in H_2O_{dest}; pH 8.5		
10 x PBS	NaCl	1.37	M
	KCl	27	mM
	Na_2HPO_4	100	mM
	KH_2PO_4	20	mM
	in H_2O_{dest}		
Blocking solution	skim milk powder	5	% (w/v)
	Tween 20	0.1	% (v/v)
	10 x PBS	10	% (v/v)
	in H_2O_{dest}		
Washing solution	skim milk powder	0.5	% (w/v)
	Tween 20	0.1	% (v/v)
	10 x PBS	10	% (v/v)
	in H_2O_{dest}		
PBS/Tween buffer	Tween 20	0.1	% (v/v)
	10 x PBS	10	% (v/v)
	in H_2O_{dest}		

Alkaline phosphate buffer	Tris-HCl	100	mM
	NaCl	100	mM
	$MgCl_2$	5	mM
	in H_2O_{dest}; pH 9.5		
Staining solution B	NBT solution	0.33	% (v/v)
	BCIP solution	0.33	% (v/v)
	in alkaline phosphate buffer		
NBT solution	nitroblue-tetrazolium	10	% (w/v)
	dimethylenformamide (DMF)	70	% (v/v)
	in H_2O_{dest}		
BCIP solution	5-brom-4-chloro-3-indolylphosphate	5	% (w/v)
	in DMF		

2.7 Enzyme Activity Assays

2.7.1 Determination of Porphobilinogen Synthase Activity

The activity of recombinantly produced and purified porphobilinogen synthase (PBGS) from *T. elongatus* was determined by using a modified Ehrlich's test. The test based on the reaction between the product porphobilinogen and 4-(dimethylamino)-benzaldehyde (DMBA). In a first reaction step porphobilinogen and DMBA form a pink reaction product which has an absorbance maximum at 555 nm. This product subsequently reacts with a second porphobilinogen molecule to form a colourless dipyrrolphenylmethane (figure 2.2). Since the second reaction proceeds very slowly porphobilinogen concentrations can be quantified *via* the Beer-Lambert law.

The Beer-Lambert law is as following:

$$c = A/(d*\varepsilon)$$

c = concentration of porphobilinogen [M]
A = absorption
d = cell diameter [cm]
ε = molar extinction coefficient of the coloured intermediate [$M^{-1}cm^{-1}$]

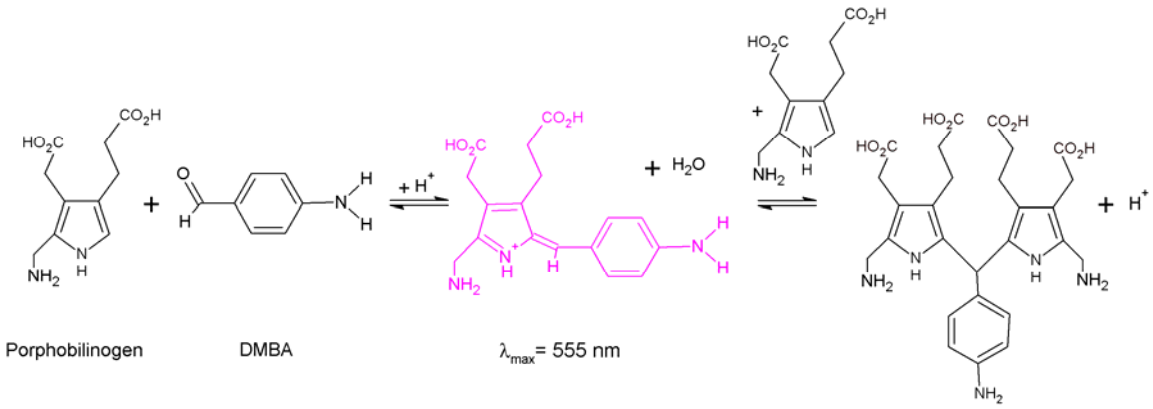

Figure 2.2 : Colorimetric Detection of Porphobilinogen.

Porphobilinogen forms a coloured complex with DMBA which can be detected at OD_{555}. This complex slowly reacts with a second porphobilinogen molecule to form colourless dipyrrolphenylmethane. The coloured intermediate has a molar extinction coefficient of ε(complex) = 60,200 $M^{-1}cm^{-1}$.

The standard assay contained a final concentration of PBGS of 10 µg/mL. Purified PBGS from *Pseudomonas aeruginosa*, which served as positive control, was kindly provided from Ilka Heinemann (Heinemann, 2007). The substrate aminolaevulinic acid (ALA) was dissolved to a concentration of 40 mM in kinetic buffer A. Stock solutions of protein and buffer were mixed and incubated at 37, 45 and 55 °C for 5 min. To start the reaction, preheated substrate was added to a final concentration of 10 mM and no ALA for the negative control, respectively. The reaction was stopped after 1 h by adding an equal amount of ice cold stop reagent. Following centrifugation (3 min and 4,000 x *g* at RT), the supernatant was treated with an equal amount of Ehrlich's reagent. After 15 min at RT, the amount of formed porphobilinogen was determined by measuring the OD_{555} and calculated using the Beer-Lambert law as described above.

Kinetic buffer A	KCl	100	mM
	$MgCl_2$	5	mM
	bis-tris-probane	100	mM
	in H_2O_{dest}; pH 8.4		
Stop reagent	trichloroacetic acid	25	% (w/v)
	in H_2O_{dest}		
Ehrlich's reagent	DMBA	2	% (w/v)
	acetic acid	27.3	% (v/v)
	hydrochloric acid	72.7	% (v/v)

2.7.2 Determination of Uroporphyrinogen III Decarboxylase Activity

2.7.2.1 Activity Assay

The uroporphyrinogen III decarboxylase (UROD) activity assay was carried out under strict anaerobic conditions in an anaerobic chamber. All solutions were saturated with N_2 prior to use. The standard assay mixture (see below) contained UROD (0.1 µM) and uroporphyrinogen III (0.025-35 µM) in potassium phosphate buffer in a total volume of 245 µL after a modified procedure as described earlier (Phillips and Kushner, 1999). After incubation at 37 °C in the dark for 30 min the reaction was stopped by addition of 10 µL concentrated hydrochloric acid and formed coproporphyrinogen III was oxidised for 15 min to coproporphyrin III by addition of 10 µL 30 % H_2O_2 (see figure 2.3). For protein removal the mixture was centrifuged (10 min and 14,000 x *g* at RT). The obtained supernatant was analysed by high performance liquid chromatography (HPLC).

Standard assay mixture

potassium phosphate buffer; pH 6.8	50 mM	42.5 µL
DTT	1 M	2.5 µL
potassium phosphate buffer; pH 6.8	1 M	20 µL
UROD in DTT (0.1 M)/ potassium phosphate buffer (0.1 M)	0.1 µM	175 µL
uroporphyrinogen III in DTT (0.1 M)/ potassium phosphate buffer (0.1 M)	0.025-35 µM	5 µL

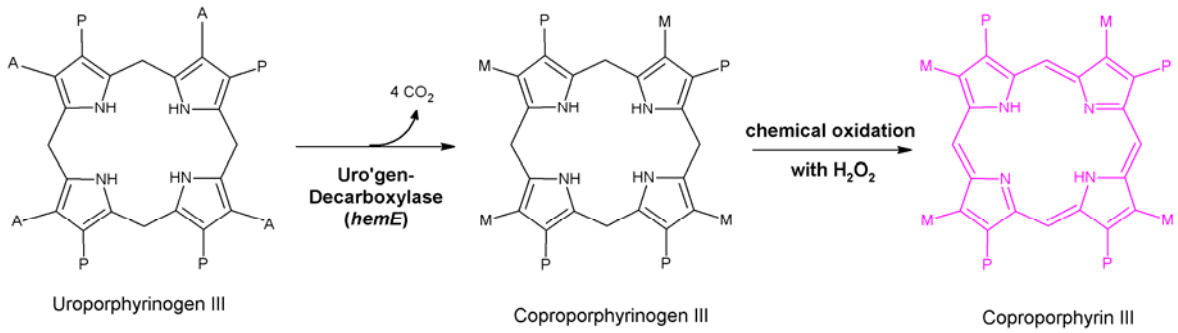

Figure 2.3 : Conversion of Uroporphyrinogen III into Coproporphyrinogen III

Uroporphyrinogen III decarboxylase catalyses the sequential decarboxylation of the four acetate residues of uroporphyrinogen III to yield the corresponding methyl groups of the product coproporphyrinogen III.

2.7.2.2 Preparation of Uroporphyrinogen III

The substrate uroporphyrinogen III (uro'gen III) was obtained by reduction of uroporphyrin III (uro III) (Frontier Scientific) according to a modified procedure described by Grandchamp and Nordmann (Grandchamp and Nordmann, 1982): 1.7 mg uro III were dissolved in 1.4 mL of KOH (50mM) and finally reduced with 1 g of 3 % sodium amalgam under nitrogen atmosphere in the dark at RT. When the reaction mixture had decoloured, it was filtered through glass wool. 36 mg DTT were added and the mixture was filled up to a volume of 4.5 mL with Tris-HCl (50 mM, pH 8.0). The pH was adjusted to 8-8.5 with 20 % (v/v) phosphoric acid and 200 µL of 1 M Tris-HCl (pH 8.0) were finally added. The uro'gen III solution, which has a final concentration of 1.88 mM, was divided anaerobically and stored at -20 °C in the dark to avoid auto-oxidation.

2.7.2.3 Uroporphyrinogen III Decarboxylase Activity Analysis by High Performance Liquid Chromatography (HPLC)

The uroporphyrinogen III decarboxylase activity was analysed by high performance liquid chromatography (HPLC). For identification the reaction products were separated by a 1,500 series Jasco HPLC System. Therefore, 100 µL of the reaction mixture supernatant was mixed with 100 µL acetone/HCl (ratio 9:10). An Equisil ODS (5 µm, 250 x 4.6 mm) C_{18} reversed phase column (Dr. Maisch GmbH, Ammerbuch) was run at 0.3 mL/min and 30 °C. Twenty µL of the sample were injected. Isocratic separation was performed using 40 % (v/v) ammonium acetate (pH 5.2) and 10 % (v/v) acetonitrile in methanol as mobile phase. Tetrapyrroles were detected by fluorescence measurement using an excitation wavelength of 409 nm and an emission wavelength of 618 nm. Uroporphyrin III and coproporphyrin III were used as standards.

3 RESULTS AND DISCUSSION

This thesis investigated several different steps of haem biosynthesis in humans and bacteria.

3.1 Characterisation of Human Uroporphyrinogen III Decarboxylase

The successive decarboxylation of the acetate subunits of uroporphyrinogen III to form coproporphyrinogen III is catalysed by the cytosolic enzyme uroporphyrinogen III decarboxylase (UROD). Under physiological conditions, the decarboxylation follows a preferred, clockwise route, starting at ring D (Jackson *et al.*, 1976; Luo and Lim, 1993). Dysfunction of the UROD leads to a disease which is commonly known as porphyria cutanea tarda. It is the most commun porphyria with a prevalence of 1 case in 25,000-50,000 population.

For that reason URODs and especially the human UROD have been examinated for a long time. Another important reason for UROD being an object of interest is that the enzyme does not require a cofactors or prosthetic groups for enzymatic activity which mark UROD as a very unusual decarboxylase (de Verneuil *et al.*, 1980; de Verneuil *et al.*, 1983; Straka and Kushner, 1983). Already early hypothesis about the reaction mechanisms had been made by Barnard and Akhtar (Barnard and Akhtar, 1979). They predicted that the enzyme itself served as proton donor for the reaction. Since then, a lot of different amino acid residues like cysteine, threonine, arginine and histidine had been exchanged by site directed mutagenesis and their impact on catalytic activity studied (Phillips *et al.*, 2009; Wyckoff *et al.*, 1996) as well natural occurring mutations had been a subject of interest (Phillips *et al.*, 2001; Phillips *et al.*, 2007).

However, none of the studied residues led to complete molecular understanding of the catalytic properties of this unusual decarboxylase. The solved structure of substrate-bound human UROD shows that the negatively charged aspartate 86 is important for substrate stabilisation in the active site (Phillips *et al.*, 2003; Whitby *et al.*, 1998). Density-functional calculations of the mechanism led to the hypothesis that arginine 37, which lies close to the substrate, may be the proton donor for the reaction (Silva and Ramos, 2005). This is supported by earlier studies which showed that UROD is inactivated by the arginine-modyfing reagent

phenylglyoxal (Jones and Jordan, 1993). Lately, Silva concluded that a second arginine 41 residue served as second proton donor as well. Conserved amino acids residues were found among all species (Figure 3.1). For example, the suggested catalytic residues Asp37, Arg41 and Arg86 (numbered by human sequence) are highly conserved in the UROD family of proteins. Whereby, the importance of Arg86 had already been proven (Phillips *et al.*, 2003; Whitby *et al.*, 1998).

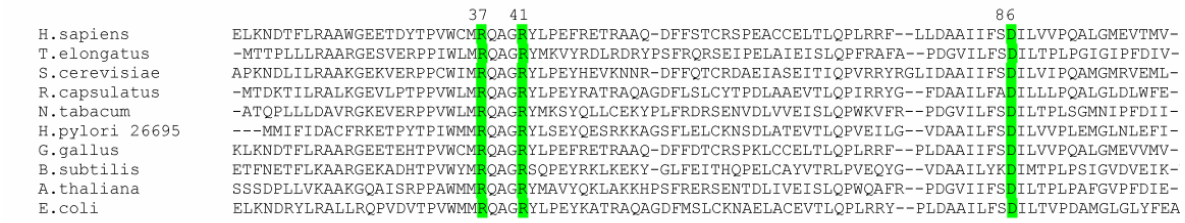

Figure 3.1: Alignment of UROD protein sequences.

Ten amino acid sequences were aligned using ClustalW2 (EMBL-EBI). Residue numbering refers to the human sequence. An extract of the sequence is illustrated. Arg37, Arg41 and Asp86 residues are green highlighted. These residues were proposed to be involved in the catalysis of UROD. GenBank database entries shown are *Homo sapiens* (U30787), *T. elongatus* (BAC08292), *S. cerevisiae* (Z49209), *Rhodobacter capsulatus* (U16796), *N. tabacum* (X82833), *Helicobacter pylori* (AE000511), *Gallus gallus* (XM422430), *B. subtilis* (M97208), *A. thaliana* (BAA97056) and *E. coli* (AAC76971).

To investigate the influence of these highly conserved arginine residues as catalytic features, mutagenesis studies of human UROD arginines 37 and 41 were performed. Wild type human UROD and respective mutant variants were recombinantly produced in *E. coli*, purified and kinetically characterised. The enzymatic influence of these residues was determined by HPLC analysis.

3.1.1 Production and Purification of Recombinant Human Uroporphyrinogen III decarboxylase (UROD)

According to the predicted mechanism of the uroporphyrinogen III decarboxylase (UROD) catalysis, a mutagenesis approach was untertaken to evaluate the chemical contribution of the residues Arg37 and Arg41 to enzymatic catalysis. Therefore, introduction of conservative and non-conservative amino acid exchanges for these residues was applied and single amino acid exchanges were conducted. Arg37 and Arg41 were individually replaced by lysine or alanine. The expression vector pHT#77 carrying the human *hemE* gene (Phillips *et al.*, 1997),

which represented the human wild type UROD, served as template for site-directed mutagenesis. The resulting constructs were verified for their correct gene sequence.

Different *E. coli* strains were transformed with the wild type expression vector pHT#77 and the mutant variants, respectively. Recombinant protein production studies revealed best results in *E. coli* BL21(DE3)pLysS for the wild type and R37K mutant variant and *E. coli* strains BL21(DE3)RIL for the mutant variants R37A, R41A and R41K, respectively. Testing different time intervals of recombinant protein production yielded a maximum concentration of protein in the cell at six hours of production. The protein concentration decreased in the cell for production of more than six hours. Therefore, an induction of gene expression with 400 µM imidazole for six hours at an incubation temperature of 25 °C was found optimal with less degradation of the protein. Recombinant UROD was produced with an N-terminal His_{10}-tag. The resulting fusion proteins were purified to apparent homogeneity in a single step *via* affinity chromatography with a Ni^{2+}-NTA affinity column using an ÄKTA Purifier^{TM}. After washing and pre-elution with a linear rising imidazole gradient unspecific bound proteins were separated (Figure 3.2, lanes 3-5). Soluble recombinant UROD was eluted with a final concentration of 250 mM imidazole. Following SDS-PAGE analysis of the purification procedure of wild type UROD revealed a dominant protein band which corresponded to a protein with a relative molecular mass of approximately 40,000 (Figure 3.2, lanes 6-11). This is in good agreement with the calculated molecular mass of the fusion protein of 43,300.

The UROD mutant variants demonstrated similar purification results like the wild type UROD (data not shown). About 8 mg of recombinant protein per litre cell culture were obtained. Since the presence of the histidine tag was shown to have no influence of enzymatic activity (Phillips *et al.*, 1997) there was no necessity for histidine tag removal. Further, in this study it was proofed that UROD did not show detectable degradation when stored at 4 °C for a time period of more than a month.

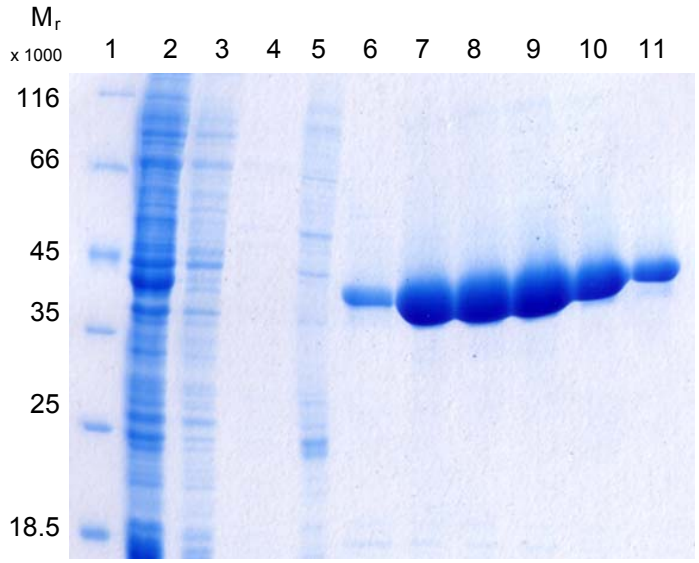

Figure 3.2: Production, purification and processing of recombinant human uroporphyrinogen III decarboxylase produced in *E. coli*.

Proteins were separated by 12 % SDS-PAGE and visualised by staining with InstantBlue. Lane 1: molecular weight marker; lane 2: total soluble protein extract after induction of gene expression with 400 µM IPTG for 6 h at 25 °C; lanes 3-5: washing steps; lanes 6-11: purified UROD eluted with 250 mM imidazole.

3.1.2 Catalytic Relevance of Arginine

The recombinantly produced wild type UROD and its constructed variants R37A, R37K, R41A and R41K, respectively, were tested for catalysis. Therefore, a UROD activity assay was carried out under standard conditions after a procedure as described earlier (Phillips and Kushner, 1999). All procedures were performed under strict anaerobic conditions. After incubation at 37 °C in the dark for 30 min the reaction was stopped by addition of concentrated hydrochloric acid. Formed coproporphyrinogen III was oxidized for 15 min to coproporphyrin III by addition of H_2O_2. Subsequently, formed coproporphyrin III was detected by HPLC analysis using an excitation wavelength of 409 nm and an emission wavelength of 618 nm for fluorescence measurement. Uroporphyrin III and coproporphyrin III with known concentrations were used as standards. The Uroporphyrin III and coproporphyrin III concentrations present in the samples were calculated *via* a calibration curve.

Wild type UROD activity resulted in the conversion into the colourless coproporphyrinogen III which was further converted into coproporphyrin III by H_2O_2 for HPLC analysis. Fluorescence emission peaks for standards of uroporphyrin III and coproporphyrin III were detected with retention times of approximately 10 min for uroporphyrin III and approximately 37 min for coproporphyrin III. Wild type UROD demonstrated normal enzymatic activity in the substrate concentration range of 0.025-35 µM, meaning that uroporphyrinogen III

was converted into coproporphyrinogen III without formation of detectable reaction intermediates (Figure 3.3).

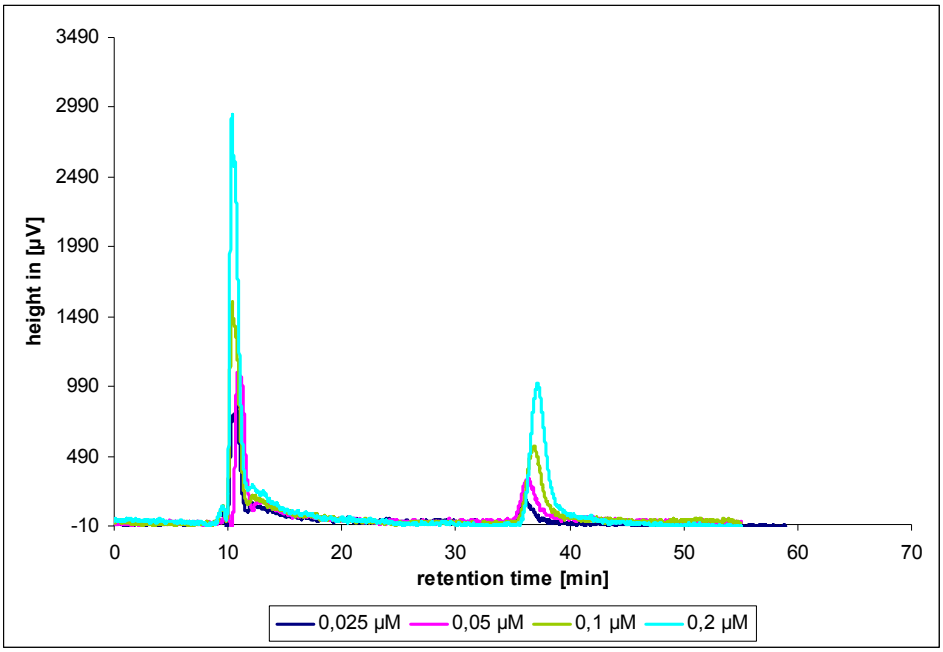

Figure 3.3: Detection of substrate and products of wild type UROD by HPLC analysis.

For analysis of UROD activity 20 µL reaction mixture were loaded on a reverse phase column for HPLC analysis. Tetrapyrroles were detected by fluorescence at an excitation wavelength of 409 nm and an emission wavelength of 618 nm. Standard curves revealed retention times of 10 min for uroporphyrin III and 37 min for coproporphyrin III. Wild type UROD demonstrates normal activity with different substrate concentrations meaning that uroporphyrinogen III was completely converted into the product coproporphyrinogen III.

The wild type UROD activity increased to a substrate concentration of approximately 5-8 µM, after which activities decreased while higher substrate concentrations were obtained (Figure 3.4, curve mark ●). Subsequently, activity experiments comparing wild type and mutant UROD's were performed in the same substrate range under the same conditions. In comparison with wild type UROD the mutant variant R37A showed enzymatic activity just at low substrate concentrations of 0.025-2 µM. However, in this range the R37A variant was just able to form small amounts of about 0.05 µM coproporphyrinogen III and failed in coproporphyrinogen III formation at higher substrate concentrations (Figure 3.4, curve mark ○). The UROD variants R37K and R41A did not show any enzymatic activity at all (data not shown). Here, neither coproporphyrinogen III nor reaction intermediates were detectable by HPLC analysis.

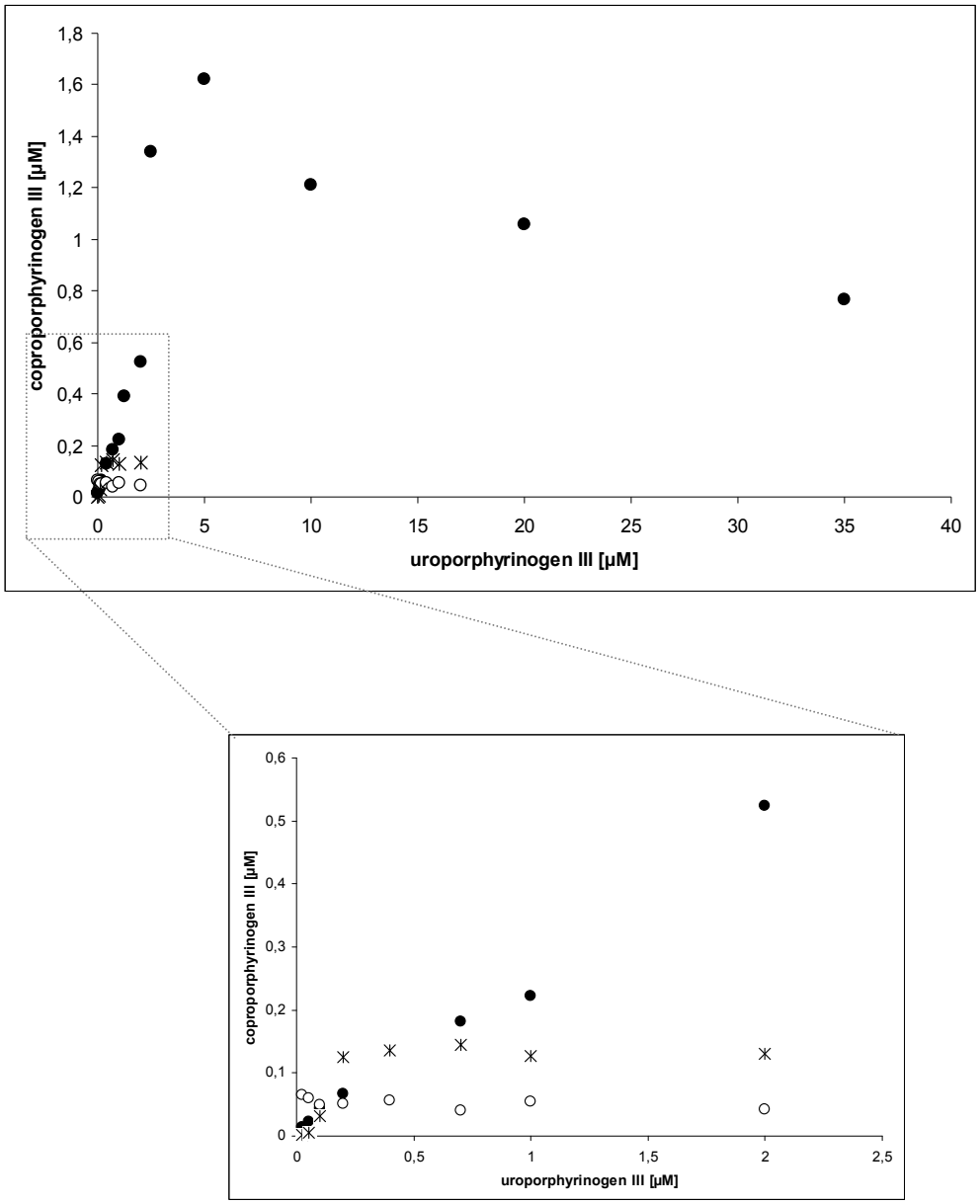

Figure 3.4: UROD activity comparison.

Wild type and variants R37A, R37K, R41A and R41K, respectively, were tested for enzymatic catalysis activity. Wild type UROD (●) demonstrated normal enzymatic activity over a substrate concentration range of 0.025-35 µM, meaning that uroporphyrinogen III was converted into coproporphyrinogen III without formation of reaction intermediates. The activity increased until a substrate concentration of approximately 5-8 µM, after which activities reached a plateau. In comparison with wild type UROD the mutant variant R37A (○) showed enzymatic activity just at low substrate concentrations of 0.025-2 µM and failed in coproporphyrinogen III formation at higher substrate concentrations. UROD-R41K (ж) demonstrated enzymatic activity at small amounts of substrate concentration of 0.025-2 µM and reached a plateau of product formation at a substrate concentration of about 0.2-0.4 µM. Variants R37K and R41A showed enzymatic activity below the detection level (data not shown).

In contrast, the R41K variant demonstrated enzymatic activity at small amounts of substrate concentration of 0.025-2 µM and reached a plateau of product formation at a substrate concentration of about 0.1-0.2 µM (Figure 3.4, curve marks ж).

Nevertheless, in this case coproporphyrinogen III as well as reaction intermediates were detectable (Figure 3.5). The attempt to identify the reaction intermediates by NMR analysis failed because of insufficient sample concentrations.

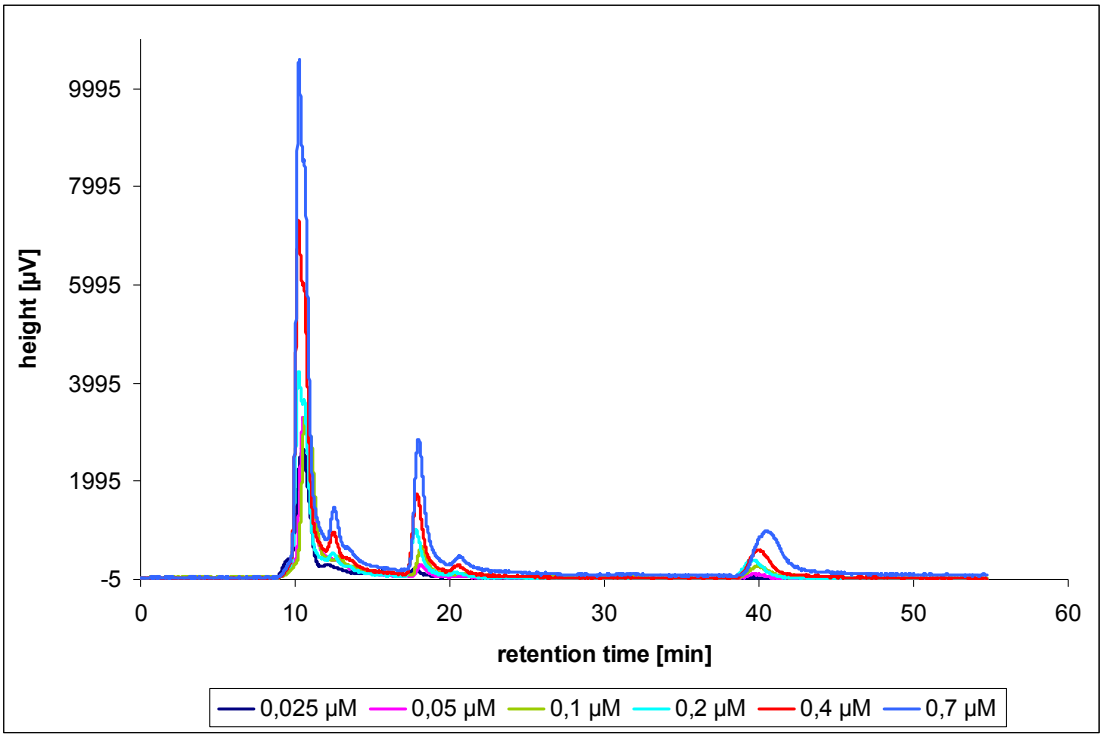

Figure 3.5: Catalysis of UROD mutant variant R41K: formation of intermediates analysed by HPLC analysis.

Mutant variant R41K was just catalytically active at low substrate concentrations of about 0.025-2 µM. In contrast to wild type and the other mutant variant R37A the product coproporphyrinogen III and additional reaction intermediates were detectable by HPLC analysis.

3.1.3 Conclusions drawn from the Active Site Mutagenesis Studies of Human Uroporphyrinogen III Decarboxylase

The catalytic investigations of UROD mutant variants in comparison with the wild type enzyme led to the conclusion that the exchange of the positively charged amino acids Arg37 and Arg41 abolished enzyme activity. This proved the essential role of these residues in UROD catalysis and endorsed the density-functional calculations of the cooperation partner Petro Silva (University Fernando Pessoa at Porto, Portugal). The calculated models computed that pyrrole protonation rather than decarboxylation are the rate-limiting steps of the mechanism. According to the UROD crystal structure (Figure 3.6) these positively charged amino acid residues (mostly arginines, histidines and lysines) are important in the active site

cleft as interaction partners for the negatively charged substrate. These residues are thought to participate orientating the substrate directly or ameliorating the charge of the substrate binding pocket.

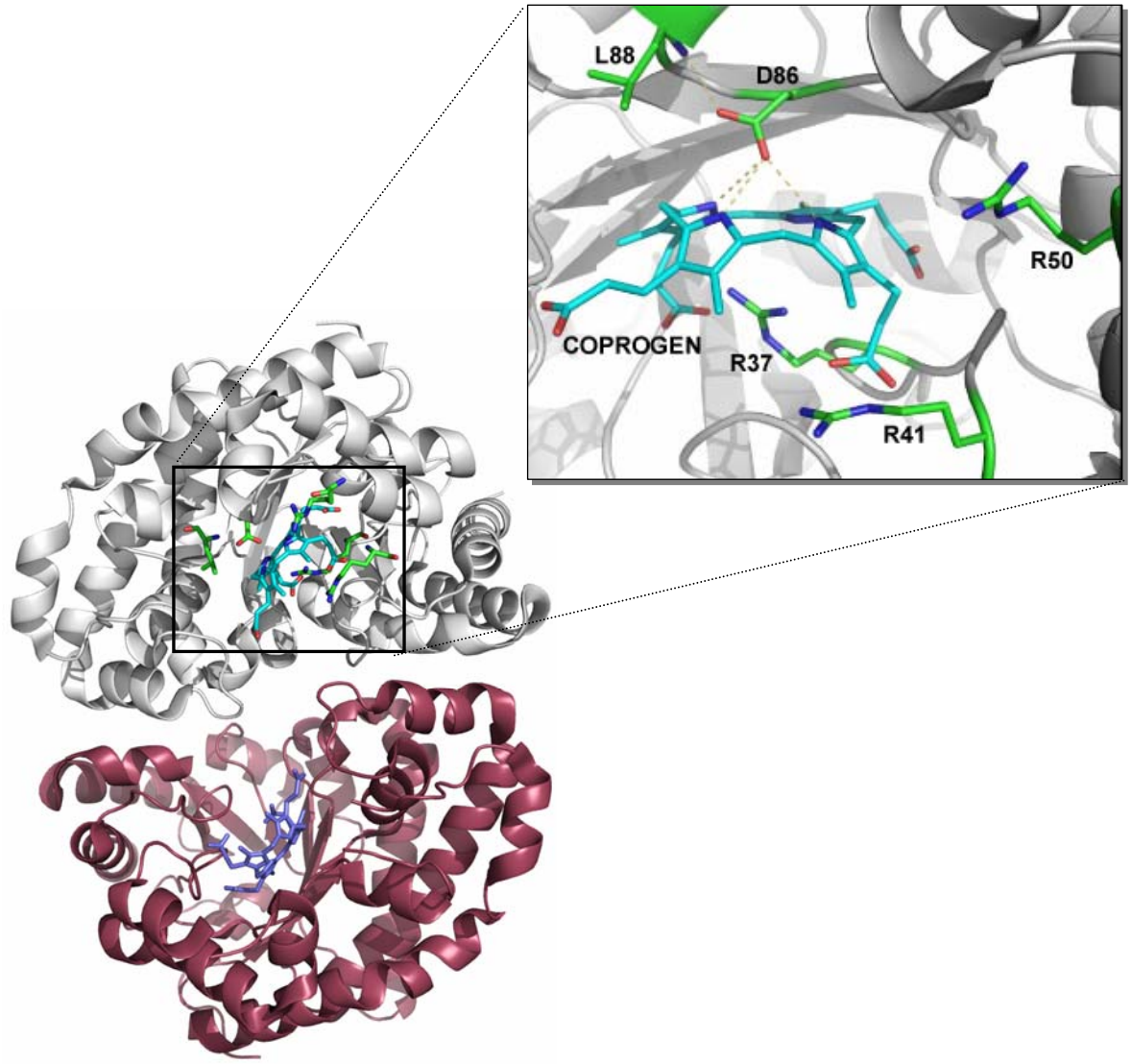

Figure 3.6: Crystal Stucture of human UROD

Solved structure (Whitby *et al.*, 1998) revealed a dimeric enzyme in which the two single domain subunits are orientated head-to-head with the active site clefts facing each other at the dimer interface arrangement of the two monomers. As a consequence, one large active site cleft is generated which is well shielded from the surrounding solvent, especially surrounding H_3O^+ ions. Recently, studies using a single chain dimeric UROD construct showed that substrate shuttling between the active sites is not required to generate coproporphyrinogen III (Phillips *et al.*, 2009). The four central NH-groups of the tetrapyrrole are in hydrogen bounding distance to the highly conserved Asp86, which is proposed to be important for substrate stabilisation. Other positively charged residues (Arg37, Arg41, Arg50, Lys263, His220, His223 and His339) are important as interaction partners for the negatively charged substrate (modified after Layer *et. al.*, 2010).

The solved structure of wild type human UROD (Whitby *et al.*, 1998) revealed a dimeric enzyme in which the two single domain subunits are orientated head-to-head with the active site clefts facing each other at the dimer interface arrangement of the two monomers. As a consequence, one large active site cleft is generated which is well shielded from the surrounding solvent, especially from the surrounding H_3O^+ ions. Moreover, it was shown that the arginine modifying reagent phenylglyoxal inactivated UROD function (Jones and Jordan, 1993). A further amino acid residue Asp86 had already been identified as an important residue for substrate stabilisation during catalysis (Phillips *et al.*, 2003).

Replacing an arginine with a lysine residue is a conservative exchange which may suggest that lysine is able to maintain the assumed ionic interaction of arginine with the substrate. However, substitution of Arg37 by lysine yielded into an inactive form of the enzyme. This suggested the very flexible basic amino acid residue Arg37 is lying close to the substrate and fulfilling the role of a general acid. Since lysine is a smaller amino acid than arginine, it was not expected to move close enough to the substrate to affect its protonation. However, it can still prevent decarboxylation of H_3O^+-protonated uroporphyrinogen III by stabilising its leaving carboxylate residue. Exchange of Arg37 by the non polar alanine residue surprisingly yielded a slightly active enzyme. This observation might be rationalised by invoking a mechanism whereby substrate binding to the mutant is much less effective due to the absence of the attracting Arg37. Thus, H_3O^+ ions might enter the enzyme active site cleft and protonates the substrate.

The observed kinetic profile of the enzyme showed very peculiar features, which were consistent with the release of partially decarboxylated intermediates from the active site of the wild-type enzyme. At low substrate concentrations, these intermediates may get back into the active site and are rapidly converted into the product coproporphyrinogen III. At higher substrate concentrations, uroporphyrinogen III competes with these intermediates for entry into the active site and prevents them from finishing conversion into coproporphyrinogen III. However, the slow rate of decarboxylation in the presence of protonated Arg37 allows the breaking of protonated uroporphyrinogen III to become a competitive reaction for the main catalytic path. In contrast, the use of Arg37 as a proton donor allows substrate protonation to occur while at the same time removing of the stabilising effect of protonated Arg37 on the leaving carboxylate proceeds.

The flexibility of Arg37, as well as its central position in the active site, allows this residue to donate the catalytic proton to every pyrrole ring in uroporphyrinogen III. This way Arg37 promotes the sequential decarboxylation of the acetic acid substituents on the intact substrate and on the partially decarboxylated intermediates without the need for different binding modes for each of these species. Since Arg37 is already in a protonated form at the physiological pH the reaction can take place by successive 90° rotation of the substrate in the active site. Simulation performed in cooperation with Silva also confirms that the proton provided by Arg37 may shuttle back and forth between the amino acid chain and each pyrrole ring allowing the sequential decarboxylation (Silva and Ramos, 2005). The completion of each decarboxylation requires the transfer of an additional proton to the methylene substituent arising from CO_2 release. Yet, the enzyme must shield its active site from solvent H_3O^+, which would be a second suitable alternative proton donor for this step.

Examination of the crystal structure suggested that Arg41, the amino acid lying at the entrance to the active site, might be the proton donor for the reactions. Arg41 is located at the protein surface, and therefore it is able to move widely, both towards the substrate and away from it. Re-protonation of Arg41, which would allow for the transfer of a new proton to the methylene formed in the reaction, is expected to occur readily. The location of Arg41 between the solvent and the active site allows this residue to react with H_3O^+ without the risk of substrate side reactions.

The HPLC analysis of R41K mutant variant revealed low coproporphyrinogen III formation, but additional intermediates were detected. Although the intermediates were collected and subjected to NMR analysis, the chemical nature of these intermediates unfortunately could not be determined due to the low amounts. Lysine may be able to maintain the ionic interaction and is particularly able to coordinate the substrate in interaction with the residue Arg37. So, Arg37 is able to conduct catalysis. However, the Lys41 can not move close enough to the substrate to affect its protonation. Exchange the Arg41 to the non polar alanine residue resulted in prevention of the decarboxylation reaction. This suggests that the surface-located Arg41 undergoes conformational changes so that the substrate molecule can not be coordinated correctly in the active side cleft and Arg37 is not even able to be close enough for catalysis.

The results are also supported by former studies. There, the crystal structure of UROD in complex with the unnatural substrate uroporphyrinogen I revealed that the enzyme undergoes conformational changes and the flexible residue Arg41 folds towards the enzyme surface (Phillips *et al.*, 2003).
The unusual use of two basic residues as general acids in two different proton donation steps in uroporphyrinogen III decarboxylase provides an elegant evolutionary adaptation. Thus, the problem of simultaneously binding the very negative uroporphyrinogen III in a positively charged active site and selectively protonating this substrate while preventing excessive carboxylate stabilisation by positive charges is excluded. These investigations revealed that minor changes in these two arginine residues cause adverse effects in the enzymatic catalysis. The interaction is important for substrate binding, coordination in the active site cleft and decarboxylation.

3.2 *Thermosynechococcus elongatus* Haem Proteins

Another object of this work was the investigation of the interaction and existence of protein complexes of different enzymes involved in early steps of tetrapyrrole biosynthesis. It is proposed that complex formation is necessary to avoid exposure of cell toxic biosynthesis intermediates. In former *in vivo* and *in vitro* studies of the terminal enzymes in the haem biosynthesis of the thermophilic cyanobacterium *Thermosynechococcus elongatus* it was already shown that the last two enzymes protoporphyrinogen IX oxidase and ferrochelatase form a complex to prevent release of the toxic intermediate protoporphyrin IX (Masoumi *et al.*, 2008). Whereas, oxygen-dependent coproporphyrinogen III oxidase was not directly involved into this complex. Furthermore, *T. elongatus* porphobilinogen deaminase (PBGD), the third enzyme in the biosynthesis order, had already been characterised in our laboratory (Frese, 2008). First, *in vitro* investigations for the interaction between porphobilinogen deaminase and uroporphyrinogen III synthase (UROS) were already performed, using PBGD from *T. elongatus* and UROS from *Bacillus megaterium*, but precise answers are absent.
In order to characterise the interaction or complex formation in *T. elongatus* the remaining haem biosynthesis enzymes porphobilinogen synthase (PBGS),

uroporphyrinogen III synthase (UROS), uroporphyrinogen III decarboxylase (UROD) and oxygen-independent coproporphyrinogen III oxidase (CPO) were object of this study. Therefore, the *T. elongatus* proteins were individually recombinantly produced and partly purified for antibody production for further interaction and complex formation studies. Furthermore, first activity studies had been performed.

3.2.1 Cloning, Purification and Characterisation of Recombinant Porphobilinogen Synthase

The *T. elongatus* porphobilinogen synthase gene (*hemB*; EC 4.2.1.24) was cloned under the control of the T7-RNA-polymerase dependent promotor (Studier *et al.*, 1990) into the standard *E. coli* expression vector pET32a using the restriction sites *Eco*RI and *Not*I resulting in the construct pET32a-TEhemB. Several *E. coli* expression strains were tested at different incubation temperatures for recombinant protein production. The best conditions for recombinant PBGS production were obtained in *E. coli* Rossetta gami 2. PBGS was produced as fusion protein with a C-terminal His_6-tag after induction of gene expression with 400 µM isopropyl-β-D-thiogalactopyranoside (IPTG) at 37 °C over night. The cell-free extract was loaded on a Ni^{2+}-NTA affinity chromatography column and PBGS was purified to apparent homogeneity in a single step using an ÄKTA Purifier™. Figure 3.7 provides documentation a SDS-PAGE of the purification procedure. After washing and pre-elution with a linear rising imidazole gradient unspecific bound proteins were separated. Soluble recombinant PBGS was eluted with a final concentration of 200 mM imidazole (Figure 3.7, lanes 13-15).

SDS-PAGE analysis of the purified protein revealed a single band corresponding to a protein with a relative molecular mass of approximately 55,000 (Figure 3.7; lanes 13-15). This is in good agreement with the calculated molecular mass of the fusion protein of 50,800. A protein concentration of about 8 mg/mL of recombinantly purified PBGS was obtained. PBGS did not show detectable degradation at 4 °C for more than three months.

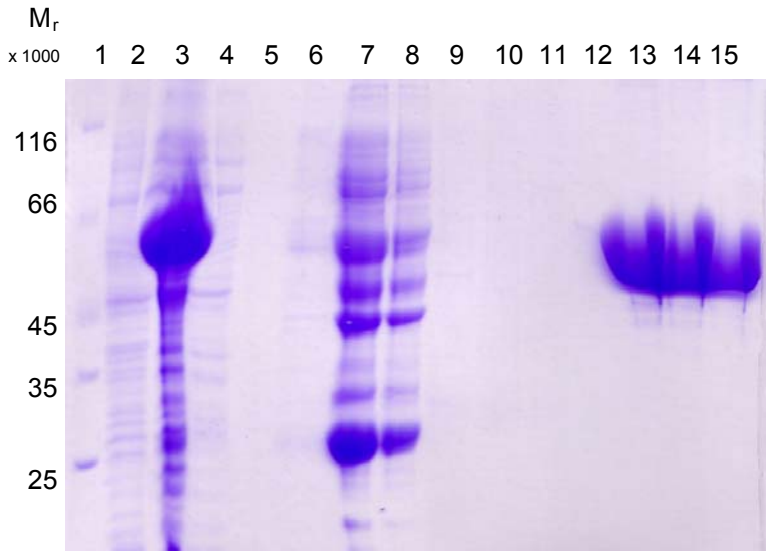

Figure 3.7: Production, purification and processing of recombinant *T. elongatus* porphobilinogen synthase produced in *E. coli*.

Proteins were separated by 12 % SDS-PAGE and visualised by staining with Coomassie Brilliant Blue. Lane 1: molecular weight marker; lane 2: total cellular extract without induction of gene expression; lane 3: total cellular extract after overnight induction of gene expression with 400 µM IPTG; lanes 4-12: washing and pre-elution steps; lanes 13-15: purified PBGS after elution with 200 mM imidazole.

PBGS is the second enzyme in the biosynthesis and catalyses the asymmetric condensation of two aminolaevulinic acid molecules to form porphobilinogen. To determine enzymatic activity of purified recombinant PBGS *in vitro* a modified Ehrlich's test was performed under standard conditions as described in MATERIALS AND METHODS using a final concentration of PBGS of 10 µg/mL. *Pseudomonas aeruginosa* PBGS was used as positive control (Figure 3.8, tube 2) which was kindly provided by Ilka Heinemann (Heinemann, 2007).

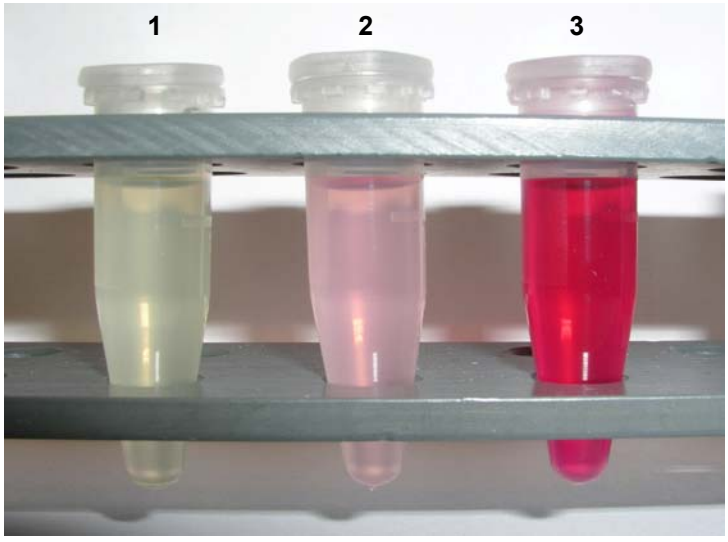

Figure 3.8: Porphobilinogen synthase (PBGS) activity assay for the recombinant purified *T. elongatus* enzyme.

The assay was carried out as described in MATERIALS AND METHODS. Tube 1: negative control; tube 2: positive control, *P. aeruginosa* PBGS; tube 3: *T. elongatus* PBGS. The activity test was carried out at 45 °C for 1 h. Tube 2 and 3 are showing a visible pink colouring, which is the result of complex formation between the reaction product porphobilinogen and 4-(dimethylamino)-benzaldehyde.

Formed porphobilinogen was verified by complex formation with 4-(dimethylamino)-benzaldehyde at an absorbance at 555 nm. Both *T. elongatus* PBGS and *P. aeruginosa* PBGS already showed visible pink colouring in the reaction tube at an incubation temperature of 45 °C (Figure 3.8). Since it is known that proteins of thermophilic bacteria are stable and enzymatic catalytic at high temperatures (Ladenstein and Antranikian, 1998) and the optimal growth-temperature of the thermophilic *T. elongatus* is 55-60 °C (DSMZ, Braunschweig, Germany), the activity test was also performed at 55 °C. In this case the *T. elongatus* PBGS showed a slightly increase in activity but the *P. aeruginosa* PBGS lost strikingly activity. On the other hand an incubation temperature of 37 °C, which is optimal for *P. aeruginosa* PBGS, decreased significantly the activity of *T. elongatus* PBGS (data not shown). With the obtained results it was possible to demonstrate optimal conditions for *T. elongatus* PBGS production and purification. Furthermore first investigations of *T. elongatus* PBGS activity were performed providing the first step towards further biochemical and structural investigations.

3.2.2 Cloning, Production and Purification of Recombinant Uroporphyrinogen III Synthase

Initial investigations to study the interaction between UROS and PBGD were performed by Frederike Frese during her diploma thesis in our laboratoury. Therefore, PBGD from *T. elongatus* and UROS from *B. megaterium* were used for interaction studies *via* co-immunoprecipitation. *T. elongatus* UROS was also cloned into an expression vector, but unfortunately the produced protein degraded during cell disruption. Consequently, another approach was attempted to find an expression system to produce UROS from *T. elongatus* without degradation.

In our group solid experiences have been made using *B. megaterium* for protein production over the years (Biedendieck *et al.*, 2007). *B. megaterium* demonstrated high plasmid stability and does not possess any alkaline proteases degrading recombinant proteins (Kim, 2003). Additionally, it has been shown that protein production in *B. megaterium* is sensitive to the codon usage of the target gene (Yang *et al.*, 2007). For that reason, the *T. elongatus hemD* DNA sequence was optimised for protein production in *B. megaterium* using the program JCAT

(www.jcat.de; Grote *et al.*, 2005). The correlation of the codon occurrence within the target gene and the preferred codons of the host are indicated as the “codon adaptation index” (CAI). This value can range from 0 (no similarity) to 1 (identical codon usage). It was found that genes with a CAI below 0.3 are not expressed in significant amounts in *B. megaterium* (Bäumchen *et al*., 2007; Yang *et al*., 2007). The original *T. elongatus hemD* DNA sequence showed a CAI of 0.29. The optimised *hemD* gene was generated by GeneArt (Regensburg, Germany) with a new calculated CAI of 0.85. The synthetic gene still encodes the original amino acid sequence of *T. elongatus* UROS. The synthetic gene was inserted into two different expression vectors. *Bgl*II and *Sph*I restriction sites were used for pN-HIS-TEV1622 (encoding an N-terminal His_6-tag) and *Spe*I and *Sph*I were used for pKMBm4 into which an additional His_6-tag was cloned as described in MATERIALS AND METHODS (Biedendieck *et al.*, 2007; Stammen *et al.*, 2010). Both constructs produced a fusion protein with an N-terminal His_6-tag and were sequenced for verification. Protoplasts of *B. megaterium* MS941 were transformed and analysed for recombinant protein production after induction of gene expression with 0.5 % xylose. Samples of proteins were taken from the cultures 3, 4, 5 and 15 hours after induction at 37 °C. The intracellular proteins were separated into soluble and insoluble fractions and were analysed by SDS-PAGE. Two clones of *B. megaterium* containing pN-HIS-TEV1622-hemD were analysed for recombinant protein production of UROS by SDS-PAGE. Analysis of soluble proteins (Figure 3.9) revealed no visible production of UROS which would be recognised by a band corresponding to a protein with a calculated relative molecular mass of 54,000. In analysis of the insoluble proteins no visible production of UROS could be determined either (data not shown).

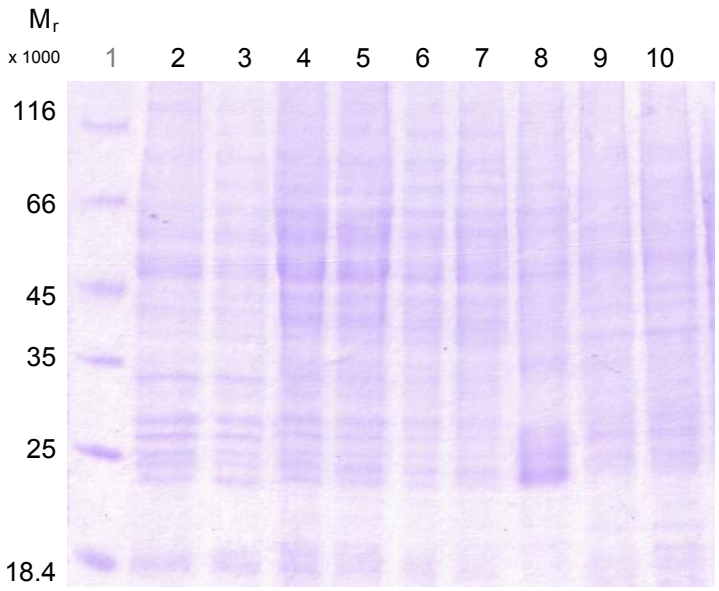

Figure. 3.9: Production of recombinant *T. elongatus* uroporphyrinogen III synthase in *B. megaterium*.

Two *B. megaterium* clones containing pN-HIS-TEV1622-hemD were analysed for protein production. Proteins were separated by 12 % SDS-PAGE and visualised by staining with Coomassie Brilliant Blue. Lane 1: molecular weight marker; lane 2: total cellular extract without induction of gene expression; lanes 3-6: total soluble protein of *B. megaterium* clone 1 after 3, 4, 5 and 15 hours induction of gene expression with 0.5 % xylose. Lanes 7-10: total soluble protein of *B. megaterium* clone 2 after 3, 4, 5 and 15 hours induction of gene expression with 0.5 % xylose. SDS-PAGE analysis revealed no protein production which would be recognised by an additional band with a calculated approximately molecular mass of 54,000.

Additionally, Western blot analysis of the soluble and insoluble proteins was performed to verify the results using a primary anti His_6-tag antibody from mouse and a secondary anti mouse antibody coupled to an alkaline phosphatase. Induction with NBT and BCIP led to visualisation of two soluble proteins (Figure 3.10). The detected protein with an approximately molecular mass of 35,000 is known to be the *B. megaterium* host protein CbiX (Leech *et al.*, 2003). CbiX is the sirohydrochlorin cobaltochelatase (EC 4.99.1.3) which is necessary for vitamin B_{12} biosynthesis and includes a natural His_6 amino acid sequence. Therefore, CbiX is always detectable in small amounts in the *B. megaterium* cell. The protein band corresponding to a protein with an approximately molecular mass of 40,000 should be the expected recombinantly produced UROS. Unfortunately, this does not correspond to the calculated relative molecular mass of the fusion protein of 54,000.

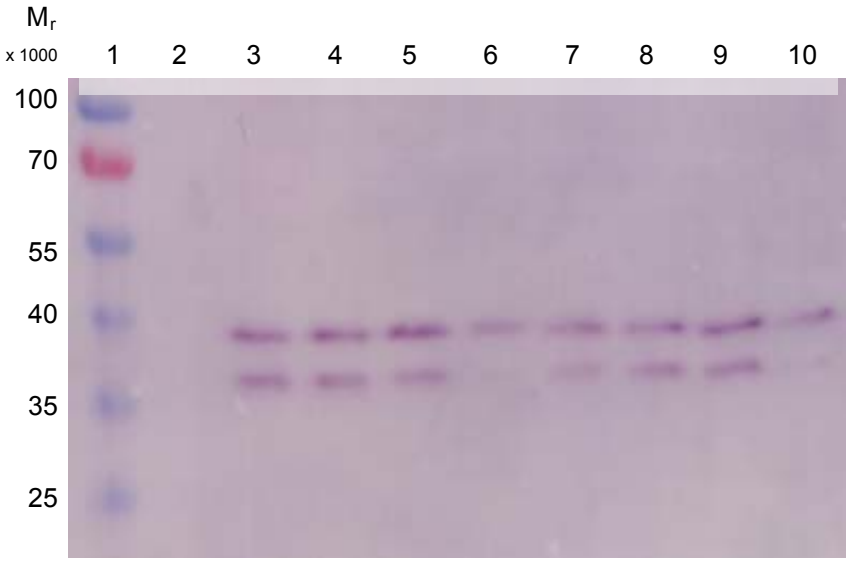

Figure 3.10: Western blot analysis of the production of recombinant *T. elongatus* uroporphyrinogen III synthase in *B. megaterium*.

Two *B. megaterium* clones were analysed for protein production by Western blot analysis. Proteins were detected with a primary anti His_6-tag mouse antibody followed by an anti mouse antibody coupled to an alkaline phosphatase. Induction with NBT and BCIP led to visualisation of proteins. Lane 1: molecular weight marker; lane 2: total cellular extract without induction of gene expression; lanes 3-6: total soluble protein of *B. megaterium* clone 1 after 3, 4, 5 and 15 hours induction of gene expression with 0.5 % xylose. Lanes 7-10: total soluble protein of *B. megaterium* clone 2 after 3, 4, 5 and 15 hours induction of gene expression with 0.5 % xylose. Two protein bands were detected. The lower approximately 35,000 protein is known to be the homolog protein CbiX of *B. megaterium* which includes a His_6 amino acid sequence. The upper detected protein with approximately 40,000 should be the expected recombinantly produced UROS.

The succeeding analysis of the *hemD* gene by sequencing did not reveal mutation of the gene or frame shift in the in the expression vector. Again the fusion protein seemed to be instable or degraded in the cell maybe because of its toxicity to *B. megaterium*. Nevertheless, the cell-free extract was purified using a Ni^{2+}-NTA affinity chromatography column and subsequently loaded onto a gel-permeation column in an attempt to separate the two remaining proteins CbiX and “UROS” by size. After the two purification steps SDS-PAGE and Western blot analyses revealed that the protein concentration decreased extremely and no obvious separation could be observed (data not shown). Another approach was to separate the two proteins by heating the protein containing solution to 70 °C for 20 min. Since *T. elongatus* proteins are stable at high temperatures (Ladenstein and Antranikian, 1998), the host’s CbiX protein should degrade while UROS stays soluble. Anyway, again Western blot analysis illustrated failure of this approach.

The other expression vector pKMBm4-hemD was tested in *B. megaterium* for recombinant UROS production according to the previous analysis of vector construct pN-HIS-TEV1622-hemD. SDS-PAGE analysis of soluble and insoluble proteins revealed no visible production of UROS (data not shown). Finally, Western blot analysis only showed the CbiX protein while UROS was not detectable, although gene analysis was proper by sequencing (data not shown).
So, the already suitable vector pGEX-6P-1 containing the *T. elongatus hemD* gene (Frese, 2008) was used for an approach for protein production. Therefore, the use of different *E. coli* bacterial strains was endeavoured to solve the problem of protein degradation during cell growth. After testing several *E. coli* strains the best result of recombinant protein production were obtained in *E. coli* Rossetta (DE3)pLysS. Induction of protein production with 400 µM isopropyl-β-D-thiogalactopyranoside (IPTG) led to successful recombinant production at 25 °C of the N-terminal glutathione-S-transferase-tag (GST) fusion protein UROS. SDS-PAGE analysis of the cell-free extract and the cell extract revealed an overproduction of a protein with a relative molecular mass of approximately 70,000 (Figure 3.11; lane 4). This is in good agreement with the calculated molecular mass of the fusion protein UROS of 78,000. However, the overproduced protein UROS was found exclusively in the insoluble cellular extract.

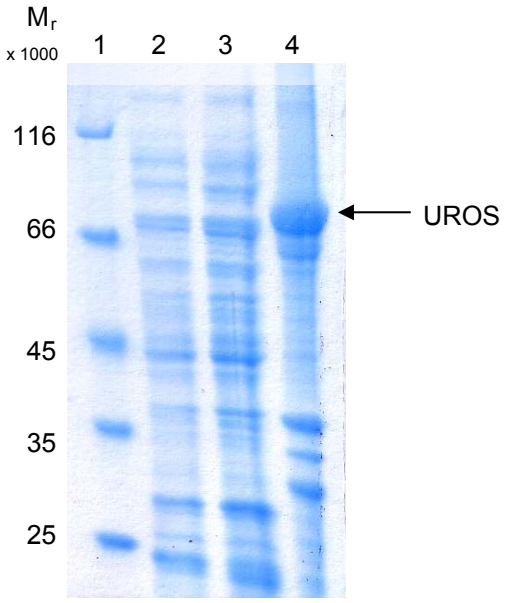

Figure 3.11: Production and solubility of recombinant *T. elongatus* uroporphyrinogen III synthase (UROS) produced in *E. coli*.

Proteins were separated by 12 % SDS-PAGE and visualised by staining with InstantBlue. Lane 1: molecular weight marker; lane 2: total cellular extract without induction of gene expression; lane 3: total soluble protein after overnight induction of gene expression with 400 µM IPTG; lane 4: total cellular extract after overnight induction of gene expression with 400 µM IPTG. Lane 4 shows a additional protein with an approximately molecular mass of 70,000.

Approaches to solubilise the protein by adding detergents like CAPS, TritonX-100, Tesit or octyl glucoside in concentrations of about 0.2 up to 2 % to the lysis buffer and repeatedly disruption of the cell extract did not show improvement. All attempts to recombinantly produce soluble UROS in other *E. coli* production strains by induction with different IPTG concentrations at varying incubation temperatures in diverse time intervals failed. If protein production was obtained, different buffers for cell lyses in a pH range of 6.8 up to 8.0 were tested, as well as using expression vectors with other affinity-tags.

3.2.3 Cloning, Production and Purification of Recombinant Uroporphyrinogen III Decarboxylase and Recombinant Oxygen-Independent Coproporphyrinogen III Oxidase

The *T. elongatus* uroporphyrinogen III decarboxylase gene (*hemE*; EC 4.1.1.37) and the oxygen-independent coproporphyrinogen III oxidase gene (*hemN*; EC 1.3.3.3) were cloned under the control of the T7-RNA-polymerase promotor into standard *E. coli* expression vectors. The *hemE* gene was inserted into pET32a with the restriction sides *Eco*RI and *Not*I, resulting in a fusion protein with a C-terminal histidine-tag. While the *hemN* gene was cloned into pGEX-6P-1 with the restriction sides *Eco*RI and *Not*I, resulting in a fusion protein with an N-terminal glutathione-S-transferase-tag (GST). Several *E. coli* strains were tested for recombinant protein production. Induction of protein production with 400 µM isopropyl-β-D-thiogalactopyranoside (IPTG) led to successful recombinant production of the C-terminal histidine-tagged fusion protein uroporphyrinogen III decarboxylase (UROD) in the *E. coli* strain Rossetta gami 2. Recombinant oxygen-independent coproporphyrinogen III oxidase (CPO) was produced in *E. coli* Rossetta (DE3)pLysS as a fusion protein with a N-terminal GST-tag by induction with 400 µM IPTG.

Samples of protein were taken from the cultures 5, 6, 7 and 20 hours after induction at 25 °C. SDS-PAGE analysis of cell-free extract and cell extract of both proteins revealed in each case an overproduction of a protein that is corresponding to a relative molecular mass of approximately 55,000 (UROD; Figure 3.12, lane 5) and 80,000 (CPO; Figure 3.12, lane 3) after 20 hours. This is

in good agreement with the calculated molecular mass of the fusion protein UROD of 53,000 and CPO of 77,000.

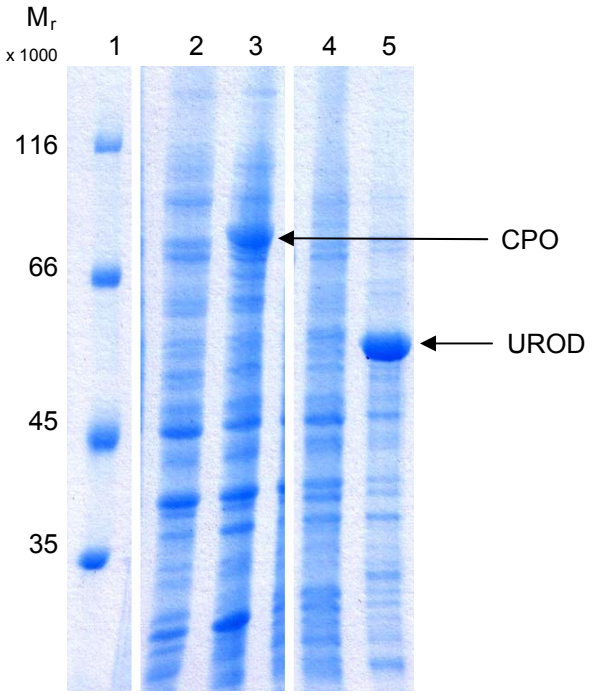

Figure 3.12: Production and solubility of recombinant *T. elongatus* uroporphyrinogen III decarboxylase (UROD) and oxygen-independent coproporphyrinogen III oxidase (CPO) produced in *E. coli*.

Proteins were separated by 12 % SDS-PAGE and visualised by staining with InstantBlue. Lane 1: molecular weight marker; lane 2: total soluble protein after overnight induction of gene expression with 400 µM IPTG for CPO production; lane 3: total cellular extract after overnight induction of gene expression with 400 µM IPTG for CPO; lane 4: total soluble protein after overnight induction of gene expression with 400 µM IPTG for UROD production; lane 3: total cellular extract after overnight induction of gene expression with 400 µM IPTG for UROD. An additional dominant protein band is visible in lane 3 for CPO with an approximately relative molecular mass of 80,000 and in lane 5 for UROD with an approximately relative molecular mass of 55,000, respectively.

However, both overproduced proteins were found exclusively in the insoluble cellular extracts (UROD: Figure 3.12, lane 5; CPO: Figure 3.12 lane 3). In order to solubilise UROD and CPO, the insoluble fractions and cell debris of *E. coli* were suspended in lysis buffer containing additionally detergents, like CAPS, TritonX-100, Tesit or octyl glucoside ranging from 0.2-2 %, and repeatedly disruption of the cell extract revealed different results. In case of UROD following SDS-PAGE analysis did not show improvement (data not shown). The test solubility of CPO with additionally TritonX-100 was increased in small amount but led to degradation of the protein (data not shown) within 24 hours, so no purification procedure was practicable. First investigations to produce recombinant soluble UROD and CPO using other *E. coli* production strains by induction with different IPTG concentrations at varying incubation temperatures in diverse time intervals failed. When protein production was obtained, different buffers for cell lyses in a pH range of 6.8 up to 8.0 were tested, as well as using expression vectors with other affinity-tags. All strategies did not show any success.

4 SUMMARY

During haem biosynthesis uroporphyrinogen III decarboxylase (UROD) catalyses the successive decarboxylation of uroporphyrinogen III acetate subunits to form coproporphyrinogen III. Dysfunction of this enzyme causes the disease porphyria cutanea tarda in humans.
Based on amino acid sequence comparison of human UROD with UROD from other organisms, the crystal structure of human UROD (Whitby *et al*., 1998) and recently newly density-functional studies of the mechanism, two highly conserved arginine residues were proposed to be important for catalysis. Therefore, the arginine 37 and 41 residues of human UROD were exchanged by site-directed mutagenesis to investigate their functional role. Wild type and mutant UROD were recombinantly produced in *E. coli*, purified and biochemically characterised. The enzymatically influence of these residues were determined by analysing the UROD activity assay mixture by HPLC analysis.
It could be shown that the exchange of the positively charged amino acids Arg37 and Arg41 abolish the enzyme activity of UROD. The necessity of the interaction of these two arginine residues for substrate binding, coordination in the active site cleft and decarboxylation was demonstrated.

A second part of this thesis focused on interactions and existence of protein complexes of different enzymes involved into early steps of tetrapyrrole biosynthesis in *Thermosynechococcus elongatus*. For the protection of highly cell-toxic tetrapyrrole intermediates in the biosynthesis, it is proposed that the involved enzymes form complexes to channel the intermediates.
Here *T. elongatus hemB* (PBGS), *hemE* (UROD) and *hemN* (CPO) were cloned into expression vectors. These proteins and an already existing cloned *hemD* gene (UROS) were recombinantly produced in *E. coli*. PBGS was successfully chromatographically purified and enzymatic activity could be revealed. However, the overproduced protein UROS, UROD and CPO were found exclusively in the insoluble cellular extract. Initial approaches to solubilise the protein were performed.

5 OUTLOOK

Characterisation of human Uroporphyrinogen III Decarboxylase:

The results of this work let conclude that the exchange of the positively charged amino acids Arg37 and Arg41 abolishes enzyme activity. The interaction of this two arginine residues are important for substrate binding, coordination in the active site cleft and decarboxylation, respectively.
Further studies using molecular analysis could be performed in order to reveal the residues importance.

1.) Mutagenesis studies of Arg37, Arg41 and Asp86 (human numbering) in other organism's UROD.
2.) Co-crystallisation experiments of the human mutant variants R37A, R37K, R41A and R41K with its substrate uroporphyrinogen III or product coproporphyrinogen III in order to study the UROD conformation and the substrate and/or product coordination in the active site cleft.

***Thermosynechococcus elongatus* Haem Proteins:**

Porphobilinogen Synthase (PBGS):

In this study it was possible to develop recombinant porphobilinogen synthase production, purification and initial corresponding activity. These were the first steps towards characterisation. Further studies have to be carried out to determine its features more closely.

1.) Determination of kinetic parameters, optimal temperature and pH dependence.
2.) Investigation on the oligomeric state of the native protein.
3.) Screening for stereochemical derivatives of alaremycin as potential PBGS inhibitors that specifically inhibit exclusively bacterial PBGS.

Uroporphyrinogen III Synthase, Uroporphyrinogen III Decarboxylase & Oxygen-independent Coproporphyrinogen III Oxidase:

In this study it was possible to develop recombinant enzyme production. However, all three enzymes were insoluble. It is necessary to perform further investigations towards the protein solubility.
Additionally, following investigations should be performed:

1.) Co-cloning of uroporphyrinogen III synthase with porphobilinogen deaminse, which may stabilise the protein and support correct folding of uroporphyrinogen III synthase.
2.) Recombinant production of uroporphyrinogen III decarboxylase and coproporphyrinogen III oxidase in *Bacillus megaterium* or co-cloning into the same expression vector, to stabilise the protein and support protein folding.
3.) Another attempt to yield soluble coproporphyrinogen III oxidase could be strict anaerobic conditions during cells disruption and purification.

All four proteins should be studied to determine their features more closely.

1.) Determination of kinetic parameters, optimal temperature and pH dependence.
2.) Investigation on the oligomeric state of the native protein.
3.) Crystallisation of *T. elongatus* proteins.
4.) Antibody production for interaction and complex formation studies *in vitro* and *in vivo*.

6 REFERENCES

Akhtar, M. (1994) The modification of acetate and propionate side chains during the biosynthesis of haem and chlorophylls: mechanistic and stereochemical studies. In *Ciba Foundation Symposium 180 - The Biosynthesis of the Tetrapyrrole Pigments*. Chadwick, D.J. and Ackrill, K. (eds). Chichester, UK: Wiley and Sons, pp. 131-151; discussion 152-135.

Amillet, J.M., and Labbe-Bois, R. (1995) Isolation of the gene HEM4 encoding uroporphyrinogen III synthase in *Saccharomyces cerevisiae*. *Yeast* **11**: 419-424.

Awa, Y., Iwai, N., Ueda, T., Suzuki, K., Asano, S., Yamagishi, J., Nagai, K., and Wachi, M. (2005) Isolation of a new antibiotic, alaremycin, structurally related to 5-aminolevulinic acid from *Streptomyces* sp. A012304. *Biosci Biotechnol Biochem* **69**: 1721-1725.

Barnard, G.F., and Akhtar, M. (1979) Stereochemical and mechanistic studies on the decarboxylation of uroporphyrinogen III in haem biosynthesis. *J Chem Soc Perkin 1* **10**: 2354-2360.

Battersby, A.R., Fookes, C.J.R., McDonald, E., and Meegan, M.J. (1978) Biosynthesis of type-III porphyrins: proof of intact enzymic conversion of the head-to-tail bilane into uro'gen-III by intramolecular rearrangement. *J. Chem. Soc., Chem. Commun.*: 185.

Battersby, A.R., Fookes, C.J.R., Gustafson-Potter, K.E., Matcham, G.W.J., and McDonald, E. (1979) Proof of synthesis that unrearranged hydroxymethylbilane is the product fram deaminase and the substrate for cosynthase in the biosynthesis of uro'gen-III. *J Chem Soc, Chem Commun*: 1155-1158.

Battersby, A.R., and Leeper, F.J. (1990) Biosynthesis of the pigments of life: mechanistic studies on the conversion of porphobilinogen to uroporphyrinogen III. *Chem. Rev* **90**: 1261-1274.

Battersby, A.R. (2000) Tetrapyrroles: the pigments of life. *Nat Prod Rep* **17**: 507-526.

Bäumchen, C., Roth, A.H., Biedendieck, R., Malten, M., Follmann, M., Sahm, H., Bringer-Meyer, S., and Jahn, D. (2007) D-mannitol production by resting state whole cell biotrans-formation of D-fructose by heterologous mannitol and formate dehydrogenase gene expression in *Bacillus megaterium*. *Biotechnol J* **2**: 1408-1416.

Beale, S.I., and Castelfranco, P.A. (1973) ^{14}C incorporation from exogenous compounds into delta-aminolevulinic acid by greening cucumber cotyledons. *Biochem Biophys Res Commun* **52**: 143-149.

Beale, S.I. (1999) Enzymes of chlorophyll biosynthesis. *Photosynthesis research* **60**: 43-73.

Biedendieck, R., Yang, Y., Deckwer, W.D., Malten, M., and Jahn, D. (2007) Plasmid system for the intracellular production and purification of affinity-tagged proteins in *Bacillus megaterium*. *Biotechnol Bioeng* **96**: 525-537.

Bogorad, L., and Granick, S. (1953) The enzymatic synthesis of porphyrins from porphobilinogen. *Proc Natl Acad Sci U S A* **39**: 1176-1188.

Bogorad, L. (1958a) The enzymatic synthesis of porphyrins from porphobilinogen. II. Uroporphyrin III. *J Biol Chem* **233**: 510-515.

Bogorad, L. (1958b) The enzymatic synthesis of porphyrins from porphobilinogen. III. Uroporphyrinogens as intermediates. *J Biol Chem* **233**: 516-519.

Breckau, D., Mahlitz, E., Sauerwald, A., Layer, G., and Jahn, D. (2003) Oxygen-dependent coproporphyrinogen III oxidase (HemF) from *Escherichia coli* is stimulated by manganese. *J Biol Chem* **278**: 46625-46631.

Breinig, S., Kervinen, J., Stith, L., Wasson, A.S., Fairman, R., Wlodawer, A., Zdanov, A., and Jaffe, E.K. (2003) Control of tetrapyrrole biosynthesis by alternate quaternary forms of porphobilinogen synthase. *Nat Struct Biol* **10**: 757-763.

Burton, G., Fagerness, P.E., Hosozawa, S., Jordan, P.M., and Scott, A.I. (1979) ^{13}C n.m.r. evidence for a new intermediate, pre-uroporphyrinogen, in the enzymic transformation of porphobilinogen into uroporphyrinogens I and III. *J. Chem. Soc., Chem. Commun.*: 202.

Cassidy, M.A., Crockett, N., Leeper, F.J., and Battersby, A.R. (1996) Biosynthesis of porphyrins and related macrocycles. Part 44. Synthetic and stereochemical studies on the proposed spiro intermediate for biosynthesis of the natural porphyrins. *J Chem Soc Perkin Trans 1*: 2079-2090.

Chadwick, D.J., and Ackrill, K. (1994) *The Biosynthesis of Tetrapyrrole Pigments.* Chichester, UK: Wiley and Sons.

Chang, C.K., and Wu, W. (1986) The porphinedione structure of heme d1. Synthesis and spectral properties of model compounds of the prosthetic group of dissimilatory nitrite reductase. *J Biol Chem* **261**: 8593-8596.

Chang, C.K. (1994) Haem *d1* and other haem cofactors from bacteria. In *Ciba Foundation Symposium 180 - The Biosynthesis of the Tetrapyrrole Pigments*. Chadwick, D.J. and Ackrill, K. (eds). Chichester, UK: Wiley and Sons, pp. 228-238; discussion 238-246.

Coomber, S.A., Jones, R.M., Jordan, P.M., and Hunter, C.N. (1992) A putative anaerobic coproporphyrinogen III oxidase in *Rhodobacter sphaeroides*. I. Molecular cloning, transposon mutagenesis and sequence analysis of the gene. *Mol Microbiol* **6**: 3159-3169.

Crockett, N., Alefounder, P.R., Battersby, A.R., and Abell, C. (1991) Uroporphyrinogen III synthase: Studies on its mechanism of action, molecular biology and biochemisty. *Tetrahedron* **47**: 6003-6014.

Dammeyer, T., and Frankenberg-Dinkel, N. (2008) Function and distribution of bilin biosynthesis enzymes in photosynthetic organisms. *Photochem Photobiol Sci* **7**: 1121-1130.

de Verneuil, H., Grandchamp, B., and Nordmann, Y. (1980) Some kinetic properties of human red cell uroporphyrinogen decarboxylase. *Biochim Biophys Acta* **611**: 174-186.

de Verneuil, H., Sassa, S., and Kappas, A. (1983) Purification and properties of uroporphyrinogen decarboxylase from human erythrocytes. A single enzyme catalyzing the four sequential decarboxylations of uroporphyrinogens I and III. *J Biol Chem* **258**: 2454-2460.

Elder, G.H., and Roberts, A.G. (1995) Uroporphyrinogen decarboxylase. *J Bioenerg Biomembr* **27**: 207-214.

Erskine, P.T., Newbold, R., Roper, J., Coker, A., Warren, M.J., Shoolingin-Jordan, P.M., Wood, S.P., and Cooper, J.B. (1999a) The Schiff base complex of yeast 5-aminolaevulinic acid dehydratase with laevulinic acid. *Protein Sci* **8**: 1250-1256.

Erskine, P.T., Norton, E., Cooper, J.B., Lambert, R., Coker, A., Lewis, G., Spencer, P., Sarwar, M., Wood, S.P., Warren, M.J., and Shoolingin-Jordan, P.M. (1999b) X-ray structure of 5-aminolevulinic acid dehydratase from *Escherichia coli* complexed with the inhibitor levulinic acid at 2.0 A resolution. *Biochemistry* **38**: 4266-4276.

Fan, J., Liu, Q., Hao, Q., Teng, M., and Niu, L. (2007) Crystal structure of uroporphyrinogen decarboxylase from *Bacillus subtilis*. *J Bacteriol* **189**: 3573-3580.

Felix, F., and Brouillet, N. (1990) Purification and properties of uroporphyrinogen decarboxylase from *Saccharomyces cerevisiae*. Yeast uroporphyrinogen decarboxylase. *Eur J Biochem* **188**: 393-403.

Frankenberg, N., Erskine, P.T., Cooper, J.B., Shoolingin-Jordan, P.M., Jahn, D., and Heinz, D.W. (1999a) High resolution crystal structure of a Mg^{2+}-dependent porphobilinogen synthase. *J Mol Biol* **289**: 591-602.

Frankenberg, N., Heinz, D.W., and Jahn, D. (1999b) Production, purification, and characterization of a Mg2+-responsive porphobilinogen synthase from *Pseudomonas aeruginosa*. *Biochemistry* **38**: 13968-13975.

Frankenberg, N., and Lagarias, J.C. (2003) Biosynthesis and biological functions of bilins. In *The porphyrin handbook*. Kadish, K.M., Smith, K.M. and Guilard, R. (eds). Amsterdam, NL: Elsevier.

Frankenberg, N., Moser, J., and Jahn, D. (2003) Bacterial heme biosynthesis and its biotechnological application. *Appl Microbiol Biotechnol* **63**: 115-127.

Fraser, D.J., Podvinec, M., Kaufmann, M.R., and Meyer, U.A. (2002) Drugs mediate the transcriptional activation of the 5-aminolevulinic acid synthase (ALAS1) gene via the chicken xenobiotic-sensing nuclear receptor (CXR). *J Biol Chem* **277**: 34717-34726.

Frere, F., Schubert, W.D., Stauffer, F., Frankenberg, N., Neier, R., Jahn, D., and Heinz, D.W. (2002) Structure of porphobilinogen synthase from *Pseudomonas aeruginosa* in complex with 5-fluorolevulinic acid suggests a double Schiff base mechanism. *J Mol Biol* **320**: 237-247.

Frere, F., Reents, H., Schubert, W.D., Heinz, D.W., and Jahn, D. (2005) Tracking the evolution of porphobilinogen synthase metal dependence in vitro. *J Mol Biol* **345**: 1059-1070.

Frere, F., Nentwich, M., Gacond, S., Heinz, D.W., Neier, R., and Frankenberg-Dinkel, N. (2006) Probing the active site of *Pseudomonas aeruginosa* porphobilinogen synthase using newly developed inhibitors. *Biochemistry* **45**: 8243-8253.

Frese, F. (2008) Wechselwirkung von Enzymen der Hämbiosynthese aus *Thermosynechococcus elongatus*. In *Institute für Mikrobiologie*. Vol. Diplomarbeit Braunschweig: Technische Universität Carolo-Wilhelmina.

Friedmann, H.C., Klein, A., and Thauer, R.K. (1990) Structure and function of the nickel porphinoid, coenzyme F430 and of its enzyme, methyl coenzyme M reductase. *FEMS Microbiol Rev* **7**: 339-348.

Grandchamp, B., and Nordmann, Y. (1982) Coproporphyrinogen III oxidase assay. *Enzyme* **28**: 196-205.

Grote, A., Hiller, K., Scheer, M., Munch, R., Nortemann, B., Hempel, D.C., and Jahn, D. (2005) JCat: a novel tool to adapt codon usage of a target gene to its potential expression host. *Nucleic Acids Res* **33**: W526-531.

Hansson, M., and Hederstedt, L. (1992) Cloning and characterization of the *Bacillus subtilis hemEHY* gene cluster, which encodes protoheme IX biosynthetic enzymes. *J Bacteriol* **174**: 8081-8093.

Hansson, M., and Hederstedt, L. (1994) *Bacillus subtilis* HemY is a peripheral membrane protein essential for protoheme IX synthesis which can oxidize coproporphyrinogen III and protoporphyrinogen IX. *J Bacteriol* **176**: 5962-5970.

Hart, G.J., and Battersby, A.R. (1985) Purification and properties of uroporphyrinogen III synthase (co-synthetase) from *Euglena gracilis*. *Biochem J* **232**: 151-160.

Heinemann, I.U. (2007) Structure and function of enzymes involved in tetrapyrrole biosynthesis. In *Institut für Mikrobiologie*. Vol. Doktorarbeit Braunschweig: Technische Universität Carolo-Wilhelmina.

Heinemann, I.U., Jahn, M., and Jahn, D. (2008) The biochemistry of heme biosynthesis. *Arch Biochem Biophys* **474**: 238-251.

Heinemann, I.U., Schulz, C., Schubert, W.D., Heinz, D.W., Wang, Y.G., Kobayashi, Y., Awa, Y., Wachi, M., Jahn, D., and Jahn, M. (2010) Structure of the heme biosynthetic *Pseudomonas aeruginosa* porphobilinogen synthase in complex with the antibiotic alaremycin. *Antimicrob Agents Chemother* **54**: 267-272.

Homuth, G., Rompf, A., Schumann, W., and Jahn, D. (1999) Transcriptional control of *Bacillus subtilis hemN* and *hemZ*. *J Bacteriol* **181**: 5922-5929.

Hunter, G.A., Zhang, J., and Ferreira, G.C. (2007) Transient kinetic studies support refinements to the chemical and kinetic mechanisms of aminolevulinate synthase. *J Biol Chem* **282**: 23025-23035.

Hunter, G.A., and Ferreira, G.C. (2009) 5-aminolevulinate synthase: catalysis of the first step of heme biosynthesis. *Cell Mol Biol (Noisy-le-grand)* **55**: 102-110.

Jackson, A.H., Sancovich, H.A., Ferramola, A.M., Evans, N., Games, D.E., Matlin, S.A., Elder, G.H., and Smith, S.G. (1976) Macrocyclic intermediates in the biosynthesis of porphyrins. *Philos Trans R Soc Lond B Biol Sci* **273**: 191-206.

Jackson, A.H., Jones, D.M., Philip, G., Lash, T.D., Batlle, A.M., and Smith, S.G. (1980a) Synthetic and biosynthetic studies of porphyrins, Part IV. Further studies of the conversion of corporporhyrinogen-III to protoporphyrin-IX: mass spectrometric investigations of the incubation of specifically deuteriated coproporhyringen-III with chicken red cell haemolysates. *Int J Biochem* **12**: 681-688.

Jackson, A.H., Lash, T.D., Ryder, D.J., and Smith, S.G. (1980b) Synthetic and biosynthetic studies of porphyrins, Part V. Evidence for an alternative pathway in the biosynthesis of haem. *Int J Biochem* **12**: 775-780.

Jacobs, N.J., and Jacobs, J.M. (1975) Fumarate as alternate electron acceptor for the late steps of anaerobic heme synthesis in Escherichia coli. *Biochem Biophys Res Commun* **65**: 435-441.

Jacobs, N.J., and Jacobs, J.M. (1976) Nitrate, fumarate, and oxygen as electron acceptors for a late step in microbial heme synthesis. *Biochim Biophys Acta* **449**: 1-9.

Jaffe, E.K., Martins, J., Li, J., Kervinen, J., and Dunbrack, R.L., Jr. (2001) The molecular mechanism of lead inhibition of human porphobilinogen synthase. *J Biol Chem* **276**: 1531-1537.

Jaffe, E.K. (2003) An unusual phylogenetic variation in the metal ion binding sites of porphobilinogen synthase. *Chem Biol* **10**: 25-34.

Jahn, D., Verkamp, E., and Soll, D. (1992) Glutamyl-transfer RNA: a precursor of heme and chlorophyll biosynthesis. *Trends Biochem Sci* **17**: 215-218.

Jahn, D., Hungerer, C., and Troup, B. (1996) [Unusual pathways and environmentally regulated genes of bacterial heme biosynthesis]. *Naturwissenschaften* **83**: 389-400.

Jones, R.M., and Jordan, P.M. (1993) Purification and properties of the uroporphyrinogen decarboxylase from *Rhodobacter sphaeroides*. *Biochem J* **293 (Pt 3)**: 703-712.

Jordan, P.M., Burton, G., Nordlov, H., Schneider, M.M., Pryde, L., and Scott, A.I. (1979) Pre-uroporphyrinogen: a substrate for uroporphyrinogen III cosynthetase. *J. Chem. Soc., Chem. Commun.*: 204.

Jordan, P.M., and Berry, A. (1980) Preuroporphyrinogen, a universal intermediate in the biosynthesis of uroporphyrinogen III. *FEBS Lett* **112**: 86-88.

Jordan, P.M., and Warren, M.J. (1987) Evidence for a dipyrromethane cofactor at the catalytic site of *E. coli* porphobilinogen deaminase. *FEBS Lett* **225**: 87-92.

Jordan, P.M., Mgbeje, B.I., Thomas, S.D., and Alwan, A.F. (1988) Nucleotide sequence for the *hemD* gene of *Escherichia coli* encoding uroporphyrinogen III synthase and initial evidence for a hem operon. *Biochem J* **249**: 613-616.

Jordan, P.M., and Woodcock, S.C. (1991) Mutagenesis of arginine residues in the catalytic cleft of *Escherichia coli* porphobilinogen deaminase that affects dipyrromethane cofactor assembly and tetrapyrrole chain initiation and elongation. *Biochem J* **280 (Pt 2)**: 445-449.

Jordan, P.M. (1994a) The biosynthesis of uroporphyrinogen III: mechanism of action of porphobilinogen deaminase. In *Ciba Foundation Symposium 180 - The Biosynthesis of the Tetrapyrrole Pigments*. Chadwick, D.J. and Ackrill, K. (eds). Chichester, UK: Wiley and Sons, pp. 70-89; discussion 89-96.

Jordan, P.M. (1994b) Highlights in haem biosynthesis. *Curr Opin Struct Biol* **4**: 902-911.

Jordan, P.M.e. (1991) Biosynthesis of tetrapyrroles. In *New comprehensive biochemistry*. Vol. 19. Neuberger, A. and van Deenen, L.L.M. (eds). Amsterdam, NL: Elservier.

Juknat, A.A., Seubert, A., Seubert, S., and Ippen, H. (1989) Studies on uroporphyrinogen decarboxylase of etiolated *Euglena gracilis Z*. *Eur J Biochem* **179**: 423-428.

Kaneko, T., Tanaka, A., Sato, S., Kotani, H., Sazuka, T., Miyajima, N., Sugiura, M., and Tabata, S. (1995) Sequence analysis of the genome of the unicellular cyanobacterium *Synechocystis* sp. strain PCC6803. I. Sequence features in the 1 Mb region from map positions 64% to 92% of the genome. *DNA Res* **2**: 153-166, 191-158.

Kauppinen, R. (2005) Porphyrias. *Lancet* **365**: 241-252.

Kikuchi, G., Kumar, A., Talmage, P., and Shemin, D. (1958) The enzymatic synthesis of delta-aminolevulinic acid. *J Biol Chem* **233**: 1214-1219.

Kim, J.Y. (2003) Overproduction and secretion of *Bacillus circulans* endo-beta-1,3-1,4-glucanase gene (*bglBC1*) in *B. subtilis* and *B. megaterium*. *Biotechnol Lett* **25**: 1445-1449.

Koch, M., Breithaupt, C., Kiefersauer, R., Freigang, J., Huber, R., and Messerschmidt, A. (2004) Crystal structure of protoporphyrinogen IX oxidase: a key enzyme in haem and chlorophyll biosynthesis. *Embo J* **23**: 1720-1728.

Kohashi, M., Clement, R.P., Tse, J., and Piper, W.N. (1984) Rat hepatic uroporphyrinogen III co-synthase. Purification and evidence for a bound folate coenzyme participating in the biosynthesis of uroporphyrinogen III. *Biochem J* **220**: 755-765.

Kohno, H., Furukawa, T., Yoshinaga, T., Tokunaga, R., and Taketani, S. (1993) Coproporphyrinogen oxidase. Purification, molecular cloning, and induction of mRNA during erythroid differentiation. *J Biol Chem* **268**: 21359-21363.

Kohno, H., Furukawa, T., Tokunaga, R., Taketani, S., and Yoshinaga, T. (1996) Mouse coproporphyrinogen oxidase is a copper-containing enzyme: expression in *Escherichia coli* and site-directed mutagenesis. *Biochim Biophys Acta* **1292**: 156-162.

Labbe, P., Camadro, J.M., and Chambon, H. (1985) Fluorometric assays for coproporphyrinogen oxidase and protoporphyrinogen oxidase. *Anal Biochem* **149**: 248-260.

Ladenstein, R., and Antranikian, G. (1998) Proteins from hyperthermophiles: stability and enzymatic catalysis close to the boiling point of water. *Adv Biochem Eng Biotechnol* **61**: 37-85.

Laemmli, U.K. (1970) Cleavage of structural proteins during the assembly of the head of bacteriophage T4. *Nature* **227**: 680-685.

Lash, T.D. (2005) The enigma of coproporphyrinogen oxidase: how does this unusual enzyme carry out oxidative decarboxylations to afford vinyl groups? *Bioorg Med Chem Lett* **15**: 4506-4509.

Layer, G., Verfurth, K., Mahlitz, E., and Jahn, D. (2002) Oxygen-independent coproporphyrinogen-III oxidase HemN from *Escherichia coli*. *J Biol Chem* **277**: 34136-34142.

Layer, G., Moser, J., Heinz, D.W., Jahn, D., and Schubert, W.D. (2003) Crystal structure of coproporphyrinogen III oxidase reveals cofactor geometry of Radical SAM enzymes. *Embo J* **22**: 6214-6224.

Layer, G., Grage, K., Teschner, T., Schunemann, V., Breckau, D., Masoumi, A., Jahn, M., Heathcote, P., Trautwein, A.X., and Jahn, D. (2005) Radical S-adenosylmethionine enzyme coproporphyrinogen III oxidase HemN: functional features of the [4Fe-4S] cluster and the two bound S-adenosyl-L-methionines. *J Biol Chem* **280**: 29038-29046.

Layer, G., Pierik, A.J., Trost, M., Rigby, S.E., Leech, H.K., Grage, K., Breckau, D., Astner, I., Jansch, L., Heathcote, P., Warren, M.J., Heinz, D.W., and Jahn, D. (2006) The substrate radical of *Escherichia coli* oxygen-independent coproporphyrinogen III oxidase HemN. *J Biol Chem* **281**: 15727-15734.

Layer, G., Reichelt, J., Jahn, D., and Heinz, D.W. (2010) Structure and function of enzymes in heme biosynthesis. *Protein Sci* **19**: 1137-1161.

Lee, D.S., Flachsova, E., Bodnarova, M., Demeler, B., Martasek, P., and Raman, C.S. (2005) Structural basis of hereditary coproporphyria. *Proc Natl Acad Sci U S A* **102**: 14232-14237.

Leech, H.K., Raux, E., McLean, K.J., Munro, A.W., Robinson, N.J., Borrelly, G.P., Malten, M., Jahn, D., Rigby, S.E., Heathcote, P., and Warren, M.J. (2003) Characterization of the cobaltochelatase CbiXL: evidence for a 4Fe-4S center housed within an MXCXXC motif. *J Biol Chem* **278**: 41900-41907.

Lermontova, I., Kruse, E., Mock, H.P., and Grimm, B. (1997) Cloning and characterization of a plastidal and a mitochondrial isoform of tobacco protoporphyrinogen IX oxidase. *Proc Natl Acad Sci U S A* **94**: 8895-8900.

Lewis, C.A., Jr., and Wolfenden, R. (2008) Uroporphyrinogen decarboxylation as a benchmark for the catalytic proficiency of enzymes. *Proc Natl Acad Sci U S A* **105**: 17328-17333.

Lieb, C., Siddiqui, R.A., Hippler, B., Jahn, D., and Friedrich, B. (1998) The *Alcaligenes eutrophus hemN* gene encoding the oxygen-independent coproporphyrinogen III oxidase, is required for heme biosynthesis during anaerobic growth. *Arch Microbiol* **169**: 52-60.

Louie, G.V., Brownlie, P.D., Lambert, R., Cooper, J.B., Blundell, T.L., Wood, S.P., Warren, M.J., Woodcock, S.C., and Jordan, P.M. (1992) Structure of porphobilinogen deaminase reveals a flexible multidomain polymerase with a single catalytic site. *Nature* **359**: 33-39.

Luer, C., Schauer, S., Mobius, K., Schulze, J., Schubert, W.D., Heinz, D.W., Jahn, D., and Moser, J. (2005) Complex formation between glutamyl-tRNA reductase and glutamate-1-semialdehyde 2,1-aminomutase in *Escherichia coli* during the initial reactions of porphyrin biosynthesis. *J Biol Chem* **280**: 18568-18572.

Luo, J., and Lim, C.K. (1993) Order of uroporphyrinogen III decarboxylation on incubation of porphobilinogen and uroporphyrinogen III with erythrocyte uroporphyrinogen decarboxylase. *Biochem J* **289 (Pt 2)**: 529-532.

Madsen, O., Sandal, L., Sandal, N.N., and Marcker, K.A. (1993) A soybean coproporphyrinogen oxidase gene is highly expressed in root nodules. *Plant Mol Biol* **23**: 35-43.

Martasek, P., Camadro, J.M., Delfau-Larue, M.H., Dumas, J.B., Montagne, J.J., de Verneuil, H., Labbe, P., and Grandchamp, B. (1994) Molecular cloning, sequencing, and functional expression of a cDNA encoding human coproporphyrinogen oxidase. *Proc Natl Acad Sci U S A* **91**: 3024-3028.

Martins, B.M., Grimm, B., Mock, H.P., Huber, R., and Messerschmidt, A. (2001a) Crystal structure and substrate binding modeling of the uroporphyrinogen-III decarboxylase from *Nicotiana tabacum*. Implications for the catalytic mechanism. *J Biol Chem* **276**: 44108-44116.

Martins, B.M., Grimm, B., Mock, H.P., Richter, G., Huber, R., and Messerschmidt, A. (2001b) Tobacco uroporphyrinogen-III decarboxylase: characterization, crystallization and preliminary X-ray analysis. *Acta Crystallogr D Biol Crystallogr* **57**: 1709-1711.

Masoumi, A., Heinemann, I.U., Rohde, M., Koch, M., Jahn, M., and Jahn, D. (2008) Complex formation between protoporphyrinogen IX oxidase and ferrochelatase during haem biosynthesis in *Thermosynechococcus elongatus*. *Microbiology* **154**: 3707-3714.

Mathews, M.A., Schubert, H.L., Whitby, F.G., Alexander, K.J., Schadick, K., Bergonia, H.A., Phillips, J.D., and Hill, C.P. (2001) Crystal structure of human uroporphyrinogen III synthase. *Embo J* **20**: 5832-5839.

Medlock, A.E., and Dailey, H.A. (1996) Human coproporphyrinogen oxidase is not a metalloprotein. *J Biol Chem* **271**: 32507-32510.

Meissner, P.N., Dailey, T.A., Hift, R.J., Ziman, M., Corrigall, A.V., Roberts, A.G., Meissner, D.M., Kirsch, R.E., and Dailey, H.A. (1996) A R59W mutation in human protoporphyrinogen oxidase results in decreased enzyme activity and is prevalent in South Africans with variegate porphyria. *Nat Genet* **13**: 95-97.

Möbius, K., Arias-Cartin, R., Breckau, D., Hannig, A.L., Riedmann, K., Biedendieck, R., Schroder, S., Becher, D., Magalon, A., Moser, J., Jahn, M., and Jahn, D. (2010) Heme biosynthesis is coupled to electron transport chains for energy generation. *Proc Natl Acad Sci U S A* **107**: 10436-10441.

Mock, H.P., and Grimm, B. (1997) Reduction of Uroporphyrinogen Decarboxylase by Antisense RNA Expression Affects Activities of Other Enzymes Involved in Tetrapyrrole Biosynthesis and Leads to Light-Dependent Necrosis. *Plant Physiol* **113**: 1101-1112.

Mock, H.P., Heller, W., Molina, A., Neubohn, B., Sandermann, H., Jr., and Grimm, B. (1999) Expression of uroporphyrinogen decarboxylase or coproporphyrinogen oxidase antisense RNA in tobacco induces pathogen defense responses conferring increased resistance to tobacco mosaic virus. *J Biol Chem* **274**: 4231-4238.

Moser, J., Schubert, W.D., Heinz, D.W., and Jahn, D. (2002) Structure and function of glutamyl-tRNA reductase involved in 5-aminolaevulinic acid formation. *Biochem Soc Trans* **30**: 579-584.

Munro, A.W., Girvan, H.M., McLean, K.J., Cheesman, M.R., and Leys, D. (2008) Heme and hemoproteins. In *Tetrapyrroles: Birth, Life and Death*. Warren, M.J. and Smith, A.G. (eds). Austin: Landes Bioscience, pp. 160-183.

Nagaraj, V.A., Arumugam, R., Chandra, N.R., Prasad, D., Rangarajan, P.N., and Padmanaban, G. (2009) Localisation of *Plasmodium falciparum* uroporphyrinogen III decarboxylase of the heme-biosynthetic pathway in the apicoplast and characterisation of its catalytic properties. *Int J Parasitol* **39**: 559-568.

Nishimura, K., Nakayashiki, T., and Inokuchi, H. (1993) Cloning and sequencing of the *hemE* gene encoding uroporphyrinogen III decarboxylase (UPD) from *Escherichia coli* K-12. *Gene* **133**: 109-113.

O'Brian, M.R., and Thony-Meyer, L. (2002) Biochemistry, regulation and genomics of haem biosynthesis in prokaryotes. *Adv Microb Physiol* **46**: 257-318.

Omata, Y., Sakamoto, H., Higashimoto, Y., Hayashi, S., and Noguchi, M. (2004) Purification and characterization of human uroporphyrinogen III synthase expressed in *Escherichia coli*. *J Biochem (Tokyo)* **136**: 211-220.

Panek, H., and O'Brian, M.R. (2002) A whole genome view of prokaryotic haem biosynthesis. *Microbiology* **148**: 2273-2282.

Phillips, J.D., Whitby, F.G., Kushner, J.P., and Hill, C.P. (1997) Characterization and crystallization of human uroporphyrinogen decarboxylase. *Protein Sci* **6**: 1343-1346.

Phillips, J.D., and Kushner, J.P. (1999) Measurement of Uroporphyrinogen Decarboxylase Activity. *Current Protocols in Toxicology*: 8.4.1-8.4.13.

Phillips, J.D., Parker, T.L., Schubert, H.L., Whitby, F.G., Hill, C.P., and Kushner, J.P. (2001) Functional consequences of naturally occurring mutations in human uroporphyrinogen decarboxylase. *Blood* **98**: 3179-3185.

Phillips, J.D., Whitby, F.G., Kushner, J.P., and Hill, C.P. (2003) Structural basis for tetrapyrrole coordination by uroporphyrinogen decarboxylase. *Embo J* **22**: 6225-6233.

Phillips, J.D., Whitby, F.G., Warby, C.A., Labbe, P., Yang, C., Pflugrath, J.W., Ferrara, J.D., Robinson, H., Kushner, J.P., and Hill, C.P. (2004) Crystal structure of the oxygen-dependant coproporphyrinogen oxidase (Hem13p) of *Saccharomyces cerevisiae*. *J Biol Chem* **279**: 38960-38968.

Phillips, J.D., Bergonia, H.A., Reilly, C.A., Franklin, M.R., and Kushner, J.P. (2007) A porphomethene inhibitor of uroporphyrinogen decarboxylase causes porphyria cutanea tarda. *Proc Natl Acad Sci U S A* **104**: 5079-5084.

Phillips, J.D., Warby, C.A., Whitby, F.G., Kushner, J.P., and Hill, C.P. (2009) Substrate shuttling between active sites of uroporphyrinogen decarboxylase is not required to generate coproporphyrinogen. *J Mol Biol*.

Rand, K., Noll, C., Schiebel, H.M., Kemken, D., Dulcks, T., Kalesse, M., Heinz, D.W., and Layer, G. (2010) The oxygen-independent coproporphyrinogen III oxidase HemN utilizes harderoporphyrinogen as a reaction intermediate during conversion of coproporphyrinogen III to protoporphyrinogen IX. *Biol Chem* **391**: 55-63.

Raux, E., Leech, H.K., Beck, R., Schubert, H.L., Santander, P.J., Roessner, C.A., Scott, A.I., Martens, J.H., Jahn, D., Thermes, C., Rambach, A., and Warren, M.J. (2003) Identification and functional analysis of enzymes required for precorrin-2 dehydrogenation and metal ion insertion in the biosynthesis of sirohaem and cobalamin in *Bacillus megaterium*. *Biochem J* **370**: 505-516.

Righetti, P.G., Gianazza, E., Gelfi, C., and Chairi, M. (1990) In *Gel electrophoresis of proteins: a practical approach*. Vol. 2nd Ed. Hames, B.D. and Rickwood, D. (eds). Oxford: Oxford University Press, pp. 149-214.

Rodgers, K.R. (1999) Heme-based sensors in biological systems. *Curr Opin Chem Biol* **3**: 158-167.

Roehl, J.C.G., Warren, M., and Hunt, D. (1998) *Purple Secret: Genes, 'Madness' and the Royal Houses of Europe.* London, UK: Bantam Press, Transworld Publishers Ltd.

Roessner, C.A., Ponnamperuma, K., and Scott, A.I. (2002) Mutagenesis identifies a conserved tyrosine residue important for the activity of uroporphyrinogen III synthase from *Anacystis nidulans*. *FEBS Lett* **525**: 25-28.

Romeo, P.H., Raich, N., Dubart, A., Beaupain, D., Pryor, M., Kushner, J., Cohen-Solal, M., and Goossens, M. (1986) Molecular cloning and nucleotide sequence of a complete human uroporphyrinogen decarboxylase cDNA. *J Biol Chem* **261**: 9825-9831.

Saito, M., Watanabe, S., Yoshikawa, H., and Nakamoto, H. (2008) Interaction of the molecular chaperone HtpG with uroporphyrinogen decarboxylase in the cyanobacterium *Synechococcus elongatus* PCC 7942. *Biosci Biotechnol Biochem* **72**: 1394-1397.

Sambrook, J., and Russell, D.W. (2001) *Molecular Cloning: A laboratory manual.* Cold Spring Harbor, NY, USA: Cold Spring Harbor Laboratory Press.

Sandberg, S., and Romslo, I. (1981) Porphyrin-induced photodamage at the cellular and the subcellular level as related to the solubility of the porphyrin. *Clin Chim Acta* **109**: 193-201.

Sanger, F., Nicklen, S., and Coulson, A.R. (1977) DNA sequencing with chain-terminating inhibitors. *Biotechnology* **24**: 104-108.

Seki, Y., Kawanishi, S., and Sano, S. (1986) Uroporphyrinogen decarboxylase purification from chicken erythrocytes. *Methods Enzymol* **123**: 415-421.

Shemin, D., and Rittenberg, D. (1945) The utilization of glycine for the synthesis of a porphyrin. *J Biol Chem* **159**: 567-568.

Shemin, D., and Rittenberg, D. (1946) The biological utilization of glycine for the synthesis of the protoporphyrin of hemoglobin. *J Biol Chem* **166**: 621-625.

Shemin, D., and Kumin, S. (1952) The mechanism of porphyrin formation; the formation of a succinyl intermediate from succinate. *J Biol Chem* **198**: 827-837.

Shemin, D., and Russel, C.S. (1953) Delta-aminolevulinic acid, its role in the biosynthesis of porphyrins and purins. *J. Am. Chem. Soc.* **75**: 4873-4875.

Shoolingin-Jordan, P.M., and Cheung, K.M. (1999) Comprehensive natural products chemistry. In *Biosynthesis of heme*. Vol. 4. Barton, D.e.K., J.W., ed.) (ed). Amsterdam, NL: Elservier Science Ltd., pp. 61-103.

Shoolingin-Jordan, P.M., Spencer, P., Sarwar, M., Erskine, P.E., Cheung, K.M., Cooper, J.B., and Norton, E.B. (2002) 5-Aminolaevulinic acid dehydratase: metals, mutants and mechanism. *Biochem Soc Trans* **30**: 584-590.

Silva, P.J., and Ramos, M.J. (2005) Density-functional study of mechanisms for the cofactor-free decarboxylation performed by uroporphyrinogen III decarboxylase. *J Phys Chem B* **109**: 18195-18200.

Silva, P.J., and Ramos, M.J. (2008) A comparative density-functional study of the reaction mechanism of the O_2-dependent coproporphyrinogen III oxidase. *Bioorg Med Chem* **16**: 2726-2733.

Smith, A.G., and Francis, J.E. (1979) Decarboxylation of porphyrinogens by rat liver uroporphyrinogen decarboxylase. *Biochem J* **183**: 455-458.

Smith, S.J., and Cox, T.M. (1997) Translational control of erythroid delta-aminolevulinate synthase in immature human erythroid cells by heme. *Cell Mol Biol (Noisy-le-grand)* **43**: 103-114.

Sofia, H.J., Chen, G., Hetzler, B.G., Reyes-Spindola, J.F., and Miller, N.E. (2001) Radical SAM, a novel protein superfamily linking unresolved steps in familiar biosynthetic pathways with radical mechanisms: functional characterization using new analysis and information visualization methods. *Nucleic Acids Res* **29**: 1097-1106.

Stamford, N.P., Capretta, A., and Battersby, A.R. (1995) Expression, purification and characterisation of the product from the *Bacillus subtilis hemD* gene, uroporphyrinogen III synthase. *Eur J Biochem* **231**: 236-241.

Stammen, S., Muller, B.K., Korneli, C., Biedendieck, R., Gamer, M., Franco-Lara, E., and Jahn, D. (2010) High yield intra- and extracellular protein production using *Bacillus megaterium*. *Appl Environ Microbiol*.

Straka, J.G., and Kushner, J.P. (1983) Purification and characterization of bovine hepatic uroporphyrinogen decarboxylase. *Biochemistry* **22**: 4664-4672.

Studier, F.W., Rosenberg, A.H., Dunn, J.J., and Dubendorff, J.W. (1990) Use of T7 RNA polymerase to direct expression of cloned genes. *Methods Enzymol* **185**: 60-89.

Tait, G.H. (1969) Coproporphyrinogenase activity in extracts from *Rhodopseudomonas spheroides*. *Biochem Biophys Res Commun* **37**: 116-122.

Tait, G.H. (1972) Coproporphyrinogenase activities in extracts of *Rhodopseudomonas spheroides* and *Chromatium* strain D. *Biochem J* **128**: 1159-1169.

Tan, F.C., Cheng, Q., Saha, K., Heinemann, I.U., Jahn, M., Jahn, D., and Smith, A.G. (2008) Identification and characterization of the Arabidopsis gene encoding the tetrapyrrole biosynthesis enzyme uroporphyrinogen III synthase. *Biochem J* **410**: 291-299.

Thauer, R.K., and Bonacker, L.G. (1994) Biosynthesis of coenzyme F_{430}, a nickel porphinoid involved in methanogenesis. In *Ciba Foundation Symposium 180 - The Biosynthesis of the Tetrapyrrole Pigments*. Chadwick, D.J. and Ackrill, K. (eds). Chichester, UK: Wiley and Sons, pp. 210-222; discussion 222-217.

Thunell, S. (2006) (Far) Outside the box: genomic approach to acute porphyria. *Physiol Res* **55 Suppl 2**: S43-66.

Tomio, J.M., Garcia, R.C., San Martin de Viale, L.C., and Grinstein, M. (1970) Porphyrin biosynthesis. VII. Porphyrinogen carboxy-lyase from avian erythrocytes. Purification and properties. *Biochim Biophys Acta* **198**: 353-363.

Troup, B., Jahn, M., Hungerer, C., and Jahn, D. (1994) Isolation of the *hemF* operon containing the gene for the *Escherichia coli* aerobic coproporphyrinogen III oxidase by in vivo complementation of a yeast *HEM13* mutant. *J Bacteriol* **176**: 673-680.

Troup, B., Hungerer, C., and Jahn, D. (1995) Cloning and characterization of the *Escherichia coli hemN* gene encoding the oxygen-independent coproporphyrinogen III oxidase. *J Bacteriol* **177**: 3326-3331.

van Serooskerken, A.M., Poblete-Gutierrez, P., and Frank, J. (2010) The porphyrias: clinic, diagnostics, novel investigative tools and evolving molecular therapeutic strategies. *Skin Pharmacol Physiol* **23**: 18-28.

Vavilin, D.V., and Vermaas, W.F. (2002) Regulation of the tetrapyrrole biosynthetic pathway leading to heme and chlorophyll in plants and cyanobacteria. *Physiol Plant* **115**: 9-24.

Warren, M.J., and Jordan, P.M. (1988) Investigation into the nature of substrate binding to the dipyrromethane cofactor of *Escherichia coli* porphobilinogen deaminase. *Biochemistry* **27**: 9020-9030.

Warren, M.J., and Smith, A.G. (2008) *Tetrapyrroles: Birth, Life and Death.* New York, USA: Landes Bioscience, Springer Science and Business Media.

Whitby, F.G., Phillips, J.D., Kushner, J.P., and Hill, C.P. (1998) Crystal structure of human uroporphyrinogen decarboxylase. *Embo J* **17**: 2463-2471.

Wittchen, K.D., and Meinhardt, F. (1995) Inactivation of the major extracellular protease from *Bacillus megaterium* DSM319 by gene replacement. *Appl Microbiol Biotechnol* **42**: 871-877.

Wood, S., Lambert, R., and Jordan, P.M. (1995) Molecular basis of acute intermittent porphyria. *Mol Med Today* **1**: 232-239.

Wyckoff, E.E., Phillips, J.D., Sowa, A.M., Franklin, M.R., and Kushner, J.P. (1996) Mutational analysis of human uroporphyrinogen decarboxylase. *Biochim Biophys Acta* **1298**: 294-304.

Xu, K., and Elliott, T. (1993) An oxygen-dependent coproporphyrinogen oxidase encoded by the *hemF* gene of *Salmonella typhimurium*. *J Bacteriol* **175**: 4990-4999.

Xu, K., and Elliott, T. (1994) Cloning, DNA sequence, and complementation analysis of the *Salmonella typhimurium hemN* gene encoding a putative oxygen-independent coproporphyrinogen III oxidase. *J Bacteriol* **176**: 3196-3203.

Yamaoka, T., Satoh, K., and Katoh, S. (1978) Photosynthetic activities of a thermophilic blue-green alga. *Plant and Cell Physiology* **19**: 943-954.

Yang, Y., Malten, M., Grote, A., Jahn, D., and Deckwer, W.D. (2007) Codon optimized *Thermobifida fusca* hydrolase secreted by *Bacillus megaterium*. *Biotechnol Bioeng* **96**: 780-794.

Zagorec, M., Buhler, J.M., Treich, I., Keng, T., Guarente, L., and Labbe-Bois, R. (1988) Isolation, sequence, and regulation by oxygen of the yeast *HEM13* gene coding for coproporphyrinogen oxidase. *J Biol Chem* **263**: 9718-9724.

Danksagung

Meinem Mentor Prof. Dr. Dieter Jahn, für die Möglichkeit meine Dissertation anzufertigen, die hervorragende Betreuung, die hilfreichen, aufmunternden Diskussionen, Anregungen und die tolle Arbeitsatmosphäre.

Dr. Gunhild Layer danke ich für ihr Interesse an meiner Arbeit, ihre Bereitschaft das Zweitgutachten dieser Dissertation zu übernehmen und ihr offenes Ohr sowie Hilfestellung bei allen Fragen zur anaeroben Arbeit.

Prof. Dr. Ralf R. Mendel für die freundliche Übernahme des Prüfungsvorsitzes.

Ganz besonderer Dank gilt Dr. Martina Jahn, für die hervorragende Betreuung, die sehr hilfreichen und motivierenden Diskussionen und Hilfestellungen und für ihren immer fröhlichen Enthusiasmus.

Ein großes Dankeschön an alle meine Labormädels Dr. Ava Masoumi, Dr. Ilka Heinemann, Dr. Nina Diekmann, Anna-Lena Hännig, Simone Huhn, Frederike Frese, Melanie Burghartz und Vanessa Hering für die nette Laboratmosphäre, die Unterstützung, die diversen lustigen Grillabende im Hause Jahn nicht zu vergessen. Unserem „Quotenmann“ Lars für so manchen Witz, Zaubertrick und sonstigen Schabernack.

Dr. Anika March, Dr. Ilka Heinemann, Dr. Ines Gruner, Isam Haddad, Melanie Burghartz, Dr. Nina Diekmann, Dr. Petra Tielen, Dr. Rebekka Biedendieck, Dr. Sabrina Thoma, Sebastian Laaß, Simon Stammen und Tanja Piekarski für die schönste Zeit während und nach der Arbeit, ihre Bereitschaft meine Backwerke zu essen, diverse Kaffee- und Mittagspausen, Feierabendbiere trinken (auch über den Atlantik hinaus), Fußball gucken, die schönsten Kaffeeflecken, Sing-Star und andere Abende, die lustigesten „Kindheits“ Geschichten und die schmerzhaftesten Lachkrämpfe.

Ich danke allen Mitgliedern der AG Jahn für die freundliche Atmosphäre in der Arbeitsgruppe, die dafür gesorgt hat, dass das Arbeiten immer Spaß gemacht hat.

Justus, Peter, Bob und John mit denen ich so manches Abenteuer erlebt habe.
Oliver Kahn für meine stetige Aufmunterung am Laborplatz: *„Niemals aufgeben! Weitermachen immer weitermachen.“*

Allen meinen „anderen“ Freunden, insbesondere Silke Jessen, Simon Hagemeister, Heidi & Guido Weiß, Alex & Franzi Brügger, Karen & Thorben Mehnert, Sonja Bockemühl, Björn Rühl und Katina Kiep, die es immer wieder schafften und schaffen mich in eine andere Welt zu entführen, ihre Aufmunterungen und ihr Verständnis in allen Lebenslagen.

Mein ganz besonderer Dank gilt meiner Mutter und meiner Schwester ohne deren Unterstützung und Ermutigung diese Arbeit nicht möglich gewesen wäre.